TUDelft

**Modelling and Optimisation of
Oil and Gas Production Systems**

Lecture notes for course ta4490 'Production Optimisation'

J.D. Jansen and P.K. Currie

Version 5c, March 2004

Title:	**Modelling and Optimisation of Oil and Gas Production Systems**
Version:	5c
Date:	March 2004
Type of report:	Lecture notes
Course code:	ta4490 (Production Optimisation)
Authors:	J.D. Jansen and P.K.Currie.
	Part of these notes (in particular parts of chapters 6 and 7, and chapter 8) have been based on the lecture notes from P.K. Currie for the former course 'Foundations of Production Technology' (mp3440). J.D. Jansen adapted and expanded the material for ta4490 and wrote the new chapters 1 to 5 and parts of 6 and 7, the appendices, and most of the MATLAB files. D.R. Brouwer assisted with the development of some of the MATLAB practicals.
Postal address:	Section Petroleum Engineering Department of Geotechnology Delft University of Technology P.O. Box 5028 2600 GA Delft The Netherlands
E-mail:	j.d.jansen@citg.tudelft.nl

Contents

1 Introduction

1.1 *What will be covered in this chapter?*

- The role of production system modelling and optimisation in the petroleum life cycle.
- An overview of the course.
- Unit and notation conventions.

1.2 *Production system modelling and optimisation*

Figure 1.1 displays a high-level overview of activities during oil and gas exploration and production (E&P). This process diagram, often referred to as the *petroleum life cycle model* can be indefinitely refined to display sub-activities at deeper levels. The course *Production optimisation* (ta4490) is of relevance to the development and production phases of the petroleum life cycle, in particular to the sub-activities involving field development planning (FDP), detailed design of wells and facilities, and operation of wells and facilities.

Explore → **Appraise** → **Develop** → **Produce** → **Abandon**

Figure 1.1: Petroleum life cycle model.

1.2.1 Development phase

Unlike what is suggested in Figure 1.1, the petroleum life cycle is not just a sequential process without feedback and repetition of activities. In particular during the design phase, a lot of activities are performed in an iterative fashion. Figure 1.2, for example, displays some of the activities involved in designing a well during a field development project, clearly indicating the iterative nature of the process. At a higher level, several cycles of re-appraisal (e.g. based on production performance or new seismic data), re-development (e.g. through re-completion of existing wells, or in-fill drilling of new ones), and production may take place during the life of a field. Each of these activities involves aspects of production optimisation. The key objective during field development is maximization of the economic benefits within the constraints of the project. This optimisation process involves comparison of a large number of development concepts, usually in combination with a large number of subsurface models to reflect geological uncertainties. Early co-operation of between geophysicists, geologists, reservoir engineers, production engineers and well engineers, supported by the appropriate integrated organizational structure and systems (software) is essential to achieve the objective.

Traditionally, the concept of production optimisation is used in a somewhat more narrow context. For example, the textbooks of Brown (1984) and Beggs (1991) focus on optimising the various components in the flow path from the reservoir to the separator, and elaborate on the detailed analysis of flow in flowlines, chokes, wells and the near-well section of the reservoir, as indicated in the centre part of Figure 1.2. The traditional use of the term production optimisation sometimes also implies the design and analysis of artificial lift methods and stimulation treatments.

All of these optimisation activities require the use of some kind of *model* of the production system. Traditionally these consisted of relatively simple mathematical models, accessible to hand analysis, sometimes with the aid of charts or tables. Nowadays, the models are usually much more complicated and require the use of a computer.
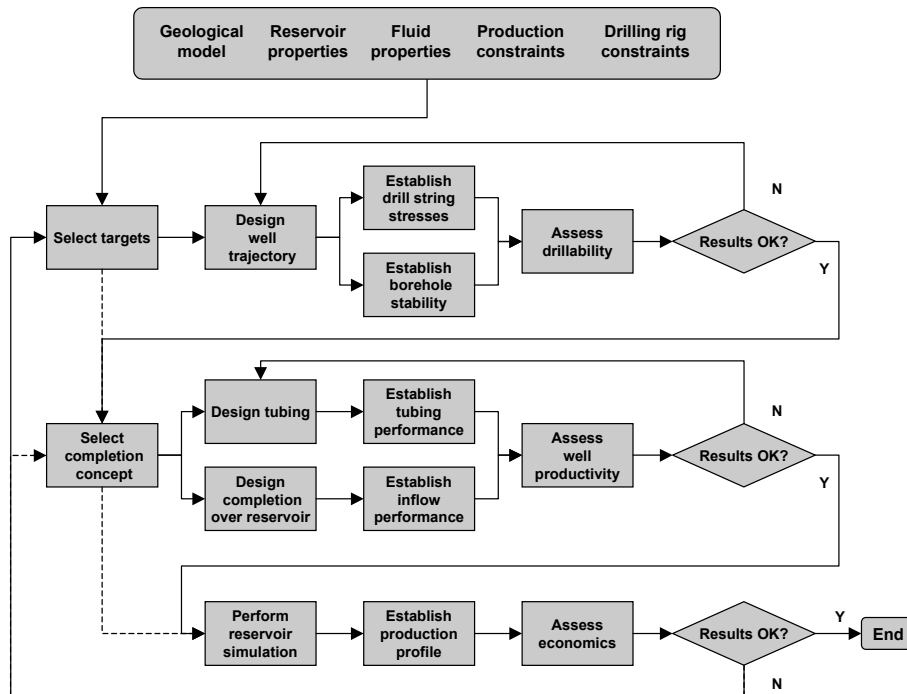
Figure 1.2: An example of iterative processes during well design in a field development project. Not shown are the links to other iterative activities during the development process such as geological modelling or design of surface facilities.

1.2.2 Production phase

Figure 1.3 shows a representation of oil and gas production as a feedback control process, involving measurement, modelling and control. Two major feedback cycles occur, each on its own time scale; see e.g. Rossi et al. (2000):

- *Daily production control*: On a scale of days to weeks, typical input variables are wellhead choke settings, water injection pressures, or lift gas rates. Measured output from the process includes production variables such as pressures, and oil, gas and water rates. Control will often be driven by short time optimisation objectives, for example production targets or utilization rates of surface facilities. Models of flow through wells and surface facilities can play an important role in the process of optimising daily production. A typical short-time optimisation problem is the distribution of a limited amount of lift gas over a number of producing wells such that oil production is maximized.

- *Reservoir management*: On a time scale of months to years, the production process essentially consists of draining the reservoir. In addition to the variables that control daily production, input includes production engineering activities such as water or gas shut off, re-completion, stimulation or even side-tracking or in-fill drilling. Measured output involves production histories, well tests and reservoir images obtained from time lapse seismic or other sources. Control is usually focused on maximizing the asset revenues, which often translates into maximizing ultimate recovery and minimizing operating expenditure. System modelling will often involve extensive reservoir simulation, in addition to wellbore and surface flow modelling. In particular when re-development activities are initiated at a later stage in the producing life of a field, the reservoir management process coincides in many aspects with the field development process described above.
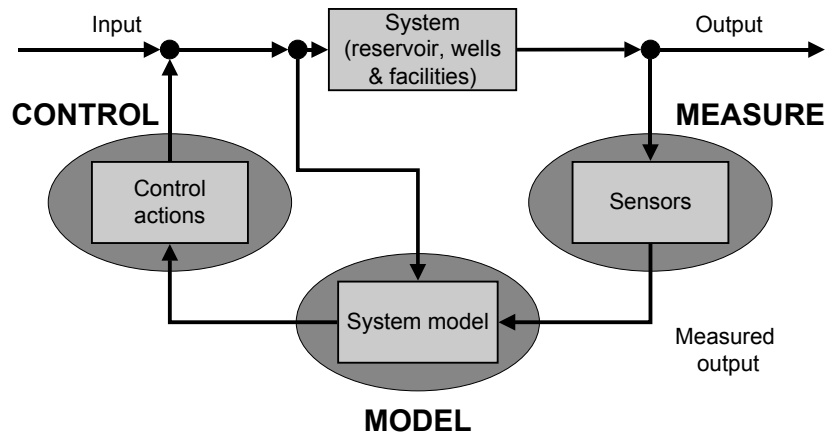
Figure 1.3: Oil and gas production represented as a feedback control process, involving measurement, modelling and control.

Sometimes short-term production optimisation is considered to be an activity for production engineers only, whereas reservoir management would then be the exclusive domain of the reservoir engineering discipline. Such a distinction is somewhat artificial and both activities are closely linked. An important production engineering activity is *surveillance*, the systematic collection and analysis of well and facilities performance data. Such production data are not only essential to optimise the production system, but also for long term reservoir management. In turn, the understanding of the long term field development objectives is essential to produce a reservoir in an optimal fashion. Because of the need to perform the short-term and long-term optimisation activities in an integrated fashion, many oil companies have re-organized their production organizations around *assets*, rather than around the traditional disciplines.

1.3   Overview of the course for 2004

1.3.1   Relationships with other courses

Pre-requisites for this course are:

- Drilling and production engineering (ta 3430).
- Properties of hydro-carbons and oilfield fluids (ta3410).
- Knowledge of physical transport phenomena as covered e.g. in Fluid flow, heat and mass transfer (ta 3220).
- Knowledge of elementary differential equations as covered e.g. in Differential equations (wi2034ta).

The course provides the knowledge of production engineering needed for

- Field development project (ta4031).

1.3.2   Course material

The course treats aspects of production optimisation in the traditional sense as well as in the wider context. The course material is completely covered in these lecture notes apart from multi-phase flow. This topic is treated in more detail in the SPE monograph *Multi-phase Flow in Wells* by Brill and Mukherjee (1999) of which the following sections form an obligatory part of the course material:

- Chapter 1: Introduction.
- Chapter 2: Single-phase-flow concepts: 2.1 – 2.4.2.

- Chapter 3: Multi-phase-flow concepts: 3.1 – 3.4.
- Chapter 4: Multi-phase flow pressure gradient predictions: 4.1, 4.2 pp. 29-31 (Hagedorn & Brown method) and pp. 44-46 (Mukherjee & Brill method), 4.3 and 4.6.

In addition,

- Chapter 6 – Well design applications,

is strongly recommended as background reading. Copies of the monograph are available via the SPE or at the 'dictatenverkoop'. A few copies can be borrowed from the TA library.

1.3.3 Exercises

Exercises are provided at the end of some chapters. Answers to the exercises can be found in Appendix D. Most of the exercises can be performed by hand, with a simple calculator, but some of them are more easily performed with the aid of a spreadsheet. Alternatively, you may want to use the MATLAB routines available from Blackboard. Make sure you inspect the content of the routines to understand their functionality. Some worked-out MATLAB exercises can be downloaded from Blackboard, see the file 'Exercises.zip'. Proficiency in MATLAB is not required for the examination. However, MATLAB exercises are an important ingredient of the five afternoons of computer practical which form an obligatory part of the course. Topics covered include

- introduction to MATLAB,
- black oil properties
- multi-phase flow in wells, and
- well performance.

Some of the practical exercises will be signed off and need to be completed to obtain a valid examination result.

1.3.4 Examination

Examination will cover
- awareness of all topics covered in the course material,
- understanding of the physical principles, and
- skills in performing engineering calculations.

The latter includes in particular
- units conversion,
- cash flow analysis,
- hydrocarbon property calculations (e.g. use of black oil correlations),
- wellbore flow analysis (single phase and multi-phase Hagedorn & Brown and Mukherjee and Brill methods),
- use of gradient curves, and
- use of inflow, tubing, well and choke performance relationships to perform nodal analysis.

Material covered during the computer exercises may form part of the examination.

The examination will be written and 'open book', i.e. course material may be taken to the exam. Additional notes and worked exercises are not allowed. A calculator will be needed. Some worked exams are provided via Blackboard.

1.4 Unit systems and notation convention

Mostly, we will present formulas, data and example calculations in *SI units*. Occasionally we will add the corresponding *field units* to allow easy comparison with results from literature, or to give you a feel for units often still used in oil field practice. The expression 'SI units' is used loosely to indicate both 'strict' SI units and 'allowable' units. The 'strict' units can be

sub-divided in the seven 'base' SI units (m, kg, s, A, K, mol and cd) and 'derived' SI units such as °C, N, or J. The 'allowable' SI units are those defined in SPE (1982) and include d (day) and a (year). For further information on the use of SI units see SPE (1982), which also contains an extensive list of conversion factors. A brief list of conversion factors is given in Appendix A of these lecture notes. In addition, a number of MATLAB 'm-files' for units conversion can be downloaded from Blackboard, see the file 'Conversion factors.zip'. They have a self-explanatory syntax. E.g. to convert a value of 1000 psi into Pa type

```
» from_psi_to_Pa(1000)
```

which produces the answer

```
ans = 6894757 .
```

SI units will be quoted directly in the text. Non-SI units will be enclosed in round brackets, whenever there is a chance for confusion. To distinguish between temperatures expressed in °C (or °F) and absolute temperatures expressed in K (or °R), we will label absolute temperatures with a subscript: T_{abs}. Dimensions will be enclosed in square brackets. For example, we could write:

"The well was completed with a 0.114 m (4 ½ inch) tubing.", or

"J_s is expressed in m^2 day^{-1} Pa^{-1} (bbl day^{-1} $psia^{-1}$ ft^{-1}) and has dimensions $[L^3 m^{-1} t]$".

Following the SPE standards, we indicate the dimensions as follows:

L	is length,
m	is mass,
n	is amount,
q	is electrical charge,
t	is time, and
T	is temperature.

For variables we will predominantly use SPE symbols as recommended in SPE (1993). Variables are always written in *italics*.

1.5 Exercises

Note: The following exercises involve unit conversions. Consult Appendix A for conversion factors and additional information. In addition, you may want to make use of the MATLAB 'm-files' for unit conversion that can be downloaded from Blackboard; see the file 'Conversion factors.zip'.

1.1 A well produces 12000 bpd of oil at a GOR of 1500 scf/stb. The oil gravity is 38 °API and the gas gravity is 0.82. What are the oil and gas production rates and densities in SI units?

1.2 A mixture of 1 lbm-mole of C_1 and 0.3 lbm-mole of CO_2 is kept at a temperature of 83 °R and a pressure of 30 psig. What are the mass, the temperature and the pressure of the gas mixture in SI units?

1.3 Calculate the pressure in Pa and in psi in a well open to the atmosphere and filled with salt water (specific gravity 1.03) at a depth of 2000 m.

1.4 The pressure drop over a choke for an incompressible liquid is given by

$$\Delta p = \rho v^2 / \left(288 g_c C^2 \right) ,$$

where Δp is the pressure drop expressed in psi, ρ is the liquid density in lbm/ft^3, v is the liquid velocity in ft/s, and C is a dimensionless choke coefficient. The nature of the dimensional constant g_c is discussed in Appendix A . Convert the expression to SI units.

2 Production system modelling

2.1 What will be covered in this chapter?

- A brief description of a typical oil and gas *production system*.
- *Systems analysis;* some basic concepts and the analogy between hydraulical, electrical and mechanical systems.
- *A first look at multi-phase flow;* in particular the difference between phase flow rates and component flow rates.
- *Nodal analysis;* a specific application of systems analysis to production systems.
- *Stability of operating point;* theoretical background to a typical aspect of multi-phase wellbore flow.

Note: Various concepts covered in this chapter, especially those in Section 2.4, may seem somewhat abstract at this stage. However, they will be of relevance later on, in particular in Chapters 3, 5 and 8. You may want to just read through these parts on the first reading, and only study them in more detail at a later stage.

2.2 Production systems

The main functions of an oil and gas production system are to

- *provide* a *conduit* for the flow of fluids from the *reservoir* to the *off take point* at *surface*, and sometimes also from the surface to the *subsurface*,
- *separate* the produced reservoir fluids from each other,
- *minimize* the production or the negative effects of *by-products*,
- *store* the produced fluids if they cannot immediately be exported
- *measure* the amounts of fluids produced and *control* the production process
- *provide* a part of the *energy* required to transport fluids through the system.

The basic elements of a production system are, see Figures 2.1 to 2.3:

- the *near-wellbore area* of the reservoir, i.e. a zone of several meters in radial direction around the *wells* at the depth of the reservoir,
- the wells from the reservoir to the *well head* at surface,
- the *flowlines* from the well heads to the *surface facilities*,
- the surface facilities, consisting of *separators*, *pumps*, *compressors* and other equipment for *treatment* and *measurement*, and
- *storage tanks* and *pipelines* up to the off take point or *sales point*, which can e.g. be a valve at the entrance of a gas transport pipeline or the off-loading point of an oil *terminal* supplying tankers.

Each element of the system can be subdevided in sub-elements. In particular, the flow path through the wellbore may consist of

- *perforations* in the *formation* (i.e. the rock) and the *cement* around the *casing*, and in the casing itself,
- *sand control equipment* consistsing of densely packed *gravel* (well sorted sand) or metal *screens* at the bottom of the well,
- the *tubing*, a pipe running from the bottom of the well to surface,
- a surface-controlled subsurface *safety valve* (SCSSV) to close-in the well if surface control is accidentally lost, and
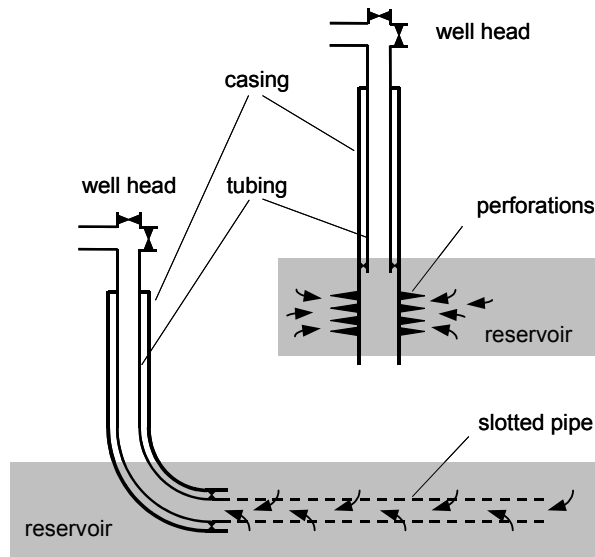
Figures 2.1 and 2.2: Schematics of a vertical and a horizontal well. The vertical well is completed with a tubing, a packer and a perforated casing. The horizontal well is completed with a tubing, a packer and an uncemented slotted pipe.

- the well head, a collection of manually or remotely-controlled *valves* to shut-in the well and allow access to the well with *wireline tools*, and a *choke* or *bean*, a variable-size restriction to control the flow from the well. Well heads are often called *christmas trees* (*Xmas tree*s).

The downhole equipment in a well is usually referred to as the *completion*. Some wells are not completed with a cemented production casing over their entire depth, but have an *open-hole completion* (just a hole in the rock without pipe, also called *barefoot completion*), or an uncemented *perforated* or *slotted* pipe in the reservoir. There is always a cemented casing present running from the top of the reservoir (the *seal* or the *cap rock*) to surface to avoid uncontrolled flow of reservoir fluids. The tubing is usually anchored to the casing just above the reservoir with the aid of an inflatable rubber *packer*. As opposed to the casing, which is cemented in place, the tubing can be changed-out if it is worn or corroded, or if the flowing behaviour of the well can be improved by changing the tubing diameter. Some wells have a *dual completion*, which means two tubings, each producing from a different reservoir at a different depths.

The surface facilities are usually more complicated than depicted in Figure 2.3. Often two or more separators are mounted in series, to allow a stepwise reduction of the pressure, rather than a single pressure drop. The reason to perform the separation in steps is to maximize the amount of oil. During separation of light and heavy hydrocarbon components, a certain amount of intermediate components disappear with the lighter ones. The lower the pressure drop that the mixture experiences, the less intermediate components disappear. A multiple separator configuration also allows to cope with a drop in *tubing head pressure* (the pressure in the tubing at the wellhead), an effect that often occurs during the life of a well when water production increases and oil production drops. In that case it is possible to connect the well to the low-pressure separator directly, while those wells that still produce at high tubing head pressures remain connected to the high-pressure separator. The pressure in the stock tank is always atmospheric, because *crude oil* (degassed and dewatered oil) is transported under atmospheric conditions.

A special role is played by the *test separator*, a separate, small, separator equipped with measurement equipment for oil, gas and water flow rates. Indvidual wells can be re-routed to the test separator to measure their oil, gas and water production. Such a *production test*, which takes several hours to obtain accurate data, is typically performed once a month for each well, and forms traditionally the only way to assess a well's production. Increasingly, however, more continuous measurements are being applied, e.g. with the aid of *multi-phase flow meters* directly connected to the flowlines. Some form of continuous measurement of pressures and temperatures at various parts of the surface production system is quite common. Downhole measurements with the aid of *permanent downhole gauges* (PDGs) are less common, although their application is steadily growing. Automatic measurements are usually stored in an electronic process control system, that may also allow full control of the surface facilities from a local or even remote control room. Such a level of instrumentation and automated process control is quite common in expensive, high production operations, typically in an offshore environment. However, many production facilities, especially those on land, are relative simple and are still operated manually.

Gas production often requires specialised *gas treatment facilities* to dry the gas and remove corrosive components such as H_2S or CO_2. Furthermore, various types of pumps and compressors, both centrifugal and reciprocating, are applied to export oil and gas or to reinject produced water or gas into the subsurface. Gas compression is also often used to enable *gas lift*, which is the injection of gas into the wellbore to reduce the hydrostatic head of the liquid and thus to increase production. This is an example of *artificial lift*, the process of supplying external energy to force the wellbore liquid from the reservoir to surface. Artificial lift is required when the reservoir pressure is too low to make the well flow naturally, a situation that often occurs at a later stage in the life of the reservoir. The most well known methods, apart from gas lift, are pumping with *beam pumps* ('*nodding donkeys*') or *electric submersible pumps* (ESPs). Fur further information on surface facilities, see e.g. Chilingarian et al. (1987) or Arnold and Stewart (1998). For further information on artifical lift, see e.g. Economides et al.(1994).
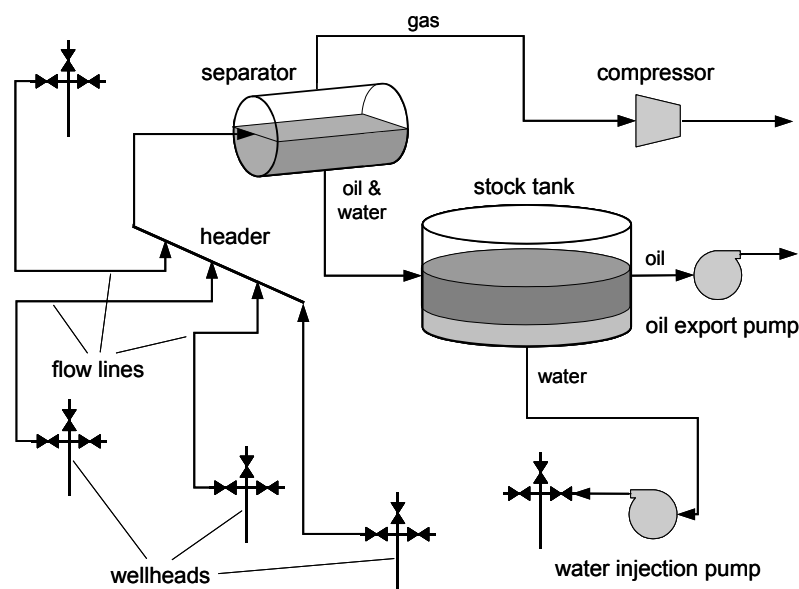

Figure 2.3: Surface facilities. The five wellheads are connected to four production wells and one water injector. Oil is exported to a terminal, gas into an export pipeline.

2.3 System models

2.3.1 Topology

Flow through a complicated system, like a production system, must be broken down into its component parts for analysis. During the course, we will examine the flow behaviour in several of the component parts: the inflow into the wells, the flow within the wells, and the flow through chokes and flowlines. But in performing these separate detailed analyses, it is essential that we realize that we are looking at only components of a larger system. Optimising the performance of each separate component will not normally result in an optimised system. For example, if we improve the well inflow behaviour so much that the tubing is unable to handle the production, we have wasted money.

We can describe the components of a production system as a *network* of *elements* connected at *nodes*. E.g., the flow from the reservoir through the well, the surface facilities and the pipeline could be represented as a series of elements and nodes as shown in Figure 2.1. The figure represents the simplest form of a network: a *cascade* or chain of elements were each node is connected to not more than two elements. In reality, a production system is not a cascade, and the associated network has a more complex *topology*. For example it may contain *branches*, i.e. three or more elements connected at a node. A next step in complexity involves *loops*: a chain of elements with a begin and end connected to the same node. Figure 2.2 displays a production system with several nested loops, formed by multiple wells, one of which is a multi-lateral, connecting two reservoirs to a single production facility. If we look in detail at some of the other components of the system, we can further refine the system model. The manifold may have more complexity, the facilities will consist of many components, and the pipeline may have branches with flow coming in from other fields.
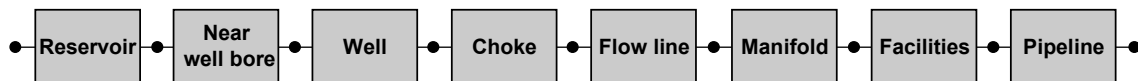
Figure 2.1: Network representation of a production system.

2.3.2 Flow and effort variables

The interaction between the various elements in a single-phase fluid flow network can usually be described in terms of two pairs of variables: *pressure* and *flow rate*, and *temperature* and *heat flow*. They are examples of pairs of *effort* and *flow variables*, concepts which play a key role in the branch of engineering known as *systems dynamics*. Other familiar pairs of effort and flow variables are the electric *potential* and *current* used in electrical network analysis, *force* and *velocity* used in mechanical systems analysis, and *torque* and *angular velocity* used also in mechanics. A common feature of most pairs of effort and flow variables is that their product represents *power flow*, also known as *energy rate* or energy per unit time:

$$p * q = V * I = F * v = M * \omega = \frac{dE}{dt} , \qquad (2.1)$$
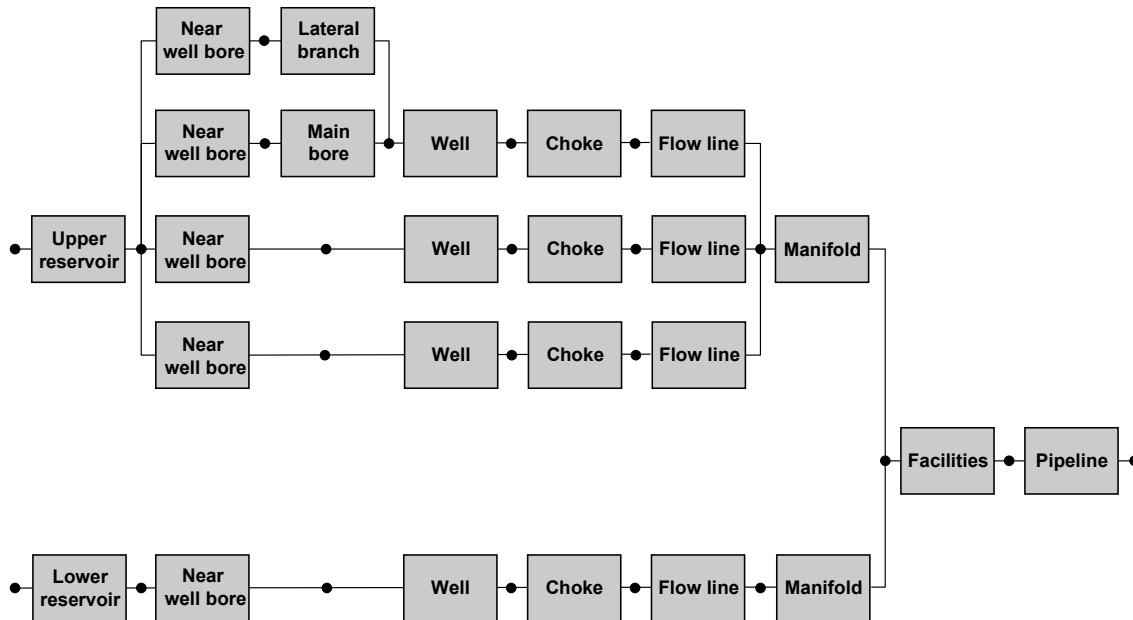
Figure 2.2: Production system represented as a network with branches and loops.

where the various symbols have been defined in Table 2.1, together with their SI units and physical dimensions. Equation 2.1 is only valid for consistent sets of units, such as SI units. For use with field units it will be necessary to introduce numerical factors, for example to account for differences between quantities expressed in feet and inches. Furthermore, it should be noted that the product of temperature and heat flow is **not** power flow. A more consistent representation of thermal systems is possible in terms of temperature and *entropy flow*, but the resulting system description is complex and outside the scope of this course. For an in-depth treatment of system dynamics, see Karnopp and Rosenberg (2000).

2.3.3 Element equations

In the following we consider *single-phase flow* of a fluid with *density* and *viscosity* that are functions of pressure and temperature. For the sake of simplicity, we neglect the occurrence of heat flow, and assume that the temperature distribution within the system is known. Within an element of a production system, pressure and temperature will generally be functions of

		Hydraulics	*Electricity*	*Translation*	*Rotation*	*Heat flow*
Effort		Pressure	Potential	Force	Torque	Temperature
Symbol		p	V	F	M	T_{abs}
SI units		Pa	V	N	N m	K
Dimension		$[L^{-1} m\, t^{-2}]$	$[L^{2} m\, q^{-1} t^{-2}]$	$[L\, m\, t^{-2}]$	$[L^{2} m\, t^{-2}]$	$[T]$
Flow		Flow rate	Current	Velocity	Angular vel.	Heat fl. rate
Symbol		q	I	v	ω	Q
SI units		$m^{3}\, s^{-1}$	A	$m\, s^{-1}$	$rad\, s^{-1}$	J
Dimension		$[L^{3}\, t^{-1}]$	$[q\, t^{-1}]$	$[L\, t^{-1}]$	$[t^{-1}]$	$[L^{2} m\, t^{-3}]$
Product		$p\, q = dE/dt$	$V\, I = dE/dt$	$F\, v = dE/dt$	$M\omega = dE/dt$	$T_{abs}Q \neq dE/dt$

Table 2.1: Analogies between system variables in different domains.

time t and spatial co-ordinates x, y, and z. Most elements, however can be represented as *one-dimensional systems* with a single *spatial co-ordinate s*. Furthermore, we generally restrict ourselves to the analysis of *steady state flow*, i.e. flow independent of t. If we consider for example a wellbore element, we can then describe the flow behaviour with the following variables:

$$\text{pressure } p(q,\rho,s,z,\alpha,T), \text{ flow rate } q(p,\rho,s,z,\alpha,T), \text{ density } \rho(p,T), \text{ and viscosity } \mu(p,T) \quad (2.2)$$

where along-hole distance s is the independent variable, while vertical depth from surface $z(s)$, wellbore inclination $\alpha(s)$, and temperature $T(s)$ are given functions of s. We need four equations to solve for the four unknowns p, q, ρ and μ. In Chapter 5 we will discuss the nature of these equations in detail. Here we only state that it is generally possible to solve the equations over the length of an element and express the pressure and flow rate at one end of the element in terms of the pressure and flow rate at the other end with *input-output relationships*:

$$\begin{cases} p_{out} = f_1(p_{in}, q_{in}) \\ q_{out} = f_2(p_{in}, q_{in}) \end{cases}, \tag{2.3}$$

where f_1 and f_2 are functions. They are usually strongly non-linear, and cannot be obtained in closed form, but may need to be determined numerically as will be treated in more detail in Chapter 5. The density and viscosity can be computed anywhere in the element since they are a function of p and T only.

We could have expressed equations (2.3) in terms of mass flow rates $w_{in} = q_{in} \rho_{in}$ and $w_{out} = q_{out} \rho_{out}$ instead of volume flow rates q_{in} and q_{out}. In that case we would have found that $w_{out} = w_{in}$ because we consider a steady state situation and therefore no mass can accumulate in an element. The same result could have been reached by expressing q_{in} and q_{out} in terms of a reference flow rate at a given pressure and temperature. In the oil industry such a reference flow rate is usually defined at *standard conditions*, representing 'typical' atmospheric conditions: 15 °C and 100 kPa. In that case equations (2.3) reduce to

$$p_{out} = f_3(p_{in}, q_{sc}), \tag{2.4}$$

where f_3 is another non-linear function, and where the subscript sc indicates standard conditions. Equation (2.4) illustrates that single-phase flow through an element can be completely determined with a single relation between pressure and flow rate. In theory it is also possible to derive the flow rate from the pressure drop with the aid of the inverse relation:

$$q_{sc} = f_4(p_{in}, p_{out}) \ . \tag{2.5}$$

For flow in oil and gas production systems, the situation is usually more complex, because we encounter *multi-phase flow*, involving a gas phase, one or two liquid phases (oil and water) and sometimes even solid phases (e.g. wax, asphaltenes, hydrates, ice). As a result we cannot use a single rate q to characterize the flow. In the following, we restrict ourselves to gas-liquid two-phase flow. Even so, each of the two phases may contain a large number of hydrocarbon components in a *composition* that varies with pressure and temperature. In this course, we will further restrict ourselves by considering an oil-gas system composed of two *pseudo-components* that are present in the gas and the oil phase in a variable composition depending on the local pressure and temperature. Each of the two phases will have its own density and viscosity, while in addition the *interfacial tension* σ comes into play. Often the

pseudo components are chosen as the gas and oil that result from surface separation at standard conditions. We can then either express the input-output relationships in terms of local oil and gas *phase* flow rates q_o and q_g, or in terms of the reference *component* flow rates $q_{o,sc}$ and $q_{g,sc}$:

$$\begin{cases} p_{out} = f_5\left(p_{in}, q_{o,in}, q_{g,in}\right) \\ q_{o,out} = f_6\left(p_{in}, q_{o,in}, q_{g,in}\right) \\ q_{g,out} = f_7\left(p_{in}, q_{o,in}, q_{g,in}\right) \end{cases} \text{ or } p_{out} = f_8\left(p_{in}, q_{o,sc}, q_{g,sc}\right) . \qquad (2.6), (2.7).$$

As was the case in single-phase flow, the difference between flow-in and flow-out vanishes in the equations expressed in (component) flow rates at standard conditions, i.e. $q_{o,in} = q_{o,out} = q_o$, and $q_{g,in} = q_{g,out} = q_g$. Equation (2.7) shows that also for two-phase flow the pressure drop over an element can be reduced to a single expression in terms of the flow rates. In this case, however, we cannot reconstruct the flow rates from the pressure drop using the inverse of equation (2.7) alone, and we need a second equation that provides information about the ratio of the flow rates $q_{o,sc}$ and $q_{g,sc}$.

2.3.4   System equations

The input-output representations (2.3), (2.4), (2.6) and (2.7) are of course perfectly suited for the analysis of cascade systems with the aid of a *marching algorithm*. We can then start from the known values for pressure and flow rate(s) at one end of the system, and work our way through to the other end by using the input-output relations f_i for the elements one after each other. Also a system with branches, but without loops, can be analysed using this approach. For a system with loops, however, the situation is more complicated, and needs to be analysed with techniques similar to those used in analysis of electrical networks. The same approach can be used for the analysis of multi-component fluid flow networks, and obviously the number of equations increases with the number of components taken into account. Furthermore, the analysis could be extended to include the temperature T and heat flow rate Q in the system. Mass flow and heat flow are strongly coupled through convective heat transport and viscous dissipation. Therefore, in the most general situation of fully thermal compositional network analysis, we end up with a large system of coupled non-linear equations that may require considerable computing power. Such an analysis is outside the scope of this course. A good introduction to the mathematical background of network analysis is given in Strang (1986).

2.4   Nodal analysis

2.4.1   Principle

The analysis of cascade systems with the aid of a marching algorithm is known in the oil industry as *nodal analysis*. Written in capitals, NODAL™ analysis has even been registered as a trade mark by a major service company.

For any given cascade network, we can march either from begin to end or vice versa. If we know the pressure *and* the flow rate at one of the ends, such a *one-pass* analysis is sufficient to obtain the pressures and flow rates at all nodes. However, often we know the value of one variable at each end of the cascade. For example we may know the reservoir pressure and the manifold pressure at the ends of a cascade representing a single well. In that case we need to guess the flow rate at one of the ends and repeat the marching algorithm several times, either upward or downward, to establish the correct flow rate in an iterative fashion. With correct flow rate we mean the flow rate that gives the correct pressure at the other end.

Instead of marching all the way from one end to the other, we could just as well perform two shorter marches, each one starting at an end and finishing in a *joint node*, also referred to as *analysis node*. Furthermore, instead of performing the iteration automatically, we could plot the two pressures (top-down and bottom-up) at that particular node for a large number of flow rates and determine the correct flow rate graphically. This is indeed the approach followed in traditional nodal analysis of production systems, which was developed in the 1950s and relied on tabulated pressure drop values and graphical analysis rather than computer methods.

2.4.2   Classical procedure

In traditional nodal analysis, popular choices for the analysis node are those representing

- the flowing *bottomhole pressure*, p_{wf}, at the bottom of the tubing,
- the flowing *tubing head pressure*, p_{tf}, just upstream of the wellhead choke,
- the *flowline pressure*, p_{fl}, at the entrance of the flowline just downstream of the wellhead choke, or
- the *manifold pressure*, p_{mf}, at the end of the flowline.

Frequently used abbreviations for (flowing) tubing head pressure and (flowing) bottomhole pressure are (F)THP and (F)BHP, where the adjective *flowing* is used to distinguish the pressures from the *closed-in* or *static* values for THP and BHP which occur when the well is closed-in at surface.

Sometimes different names are used for pressure drop calculations depending on whether the algorithm marches in the direction of the flow or against it. If, for a given input pressure and flow rate, we calculate the output pressure, this is known as a *pressure drop calculation*. Alternatively, if we specify the output pressure, and calculate the input pressure for a cascade at the given flow rate, this is called an *operating point calculation*. For example, if the THP is specified and the BHP is calculated, this is an operating point calculation. If the BHP is specified and the THP is calculated, it is called a pressure drop calculation. In practice, we use a mixture of pressure drop and operating point calculations to analyse the particular feature of a production system, as shown in Figure 2.3.

For example, we may want to look at the effect of inflow performance on the production rate $q_{o,sc}$ of a well, for a given manifold pressure. We choose the bottom of the tubing as the analysis node. For a fixed (surface) flow rate $q_{o,sc}$, we work back down the well, using operating point calculations for the various components (choke and tubing) and determine the pressure at the analysis node. Repeating this procedure for different flow rates, gives a relationship between the flow rate $q_{o,sc}$ and the pressure p_{wf} at the analysis node. Such a *p-q* relationship we call an *operating point performance curve*.
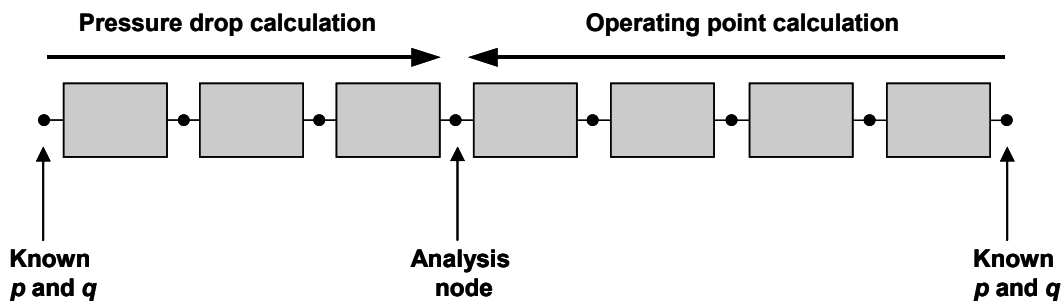

Figure 2.3: Procedure for nodal analysis.

Similarly, starting from the given reservoir pressure, we can perform pressure drop calculations for each component (reservoir, near wellbore region, perforations etc.) to determine a *pressure drop performance curve* for p_{wf} and $q_{o,sc}$. These two curves can be plotted on the same *p-q* graph. There will be two possibilities, as shown in Figure 2.4.

1. *The two curves do not intersect*. The system cannot be operated under the assumed conditions (given reservoir and manifold pressure).
2. *The curves intersect at one or more points*. Because the relationship between pressure drop and flow rate is non-linear for most elements of the production system, the *p-q* graphs are usually curved and may intersect at more than one point. Typically, we encounter two intersections, one representing a stable and one an unstable (physically unrealistic) *operating point*.

2.4.3 Stability of an operating point

To understand why an operating point can be unstable, we need to consider the dynamics of the system. Nodal analysis is based on the steady-state relationship between pressure drop and flow rate. For example, the operating point and pressure drop performance curves in Figure 2.4 can be represented schematically as:

$$p = f(q) \text{ and } p = g(q), \tag{2.8}$$

where *f* and *g* are non-linear functions. The flow rate *q* refers to the oil flow rate at standard conditions $q_{o,sc}$, but in this section we will drop the subscript '*o,sc*' to avoid confusion with the subscript '0' (zero) used to indicate an operating point. In an operating point (p_0, q_0) we find that

$$p_0 = f(q_0) \text{ and } p_0 = g(q_0) . \tag{2.9}$$

We are interested in the effect of small disturbances $\widetilde{p}$ on the flow in the neighbourhood of an operating point:
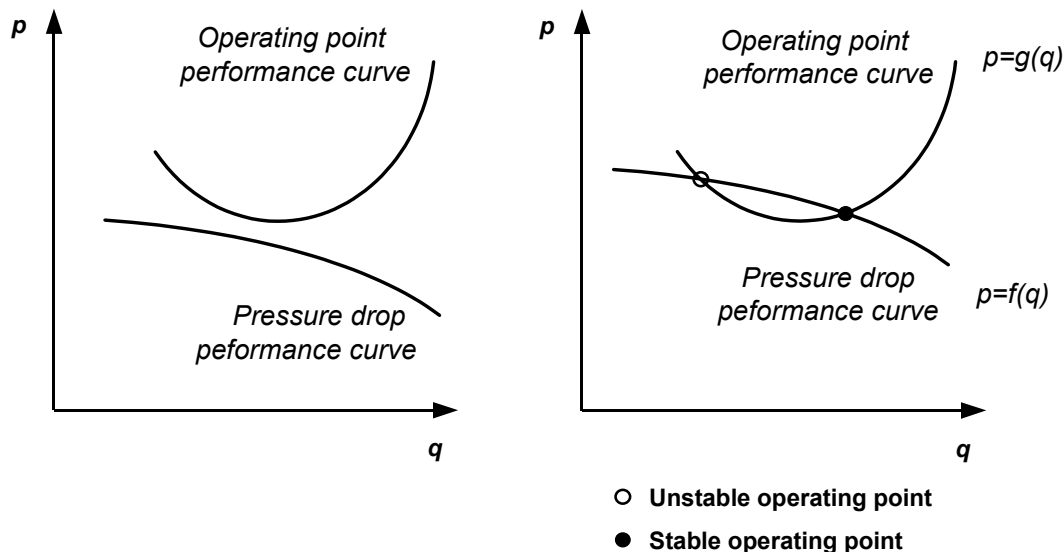

Figure 2.4: Nodal analysis using performance curves. Left: no intersection between curves. Right: two intersections representing two operating points, of which only one is physically realistic.

$$p_0 + \tilde{p} = f(q_0 + \tilde{q}) \text{ and } p_0 + \tilde{p} = g(q_0 + \tilde{q}). \tag{2.10}$$

Because we only consider small disturbances, we can linearize f and g. In other words, we can take the Taylor expansions for f and g around q_0, defined as

$$f = f(q_0) + \left(\frac{df}{dq}\right)_{q=q_0} * (q - q_0) + \frac{1}{2}\left(\frac{d^2 f}{dq^2}\right)_{q=q_0} * (q - q_0)^2 + \dots$$

$$g = g(q_0) + \left(\frac{dg}{dq}\right)_{q=q_0} * (q - q_0) + \frac{1}{2}\left(\frac{d^2 g}{dq^2}\right)_{q=q_0} * (q - q_0)^2 + \dots \tag{2.11}$$

and maintain only the constant and linear terms. If we substitute expansions (2.11) into equations (2.9) and (2.10) and subtract the results, we obtain linear relations for $\tilde{p}$ and $\tilde{q}$:

$$\tilde{p} = f'\tilde{q} \text{ and } \tilde{p} = g'\tilde{q}, \tag{2.12}$$

where f' and g' are constants that follow from equations (2.11) as:

$$f' = \left(\frac{df}{dq}\right)_{q=q_0} \text{ and } g' = \left(\frac{dg}{dq}\right)_{q=q_0}. \tag{2.13}$$

Small fluctuations in flow rate imply that the flow accelerates and decelerates with small amounts. These accelerations cause pressure fluctuations which we can represent in equations (2.12) by adding inertia terms. We now assume that f represents the pressure drop performance curve, and g the operating point performance curve. In that case we can write

$$\tilde{p} = f'\tilde{q} - f_{in}\frac{d\tilde{q}}{dt} \text{ and } \tilde{p} = g'\tilde{q} + g_{in}\frac{d\tilde{q}}{dt}, \tag{2.14}$$

where $f_{in} \geq 0$ and $g_{in} \geq 0$. The two equations (2.14) are relationships between the pressure and the flow rate in the analysis point and represent the effect of the flow dynamics in the well upstream and downstream of that point respectively. The two acceleration terms have different signs because an increase in pressure in the analysis node causes a deceleration of the flow in the upstream part of the system and an acceleration of the flow in the downstream part. In the operating points the pressures resulting from the upstream and the downstream part have to be equal, and therefore we can write:

$$f'\tilde{q} - f_{in}\frac{d\tilde{q}}{dt} = g'\tilde{q} + g_{in}\frac{d\tilde{q}}{dt}, \tag{2.15}$$

which can be rewritten as

$$(f_{in} + g_{in})\frac{d\tilde{q}}{dt} - (f' - g')\tilde{q} = 0. \tag{2.16}$$

Equation (2.16) is a linear first order differential equation for $\tilde{q}$. To obtain a complete solution we need one initial condition. If we assume that a pressure disturbance with magnitude $\tilde{q}_0$ takes place at time $t = 0$, the initial condition becomes:

$$t = 0 : \tilde{q} = \tilde{q}_0. \tag{2.17}$$

Solving equation (2.16) results in

$$\tilde{q} = C \exp\left(\frac{f' - g'}{f_{in} + g_{in}} t\right), \tag{2.18}$$

where C is an integration constant which can be determined with the aid of initial condition (2.17). That results in $C = \tilde{q}_0$, and therefore

$$\tilde{q} = \tilde{q}_0 \exp\left(\frac{f' - g'}{f_{in} + g_{in}} t\right). \tag{2.19}$$

Equation (2.19) represents an exponentially growing or decreasing magnitude of disturbance $\tilde{q}$ with time, depending on the sign of $(f' - g') / (f_{in} + g_{in})$. Because we defined that $f_{in} \geq 0$ and $g_{in} \geq 0$, it is the sign of $(f' - g')$ that determines the stability of the flow in an operating point. With the aid of equation (2.13) we can interpret f' and g' as the slopes of the pressure drop performance curve and the operating point performance curve. Note that a performance curve that decreases with increasing q has a negative slope. Referring back to Figure 2.4, we find that the operating point to the left is unstable, and the one to the right stable. Stable wellbore flow can therefore only occur at the pressure and flow rate corresponding to the operating point to the right.

2.5 Exercises

2.1 An electric motor operates with 90 % efficiency at 300 V and draws a current of 16 A. The shaft of the motor rotates with 240 revolutions per minute (rpm) and drives an oil pump, via a reduction gear with an efficiency of 98 %. The pump creates a pressure differential of 160 kPa at a flow rate of $22 * 10^{-3}$ m³/s. What is the torque generated by the motor? What is the efficiency of the pump?

3   Optimisation objectives and constraints

3.1   What will be covered in this chapter?

- Economic objectives. Particular attention is paid to the importance of discounting to capture the effect of time in economic optimisation.
- Environmental objectives.
- Technical objectives.
- Constraints imposed by nature, technology and socio-economic conditions.

3.2   Economic objectives

3.2.1   Cash flow analysis

Optimisation of a process requires a clearly defined *objective* together with the relevant *constraints*. In most E&P projects, the objective is to maximize the economic value of the project in some sense. Figure 3.1 displays a typical annual *cash flow* of an oil or gas development project, i.e. the yearly difference between cash-in, consisting of revenues from oil or gas sales, and cash-out consisting of capital expenditure (CAPEX), operating expenditure (OPEX), royalties and taxes. The sum of OPEX and CAPEX is also known as *technical costs*, the sum of royalties and taxes as *host government take*. OPEX is often devided in a fixed part, expressed as a percentage of the cumulative project CAPEX, and a variable part, expressed as a cost per unit of liquid or gas produced. The sum of CAPEX and OPEX per unit volume of oil produced is known as the *unit technical cost* (UTC), which is a frequently used indicator of the cost-efficiency of production operations. Royalties are a percentage of the oil produced and are payed either in the form of money or 'in kind', i.e. in the form of oil. Taxes are paid in the form of a percentage of the *taxable income* which consists of the revenues minus the sum of the royalties, the OPEX and the *depreciation*. In the context of project economics, depreciation is a fiscal tool to spread the CAPEX spent in one year over several fiscal years, and rules for depreciation are set by the host government. The annual cashflow F_k in year k can therefore be expressed as

$$F_k = R_k - E_k = \underbrace{p_o N_k}_{\text{revenues}} - \underbrace{O_k - C_k}_{\text{technical costs}} - \underbrace{r_R p_o N_k - T_R I_{bt,k}}_{\text{government take}} \ , \tag{3.1}$$

where R are the revenues, E are the expenses, p_o is the oil price, N is the annual production, O is the OPEX, C is the CAPEX, r_R is the royalty rate, and T_R is the tax rate, and where I_{bt} is the taxable income (or *income before tax*) defined as

$$I_{bt,k} = p_o N_k (1 - r_R) - O_k - D(C_k, C_{k+1}, \cdots, C_{k-K}) \ , \tag{3.2}$$

where D is the depreciation function and K the number of years over which the CAPEX can be depreciated. In it's simplest form, known as *straight line depreciation*, the CAPEX is simply devided in equal parts over a period of K years. Figure 3.2 displays the *cumulative cash flow* corresponding to Figure 3.1. It illustrates the initial *maximum exposure* (expressed in $) caused by up-front investments, the *break-even point* or *pay-out time* (expressed in years), when the investments are recovered through the revenues, and the *cumulative cash surplus* (expressed in $) at the end of the project life.

3.2.2   Discounting

The cash flows in Figures 3.1 and 3.2 are given in '*constant value money*', i.e. they do not take into account inflation. If we would take into account inflation, the resulting cumulative cash flow in '*money of the day*', would be higher, but we will not address this issue further.

However, we will take into account another effect: Money has a tendency of apparently loosing its value during the course of a project because it could have been used for other, more profitable, investments. In the analysis of project economics, this effect is taken into account through *discounting* the project cash flow, i.e. through reducing the value of money over time to reflect the return on investment that could have been made by investing the money elsewhere. The interest rate of this imaginary alternative investment is known as the *discount rate*, and we can therefore write

$$S_{alt} = S(1 + R_{disc}/100)^n,\qquad(3.3)$$

where

S_{alt} is the value in year n from the alternative investment of S expressed in \$,
S is the sum of money invested in year 0 in \$,
R_{disc} is the discount rate in % per year, and
n is the number of years since the investment.

The value of a sum S to be paid or received in year n should therefore be reduced to a discounted value S_{disc} according to

$$S_{disc} = S * \frac{S}{S_{alt}} = S * \underbrace{\left[\frac{1}{(1 + R_{disc}/100)^n}\right]}_{\text{discount factor}},\qquad(3.4)$$
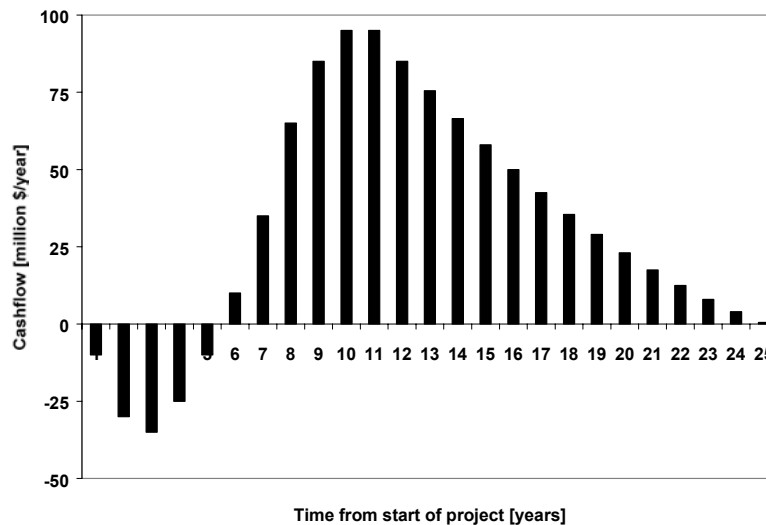

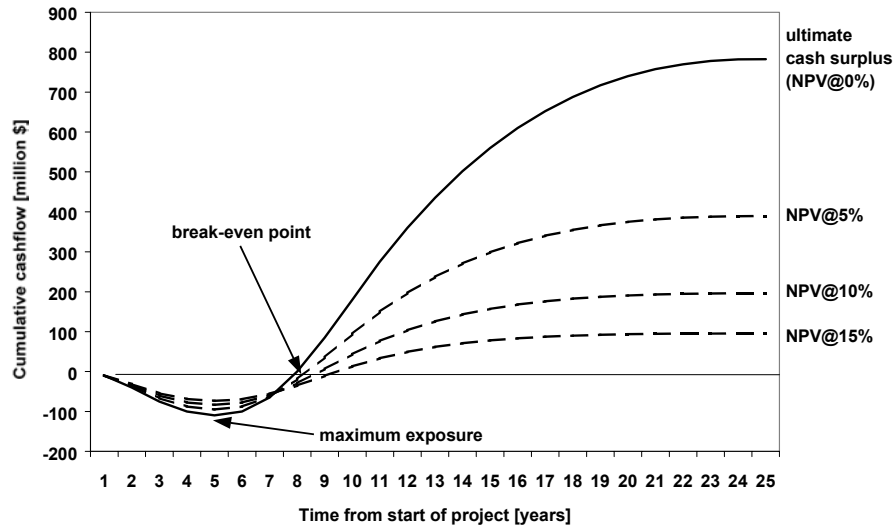Figure 3.1: Annual cash flow of a typical oil or gas development project.

Figure 3.2: Cumulative cash flow corresponding to the values of Figure 3.1.

where the multiplication factor at the right-hand side is known as the *discount factor.* Discounting is a method to quantify the effect that it is economically attractive to receive payments as early as possible: until they have been received they cannot be used by the receiver to make a return on investment and therefore gradually loose value. Conversely, it is economically attractive to delay expenses, because until the money actually changes hands, the spending party can use it to make a return, which effectively results in a reduced expenditure. The discounted cumulative cash surplus of a project is often referred to as the *net present value* (NPV) at a particular discount rate. Because of the large influence of oil prices on revenues and therefore on E&P project economics, the NPV is usually quoted together with the oil price and the discount rate used for its computation.

During the design phase of a development project, in particular during the FDP phase, the objective is maximization of the NPV within the constraints of the project. This involves comparison of a large number of development concepts, usually in combination with a number of potential subsurface models to reflect geological uncertainties. An important aspect is the phasing of the investments, because money spent at a later date has effectively a lower value, because it has been discounted. Similarly, oil produced during the early days of the project has a more beneficial effect on the NPV than oil produced at a later date, and sometimes expensive completion concepts may be justified based on their potential to speed up production. For a more detailed treatment of cash flow analysis and other aspects of petroleum economics, see e.g. Seba (1998).

3.2.3 Example

A well could be completed with a 0.089 m (3-½ inch) tubing at a cost of 160,000 $. The expected daily production rates are given in allowable SI units and field units in columns 2 and 3 of Table 3.1. Alternatively, the well could be completed with a 0.102 m (4 inch) tubing at a cost of 210,000 $, resulting in a production rate according to columns 4 and 5 of Table 3.1. Reservoir simulations indicate that the 0.102 m completion will stop producing after 8 years because of lift die-out caused by an increased watercut. Re-completion with a 0.089 m tubing, at a cost of 800,000 $ for the workover, will extend the life of the well with another 6 years, during which time it will produce just as if it were completed with a 0.089 m tubing right from the start.

Table 3.1: Daily production rates for two tubing sizes.				
Time (year)	Production rate 0.089 m (3-½ inch) tubing		Production rate 0.114 m (4 inch) tubing	
	m^3/d	bpd	m^3/d	bpd
1	119.3	750	141.5	890
2	119.3	750	141.5	890
3	119.3	750	141.5	890
4	115.3	725	132.0	830
5	91.4	575	91.4	575
6	55.7	350	42.1	265
7	31.8	200	15.9	100
8	27.8	175	4.0	25
9	24.6	155		
10	22.3	140		
11	20.7	130		
12	19.9	125		
13	19.1	120		
14	8.0	50		

Question:

What is the most economic completion under an assumption of an oil price of 15 $/bbl, and using a discount rate of 12%? To simplify the analysis, assume that the government take is only in the form of a 20% royalty, and no taxes are being paid.

Answer:

Column 2 of Table 3.2 displays the differential daily oil production Δq_o of the two completions, and column 3 the associated yearly differential revenues ΔR computed as:

$$\Delta R = p_o * \Delta q_o * 365 , \qquad (3.5)$$

where p_o is the oil price in $/bbl. Column 4 displays the differential annual expenses ΔE. They are zero except for 50,000 $ in year 1 because of the difference in initial completion costs, and 800,000 $ in year 9 for the workover and re-completion. After year 9, there is no difference in revenues or expenses, and we do not have to consider this period in the rest of the analysis. The differential annual cash flow, taking into account the 20% royalties, can be expressed as $\Delta F = (1 - 0.2) * \Delta R - \Delta E$ and is given in column 5. The discounted differential annual cash flow ΔF_{disc} is obtained by reducing the value of ΔF according to equation (3.4) resulting in

$$\Delta F_{disc} = \frac{\Delta F}{(1 + R_{disc}/100)^n} . \qquad (3.6)$$

Summation of the discounted differential annual cash flow results in the discounted cumulative differential cash surplus, in other words, the differential NPV. As displayed at the

bottom of column 6 of Table 3.2, the undiscounted cumulative differential cashflow is just negative, suggesting that the recompletion option is unattractive. However, the discounted differential cashflow equals nearly 780,000 dollar, which clearly indicates that under a 15 $/bbl oil price and a 12 % discount rate it is economical to initially complete the well with the larger size tubing and pay for the extra costs of the workover in year 9. The reason for the difference is the strong production increase during early years which is much heavier weighted than the reduced production and the workover costs later in time. Note: A further improvement in NPV could be obtained by changing out the tubing earlier; see exercise 3.4.

Table 3.2: Differential NPV calculation.					
Time (year)	Differential production rate (bpd)	Differential annual revenue ($)	Differential annual expenses ($)	Differential annual cash flow ($)	Discounted differential annual cash flow ($)
1	140	766,500	50,000	563,200	502,857
2	140	766,500	0	613,200	488,839
3	140	766,500	0	613,200	436,464
4	105	574,875	0	459,900	292,275
5	0	0	0	0	0
6	-85	-465,375	0	-372,300	-188,619
7	-100	-547,500	0	-438,000	-198,129
8	-150	-821,250	0	-657,000	-265,351
9		0	800,000	-800,000	-288,488
	190	1,040,250	850,000	-17,800	**779,848**

3.2.4 Treatment of uncertainties

Geological or operational uncertainties may have an effect on the economics of a production optimisation project. For example the time to remove the packer and the tubing from a well during a workover may vary strongly because of corrosion and ageing of the packer elements. Sometimes it is possible to make an estimate of the probability of occurrence of uncertain events, and in that case one can compute the risk-weighted NPV of the project which is also known as the *expected monetary value* (EMV). For example, operational experience in a certain area may have revealed that there is an 80% chance of performing a tubing change-out in 4 days, but a 20 % chance that it takes about two weeks. At a rig rate of 100,000 $/d such a delay of 10 days would mean an increase in the workover costs of 1,000,000 $. Applying this situation to the example given in Section 3.2.3 above, the discounted additional costs would be

$$\frac{1,000,000}{\left(1+12/100\right)^9} = 360,610 \text{ \$.} \tag{3.7}$$

In that case the EMV of the tubing change-out option would be given by

$$V_e = 0.8*779,848 + 0.2*\left(779,848 - 360,610\right) = 707,726 \text{ \$.} \tag{3.8}$$

3.3 Environmental objectives

Economic aspects of an oil and gas development project cannot be considered in isolation from the *environmental aspects* and the *social impact* on the population in the neighbourhood. Environmental objectives can be specified in terms of allowable limits such as the amount of residual oil in discharged water, the amount of hydrocarbons vented during processing, or the noise level of production facilities. These limits may originate from local, national or international *legislation* or from an oil company's own *policies* and *environmental targets*. Sometimes it is possible to translate environmental objectives directly into economic ones, for example through imposing a financial penalty on discharges. Often, however, this is not possible and environmental objectives have to be balanced against economic objectives, both during the field development process, as well as during the producing life of the field.

Essential in an up-front reduction of the environmental impact of a development process is to consider the process of hydrocarbon production from cradle to grave, including waste generation and handling, and abandonment of the facilities. *Waste management* should focus on minimization, re-use, and re-cycling of waste and only thereafter consider the best option for disposal. The major waste stream from a production process is water. Unfortunately, also gas is often considered an unwanted by-product, in particular when there is no local market to sell it. The most widely accepted solution for produced water and gas disposal is re-injection in the sub-surface, although this is also not without environmental risks, in particular when there is a possibility that produced water may pollute fresh-water bearing aquifers. Disposal of produced water at sea, after treatment to minimize the oil-in-water content, may in some instances be acceptable; surface disposal (flaring) of gas is almost never. Minimization of water and gas production are therefore usually the most important environmental objectives. Other commonly encountered environmental objectives are minimization of the discharges from drilling and workover operations, and minimization of the land take by production facilities and pipelines. This may lead to field development with deviated wells and clustered wellheads in a small number of surface locations. For further information on environmental aspects of oil and gas production see e.g. Reis (1996).

3.4 Technical objectives

During the design process of a production system it is often not feasible to directly assess the economic and environmental consequences of technical solutions. Similarly, during production operations it may be impossible to directly assess the consequences of operational activities. Therefore, it is necessary to specify *technical objectives*, that can serve as intermediate goals during the development and production processes.

A production system is designed to transfer hydrocarbons at the point of delivery to the customer, and return waste products to the subsurface or treatment facilities. The *delivery commitment* for hydrocarbons is usually in terms of volume and, in case of gas projects, pressure and composition. Thus an important technical objective is to design the production system such that it can sustain the required *system capacity* or *throughput*, making allowance of course for normal downtime. This involves matching of the various components in the flow path from the reservoir to the point of delivery to ensure maximum flow rate at a given pressure drop, or minimum pressure drop at a given flow rate. This optimisation process should take into account that the reservoir pressure and the composition of produced fluids change drastically over the life of the reservoir. A related technical objective is to ensure a production stream that will remain stable over a considerable part of the of the producing life of the reservoir. As will be shown during the course, improperly designed components in a well may result in unstable flow, or, in the worst case no flow at all.

Technical objectives during production are usually short-term production targets or facility utilization rates, and cost reduction. The most important longer-term technical objective is maximizing ultimate recovery. As already discussed in Section 1.2, short term production optimisation and longer term reservoir management are closely linked, both in the development phase as well as in the production phase of the petroleum life cycle.

3.5 Constraints

Many constraints have to be taken into account during production optimisation.

Location: In particular the difference between onshore and offshore has dramatic consequences. In deep offshore locations well construction and well servicing are extremely costly and therefore justify development concepts that would not be economically onshore.

Reservoir and fluid properties: High reservoir pressures and temperatures can severely influence the design of wells and processing facilities. Similar effects have the presence of aggressive components such as H_2S or CO_2 in the reservoir fluids.

Time: Lead time for the procurement of well tubulars or production equipment may exceed many months and is often more than a year. Furthermore, the time spent on engineering and design optimisation needs to be balanced against the economic objective to produce oil as early as possible.

Legislation and regulations: Legislation, tax regimes and operating agreements with the host government may influence the development concept. E.g., many governments do not allow *commingled production*, i.e. production from different reservoirs through a single tubing. Also, the extent to which development expenses can be treated as CAPEX or OPEX can lead to major differences in taxation for different development concepts.

Standardization: Oil company regulations for standardization sometimes limit the scope for detailed optimisation of a design on a project by project basis. Obviously, the idea is that these short-term losses are offset against the longer term benefits of standardized equipment, such as simplified maintenance and reduced stock levels of spare parts.

Rig capacity and availability: The scope for complicated wells may be reduced by technical limits of the available drilling rigs, in particular hoisting and pumping capacity required for extended-reach wells. Opportunities for well modification or repair (*workover*) may be restricted by limited availability of workover rigs.

Many more constraints may be encountered during the various activities involved in production optimisation. Sometimes environmental objectives can be considered as constraints for economic or technical optimisation, or vice versa.

3.6 Exercises

Cash flow calculations can be most easily performed with the aid of a spreadsheet. Alternatively, you may want to use the MATLAB routines available from Blackboard; see the file 'Economics.zip'. Make sure you inspect the content of the routines to understand their functionality.

3.1 What is the discounted value of a sum of $10*10^6$ \$ after 5, 10 and 20 years at a discount rate of 7%?

3.2 What is the NPV of the following cash flow at discount rates of 0 and 15%?

Table 3.3: Undiscounted cash flow						
Time (year)	1	2	3	4	5	6
Cash flow (10^6 \$)	-5.3	-1.2	1.8	3.9	2.5	1.4

3.3 In a field development plan (FDP) it is proposed to drill 10 wells, phased as indicated in Table 3.4 below, at a cost of 5 million $ each. The wells are expected to produce according to Table 3.5, starting the year after they have been drilled. The oil company's guidelines for project screening use an oil price of 15 $/bbl and a discount rate of 15%. The asset manager challenges the FDP and states that an aggressive use of multi-lateral (ML) wells could improve the project economics. He states that 5 ML wells could give the same production as the 10 proposed wells, at a cost of 8 million $ per well. The FDP project team responds that they have looked into this option, but that the long lead time for equipment makes the proposal unattractive, because the first two wells would be delayed by a year. Make a quick re-evaluation of the two options. Disregard royalties and taxes. Make use of the ML well drilling sequence presented in Table 3.4, and the cash flow analysis for a well drilled in year 1 presented in Table 3.5. Is there a better option?

Table 3.4: Drilling sequence for conventional and ML wells			
Year	1	2	3
Conv. well	1,2	3,4,5,6	7,8,9,10
ML well	-	1,2,3	4,5

Year	Oil rate (bpd)	Yearly prod. (10^6 bbl)	Cash in (10^6 \$)	Cash out (10^6 \$)	Cash flow (10^6 \$)	Cash flow @ 15% (10^6 \$)	Cum. disc. cash flow (10^6 \$)
1	0	0.000	0	5.00	-5.00	-4.35	-4.35
2	5000	1.825	27.38		27.38	20.70	16.36
3	4800	1.752	26.28		26.28	17.28	33.63
4	2500	0.913	13.69		13.69	7.83	41.46
5	1900	0.694	10.40		10.40	5.17	46.63
6	1400	0.511	7.67		7.67	3.32	49.95
7	1000	0.365	5.48		5.48	2.06	52.01
8	700	0.256	3.83		3.83	1.25	53.26
9	500	0.183	2.74		2.74	0.78	54.04
10	400	0.146	2.19		2.19	0.54	54.58
11	350	0.128	1.92		1.92	0.41	54.99
12	300	0.110	1.64		1.64	0.31	55.30
13	300	0.110	1.64		1.64	0.27	55.57
14	300	0.110	1.64		1.64	0.23	55.80
15	300	0.110	1.64		1.64	0.20	56.00
16	300	0.110	1.64		1.64	0.18	56.18
17	300	0.110	1.64		1.64	0.15	56.33
18	300	0.110	1.64		1.64	0.13	56.46
19	300	0.110	1.64		1.64	0.12	56.58
20	300	0.110	1.64		1.64	0.10	56.68

3.4 Consider the example in Section 3.2.3. Determine the optimal time to change out the 0.102 m (4 inch) tubing for the 0.89 m (3-½ inch) tubing. How far should the oil price drop before changing out the tubing becomes unattractive at a discount rate of 12%?

4 Properties of reservoir fluids

4.1 What will be covered in this chapter?

- The most common fluid properties used in petroleum engineering.
- The pressure-temperature phase diagram, and the associated classification of reservoirs types and hydrocarbon fluids.
- Black oil and volatile oil models.
- Black oil correlations.

4.2 Fluid properties

The thermodynamic properties of reservoir fluids, like pressure, temperature, density or viscosity, can have a strong influence on the flow in a well and the production rate. An overview of the subject was given in course ta 3410 'Properties of hydrocarbons and oilfield fluids'; see Zitha and Currie (2000). For further engineering-oriented information see also Whitson and Brulé (2000), Danesh (1998), McCain (1990), Ahmed (1989) or Pedersen, Fredenslund and Thomassen (1989), while for a more theoretical treatment see Firoozabadi (1999). For a general introduction to thermodynamics see e.g. Moran and Shapiro (1998).

During the exploration and appraisal phase of an oil or gas field, determination of the fluid properties is an important activity. Fluid samples, often called *bottomhole samples*, can be collected from the bottom of the wellbore with the aid of specialized wire line tools. Also, samples can be collected from the production stream to surface if a well test is performed. Specialized laboratories perform *pressure-volume-temperature (PVT) analyses* to determine the *composition,* i.e. the type and relative quantity of each component in the fluid mixture, and the *properties* of the fluids at a wide range of pressures and temperatures. The composition is usually specified in terms of fractions of the various components per kmol or lbm-mole of fluid sample. For a good description of the reporting of other properties, see Whitson and Brulé (2000). Some important properties of the most frequently encountered reservoir fluid components have been reproduced in Tables B.1 and B.2 in Appendix B.

To analyse multi-phase flow of hydrocarbons in production systems we need to know the *state*, i.e. the thermodynamic condition, of the fluid mixture in each point of the production system. Apart from the thermodynamic properties of the components, this requires knowledge of the *phase behaviour* of the mixture. We usually distinguish three distinct *phases*: gas, oil and water, where we consider oil and water as different phases because they are immiscible. In this course we will not consider the effect of the presence of a solid phase as may occur when e.g. asphaltenes or waxes are present. To what extent the various components of a reservoir fluid mixture are in the liquid or the gas phase is fully determined by the composition of the mixture, and a minimal set of fluid properties, the *state variables*: pressure, volume and temperature. The state variables are related to each other through an *equation of state* (EOS), an algebraic relationship that will be discussed in more detail in Section 4.4 below. Therefore it suffices to know only two of the three variables to completely specify the state of an oil-gas mixture.

It is customary to specify fluid properties at a reference state. In the E&P industry, this is done through the definition of a reference pressure and temperature, known as *standard conditions*: a pressure p_{sc} = 100 kPa (14.7 psi) and a temperature T_{sc} = 15 °C (60 °F), which can be considered as typical for atmospheric conditions in temperate climates. Oil at standard conditions is often referred to as *stock tank oil*, gas at surface conditions sometimes as *stock tank gas*. The term *separator gas* usually refers to gas at a slightly higher than atmospheric pressure, and should not be confused with gas at standard conditions. The fluid properties that are of most interest for production engineering calculations are:

- *Oil density at standard conditions $\rho_{o,sc}$.* In SI units, this is the density of the oil in kg/m^3. In field units, oil density is usually specified by the oil specific gravity γ_o, which is the density of the oil relative to that of pure water, both measured at standard conditions; $\rho_{w,sc}$ = 999 kg m^{-3} (62.4 lbm ft^{-3} or 8.34 lbm gal^{-1}). However it is common to also use the API gravity γ_{API}, which is related to the specific gravity as $\gamma_o = 141.5 / (131.5 + \gamma_{API})$, and therefore to the density as $\rho_o = 141.5 * 10^3 / (131.5 + \gamma_{API})$.

- *Gas density at standard conditions $\rho_{g,sc}$ or gas specific gravity γ_g.* The latter is the density of the gas relative to air, both measured at standard conditions; $\rho_{air,sc}$ =1.23 kg m^{-3} (76.3 * 10^{-3} lbm ft^{-3}). This is equal to the ratio of the gas *molar mass M* to the molar mass of air; M_{air} = 28.97 kg kmol^{-1} (lbm lbm-mole^{-1}).

- *Water density at standard conditions $\rho_{w,sc}$ or water specific gravity γ_w,* which is the density of the formation water relative to that of pure water, both measured at standard conditions. The formation water will contain many dissolved salts. An equivalent measurement is therefore the NaCl equivalent water salinity.

- *Bubble point pressure p_b.* This is the pressure at which first gas is formed when oil is subjected to a decreasing pressure at a given temperature. If the pressure at the top of a reservoir is above the bubble point pressure, all gas is dissolved in the oil. However, if the top part of the reservoir is below bubble point pressure, a gas cap exists, and the oil is *gas-saturated*. The bubble point pressure is therefore also known as the *saturation pressure*. Going deeper down in the reservoir, the pressure increases, and when the bubble point pressure is reached we encounter the gas-oil contact (GOC).

- *Solution gas-oil ratio R_s.* This is the volume of stock tank gas which will dissolve in a unit volume of stock tank oil when both are transferred to the given pressure and temperature conditions. R_s, which is also referred to as *gas solubility*, is a ratio of volumes, and hence dimensionless, but it is dependent on the choice of units (m^3/m^3 or scf/stb). The abbreviation 'scf' indicates 'standard cubic feet' or 'ft^3 at standard conditions'; 'stb' indicates 'standard barrel' or 'bbl at standard conditions'.

- *Producing gas-oil ratio R_p.* This is the volume of stock tank gas which will dissolve in a unit volume of stock tank oil when both are transferred to bubble point pressure at reservoir temperature. The producing gas-oil ratio (GOR) R_p is therefore equal to the solution GOR R_s at (or above) bubble point pressure and at reservoir temperature. Just like R_s, R_p is a ratio of volumes, and hence dimensionless, but dependent on the choice of units (m^3/m^3 or scf/stb). R_p can be determined from a laboratory analysis of a bottomhole sample in a so-called *separator test* or *flash test* where oil at bubble point pressure and reservoir temperature is brought to standard conditions. Oil with a very low producing GOR is often referred to as *dead oil*. The same indication is also used for oil after it has released its gas during the separation process at surface.

- *Solution oil-gas ratio r_s.* This is the volume of stock tank oil which will vaporize in a unit volume of stock tank gas, when both are transferred to the given pressure and temperature conditions. The oil-gas ratio (OGR) plays an important role in the production of *gas-condensates*, and is therefore also referred to as *solution condensate-gas ratio* or simply *condensate-gas ratio* (CGR). Also r_s is a ratio of volumes, and hence dimensionless, but it is dependent on the choice of units (m^3/m^3 or stb/scf).

- *Producing oil-gas ratio r_p.* In analogy to the producing GOR, this is the volume of stock tank oil (or condensate) which will vaporize in a unit volume of stock tank gas, when both are transferred to the dew point pressure at reservoir temperature. The producing OGR r_p is therefore equal to the solution OGR r_s at (or above) dew point pressure and at reservoir temperature. The same comments on dimensions apply as were made for r_s. Gas

with a very low producing OGR is referred to as *dry gas.* Note that the same indication is also used for gas after it has been dried during processing at surface.

- *Oil formation volume factor B_o.* This is the volume occupied by one stock tank unit volume of oil, transferred to another condition with a given pressure p and temperature T, where it will include dissolved gas. In reservoir engineering, B_o is usually specified at reservoir conditions p_R and T_R, but in production engineering, B_o may also be specified at other conditions that occur in between the reservoir and the separator. B_o is a ratio of volumes, and hence dimensionless, and, unlike the GOR and OGR, it is *in*dependent of the choice of units (m^3/m^3 or bbl/stb).

- *Gas formation volume factor B_g.* This is the volume occupied by a unit volume of gas at standard conditions, transferred to another condition with a given pressure p and temperature T, where it will include the oil that was present as condensate at standard conditions. B_g is also a dimensionless ratio of volumes, but in field units different definitions can be used, leading to a dependency on the choice of units (m^3/m^3, ft^3/scf, or bbl/scf).

- *Water formation volume factor B_w.* Not surprisingly, this is the volume occupied by a unit volume of water at standard conditions, transferred to another condition with a given pressure p and temperature T. Also B_w is dimensionless, but independent of the choice of units (m^3/m^3 or bbl/stb). B_w usually has a value very close to one, because of the low compressibility and low gas solubility capacity of water.

- *Oil, gas and water viscosities*: Usually the dynamic viscosities are used, with SI units Pa s or field units cp. The viscosities are strongly varying functions of temperature.

- *Interfacial tensions σ_{og}, σ_{ow}, σ_{gw}.* These quantities, in theory, play a role in multi-phase flow behaviour in production systems, however to a much lesser extent than in flow through porous media. They occasionally occur in models for multi-phase flow through pipes.
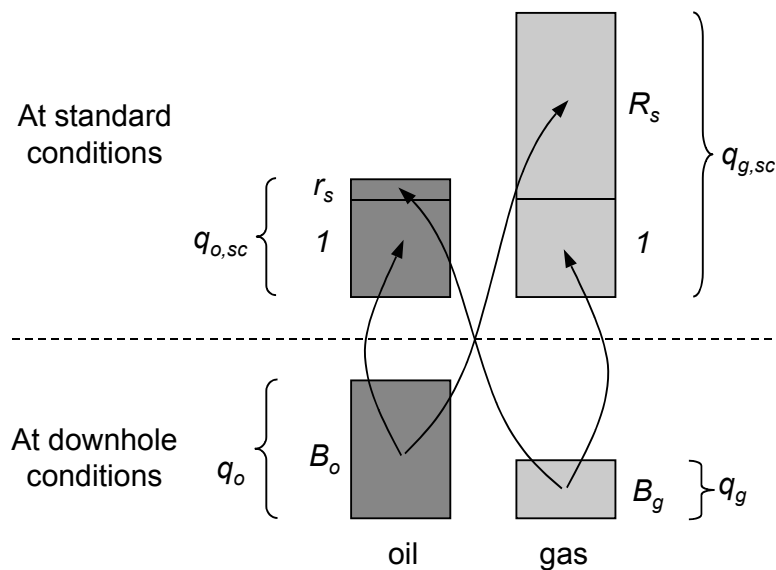

Figure 4.1: Oil and gas volume flows at different pressures.

A simple interpretation of the oil and gas formation volume factors is depicted in Figure 4.1. When an amount of B_o m^3 of oil at downhole conditions is brought to surface it yields one m^3 of stock tank oil, and R_s m^3 of stock tank gas. Or, when one m^3 of oil at downhole conditions is brought to surface it yields $1/B_o$ m^3 of stock tank oil and R_s/B_o m^3 of stock tank gas. Although the oil itself slightly expands under reducing pressure, the escaping gas makes the oil effectively shrink when it comes to surface. Therefore the ratio $1/B_o$ is known as the *shrinkage factor*, where $1/B_o < 1$. Similarly, when an amount of B_g m^3 of gas at downhole conditions is brought to surface it yields one m^3 of stock tank gas, and r_s m^3 of stock tank oil (condensate). Even at large amounts of condensate drop-out, the gas still expands so much under reducing pressure, that the ratio $1/B_g$ is always much larger than one. In gas engineering it is common practice to use the symbol E to indicate this gas *expansion factor*: $E = 1/B_g$, where E and B_g are both expressed in m^3/m^3 or ft^3/ft^3.

Related to the fluid properties R_s, R_p, r_s and r_p defined above are two frequently used *process parameters*:

- *Gas-oil ratio R_{go}.* This is the ratio of the gas and oil *flow rates* measured at surface during actual production: $R_{go} = q_{g,sc} / q_{o,sc}$. If water is present in the production stream we can extend the concept of the GOR to a gas-liquid ratio (GLR) $R_{gl} = q_{g,sc} / (q_{o,sc} + q_{w,sc})$. These quantities are also referred to as the actual GOR and GLR, or, confusingly, as the producing GOR and GLR. When producing oil from a reservoir above bubble point pressure, R_{go} will be identical to R_p, and therefore to R_s at bubble point pressure and reservoir temperature. However, if the reservoir is below bubble point pressure, *free gas* may be produced from the gas cap together with the *associated gas* that is released from the oil during its travel up the wellbore, and R_{go} may be considerably above R_p. In general, when reservoir engineers refer to the producing GOR, they mean R_p, i.e. the fluid property. When production engineers refer to the producing GOR, they usually mean R_{go}, i.e. the process parameter.

- *Oil-gas ratio r_{og}.* In analogy to the GOR, this is the ratio of the oil and gas flow rates measured at surface: $r_{og} = q_{o,sc} / q_{g,sc}$. As mentioned before, the OGR plays an important role in the production of gas-condensates, and is therefore also referred to as CGR. The same comments on dimensions apply as were made for r_s.

A third frequently used process parameter concerns the combined production of water and oil:

- *Water-oil ratio R_{wo}.* This is the volume of water produced at surface together with a unit volume of oil, both measured at standard conditions, or, in terms of flow rates: $R_{wo} = q_{w,sc} / q_{o,sc}$. An alternative measure is the *watercut*: the fraction (or percentage) of water in the total volume of produced liquids (oil and water) measured at standard conditions: $f_{w,sc} = q_{w,sc} / (q_{o,sc} + q_{w,sc})$. Both measures are dimensionless, and independent on the choice of units (m^3/m^3 or stb/stb). Oil with a zero or very low water-oil ratio (WOR) is often referred to as *dry oil*. Sometimes the concept of *base sediment and water* (BSW) is used to indicate the amount of solids and water as a fraction of the total amount of solids and liquids in the wellbore flow. Because the amount of solids is usually very low, the BSW value is in practice almost identical to the watercut.

4.3 Pressure-temperature phase diagram

Figure 4.2 displays the *phase diagram* for a hydrocarbon mixture. To the left of the *bubble-point line*, the system acts as a single phase liquid and all the gas is dissolved. To the right of the *dew-point line* the system acts as a gas. Moving from left to right at a pressure above the *cricondenbar* we experience a gradual transition from liquid to gas. However, if the bubble-point line is crossed when coming from the liquid phase, gas is liberated to form a two-phase

system. Moving further towards the dew point line, an increasing amount of gas comes out of solution. Conversely, if the dew point line is crossed when coming from the gas phase, liquid condenses. At the *critical point*, the distinction between liquid and gas cannot be made, because at that particular pressure and temperature the liquid and gas phases have identical densities. Also shown in Figure 4.2 is the classification of reservoir types based on this diagram.

- *Undersaturated oil reservoirs* have initial pressures above the bubble point line and temperatures to the left of the critical point. During production of a reservoir, the reservoir pressure will drop while the reservoir temperature remains unchanged. This can be represented by a vertical line in *p-T* space. When the line crosses the bubble point line, gas is liberated and a gas cap is formed.
- *Saturated oil reservoirs* or *gas cap reservoirs* have initial pressures already below the bubble point line.
- *Gas-condensate reservoirs* have initial pressures above the dew point line, and initial temperatures between the critical temperature and the *cricondentherm*. During production of a gas-condensate reservoir, condensation occurs when the pressure drops below the dew point line. This effect, which is called *retrograde condensation*., may seem somewhat counter-intuitive because we usually experience condensation when the pressure of a gas-liquid mixture increases rather than decreases. Although it appears from the phase diagram that at even lower pressures the condensate would return to the gas phase again, this is usually not the case. Because the condensed liquids are much less mobile than the gas, they stay behind in the matrix while the gas is produced. As a result, the reservoir fluid composition changes and the entire phase diagram changes its form and moves to the right such that vaporization of the remaining condensate will never occur.
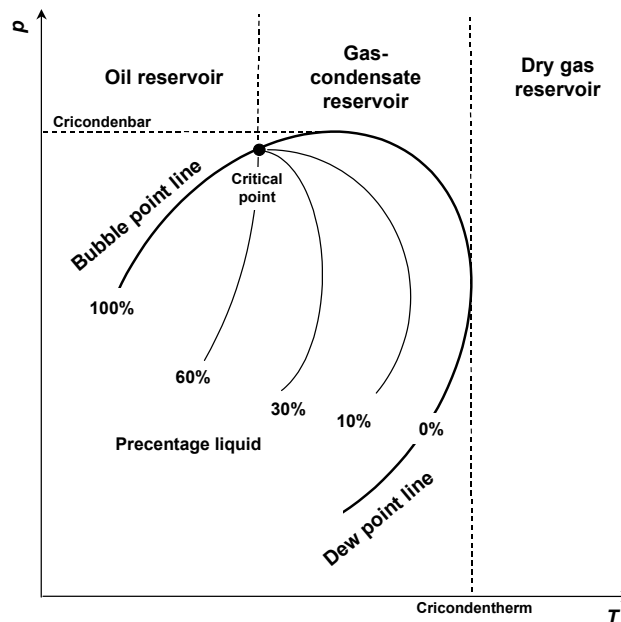- *Dry gas reservoirs* have temperatures to the right of the cricondentherm and do not experience this problem.

Figure 4.2: Phase diagram for a hydrocarbon system.

Using a similar terminology but a slightly different classification, we can distinguish four categories of hydrocarbon fluids:

- *Black oil*: oil for which the producing gas-oil ratio $R_p < 350$ m^3/m^3 (about 2000 scf/stb).
- *Volatile oil*: oil for which the producing gas-oil ratio $R_p > 350$ m^3/m^3 (about 2000 scf/stb).
- *Gas condensate*: gas-condensate for which the producing condensate-gas ratio $r_p > 30$ m^3/million m^3 (about 5 stb/million scf).
- *Dry gas*: a gas or gas/condensate for which the producing condensate-gas ratio $r_p < 30$ m^3/million m^3 (about 5 stb/million scf).

As shown in Figure 4.3, when oil flows up the production tubing, it follows a path in *p-T* space in which gas is liberated and expands as it goes up the tubing. As a result, the amount of liquid decreases, so there is a shrinkage in the volume of oil. Furthermore, unlike the pressure drop in the reservoir, which is isothermal, the pressure drop in the tubing is accompanied by a drop in temperature. When producing from a gas reservoir, this may result in condensation of liquids and the formation of *wet gas*.

4.4 Equations of state

4.4.1 Vapour-liquid equilibrium

As discussed in Section 4.2, an *equation of state* (EOS) specifies an algebraic relationship between state variables. More specifically, we address the relationship between pressure, volume and temperature. With the aid of such an EOS, all properties of hydrocarbon mixtures as required in production engineering can be determined, provided an accurate compositional description is available from laboratory experiments on fluid samples. In particular, we can use an EOS to determine the so-called *equilibrium factors* (*K* values) that are needed to describe the equilibrium between components in the liquid and the vapour phase. The *K* values allow us to compute the composition of the liquid and the gas phases in a multi-phase fluid mixture at any given pressure and temperature. These so called *flash calculations* or *liquid-liquid equilibrium (VLE) calculations* that use an EOS to determine the *K* values, require a level of numerical computation outside the scope of this course. For more information on the EOS-based approach, see Whitson and Brulé (2000), Danesh (1998) or Firoozabadi (1999).
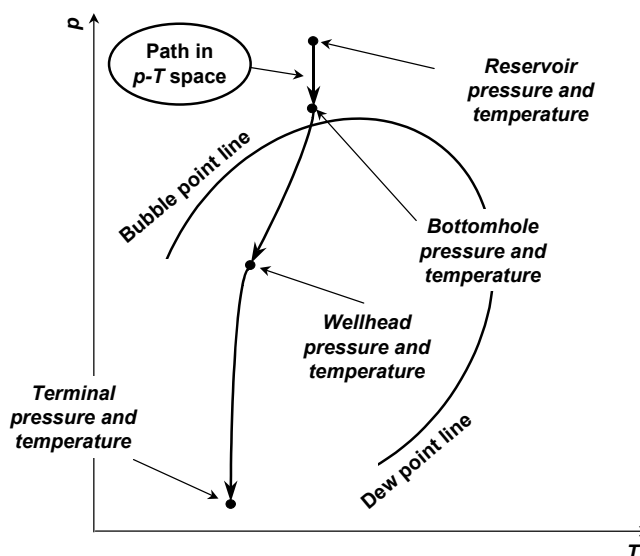

Figure 4.3: Path in p-T space as the oil/gas mixture flows from the reservoir to the terminal.

4.4.2 Single-phase gas compressibility

Another use of an EOS is to describe the change in volume of oil or gas under changing pressure and temperature. The relationship between the properties of an *ideal gas* follow from the EOS known as the ideal gas law which can be expressed as

$$pV = nRT_{abs} \quad \text{or} \quad pV = \frac{mRT_{abs}}{M} \quad \text{or} \quad \frac{p}{\rho_g} = \frac{RT_{abs}}{M} \; . \qquad (4.1, 4.2, 4.3)$$

where

p is pressure, Pa, (psia),
V is volume, m^3, (ft^3)
n is the amount of gas, kmol, (lbm-mole)
R is the universal gas constant equal to 8314 J K^{-1} kmol^{-1}, (10.73 psia ft^3 °R^{-1} lbm-mole^{-1}),
T_{abs} is absolute temperature K, (°R),
m is mass, kg, (lbm),
ρ_g is gas density, kg m^{-3}, (lbm ft^{-3})
M is molar mass, kg kmol^{-1}, (lbm (lbm-mole)$^{-1}$).

See Section A.5 of Appendix A for the numerical relationship between the *molar mass M*, which is also known as the *molecular weight*, the specific gravity γ_g and the density $\rho_{g,sc}$.

The ideal gas law is only valid at pressures much below those normally encountered in the E&P industry. Approximate relationships valid at higher pressures are given by

$$pV = nZRT_{abs}, \quad \text{or} \quad pV = \frac{mZRT_{abs}}{M} \quad \text{or} \quad \frac{p}{\rho_g} = \frac{ZRT_{abs}}{M} \; , \qquad (4.4, 4.5, 4.6)$$

where Z is the *gas deviation factor,* also known as the *gas compressibility factor* or simply the *Z factor*. Correlations developed by Standing and Katz (1942) are normally used to extend this relationship to hydrocarbon gas mixtures; see Appendix B. An expression for the gas formation volume factor follows from the gas law for non-ideal gasses as:

$$B_g = \frac{q_g}{q_{g,sc}} = \frac{V_g}{V_{g,sc}} = \frac{\rho_{g,sc}}{\rho_g} = \frac{p_{sc} T_{abs} Z}{p T_{sc,abs} Z_{sc}} \; . \qquad (4.7)$$

4.4.3 Single-phase oil compressibility

Oil compressibility is usually described with the aid of an experimentally determined compressibility coefficient that is itself a function of pressure, temperature and composition. The large heat capacity of an oil reservoir allows the assumption that oil expansion in the reservoir during production is an iso-thermal process. When flowing through the wellbore to surface, the fluid mixture gradually cools down, but it is often still assumed that the expansion occurs iso-thermally, although with a compressibility coefficient that gradually changes with decreasing pressure and temperature. The iso-thermal oil compressibility coefficient c_o is defined as the (negative) increase in volume per unit of pressure, $-\partial V/\partial p$, per unit of volume V, at constant temperature T:

$$c_o(p) = -\frac{1}{V} \left(\frac{\partial V}{\partial p} \right)_T \; . \qquad (4.8)$$

An empirical correlation for c_o is given in Section B.2.5 in Appendix B. Equation (4.8) can be interpreted as a differential equation in V and p that allows for separation of variables:

$$\frac{\partial V}{V} = -c_o(p)\partial p .\tag{4.9}$$

We define a 'boundary condition' by specifying that $V(p_{ref}) = V_{ref}$, and assume that the dependence of c_o on p is small enough to linearize the right-hand side of equation (4.9). The solution can then be written as:

$$V = V_{ref} \exp\left[-c_o\left(p - p_{ref}\right)\right] .\tag{4.10}$$

Remembering that c_o is a function of p and T, equation (4.10) can be interpreted as an equation of state which describes the PVT behaviour of single-phase oil. Because the density ρ_o is inversely proportional to the volume V we can also write equation (4.10) as

$$\rho_o = \rho_{o,ref} \exp\left[c_o\left(p - p_{ref}\right)\right] .\tag{4.11}$$

A natural choice for the reference pressure p_{ref} is the bubble point pressure at temperature T, leading to

$$\rho_o = \rho_{ob} \exp\left[c_o\left(p - p_b\right)\right] \text{ for } p > p_b,\tag{4.12}$$

where the values of p_b and ρ_{ob} can be determined from laboratory experiments or from empirical correlations as discussed in Appendix B. For pressures above the bubble point pressure the oil formation volume factor is therefore given by:

$$B_o = \frac{V_o}{V_{o,sc}} = \frac{\rho_{o,sc}}{\rho_o} = \frac{\rho_{o,sc}}{\rho_{ob}} \exp\left[-c_o\left(p - p_b\right)\right] = B_{ob} \exp\left[-c_o\left(p - p_b\right)\right].\tag{4.13}$$

4.4.4 Multi-phase gas and oil compressibility

For a multi-component oil-gas mixture, the prediction of PVT properties, and therefore of the formation volume factors B_g and B_o, can be performed by combining a compositional analysis with a semi-empirical EOS. However, in this course we will follow a simpler approach as described in the following section.

4.5 *Oil models*

4.5.1 Compositional models

In a compositional model of a two-phase hydrocarbon mixture, the composition of the liquid and the gas phase are functions of pressure and temperature and need to be determined with flash calculations using an EOS. Hydrocarbon mixtures may consist of many tens of components, and a full compositional analysis taking into account all components would be very time consuming. Furthermore, it is often quite difficult to accurately establish the amount and the properties of all components, in particular those with a high molar mass, the so called the *heavy fractions*. Therefore it is customary to lump these into a *pseudo component*. This is typically done for heptane and all heavier fractions, in which case the pseudo component is referred to as C_{7+}. In its most simple form, a compositional model consists of only two pseudo components, one for the lighter and one for the heavier hydrocarbons, usually referred to as *heavies* and *lights*. Such a *two-component model* or *binary mixture model* is too crude to accurately describe the behaviour of gas-condensate systems. However, it is usually sufficient to describe the behaviour of black oils or even volatile oils.

4.5.2   Volatile oil model

The *volatile oil model* is a two-component model, that accounts for compositional variations in both the liquid and the gas phase. The pseudo components in the volatile oil model are stock tank oil and stock tank gas which can each be characterized with a single parameter only: $\rho_{o,sc}$ and $\rho_{g,sc}$ (or γ_g) in SI units, or γ_o (or γ_{API}) and γ_g in field units. The change in state with changing pressure and temperature is then described in terms of the change in densities of the oil and gas phases, with the aid of the oil and gas formation volume factors B_o and B_g and the solution gas-oil and oil-gas ratios R_s, and r_s. With the aid of Figure 4.1 we can derive the mass balance equations for oil and gas that are brought from downhole conditions to standard conditions:

$$B_o \rho_o = \rho_{o,sc} + R_s \rho_{g,sc} \; ,$$
$$B_g \rho_g = \rho_{g,sc} + r_s \rho_{o,sc} \; , \qquad\qquad (4.14, 4.15)$$

which give us the required expressions in terms of densities:

$$\rho_o = \frac{\rho_{o,sc} + R_s \rho_{g,sc}}{B_o} \text{ and } \rho_g = \frac{r_s \rho_{o,sc} + \rho_{g,sc}}{B_g} \; . \qquad (4.16, 4.17)$$

Since B_g, B_o, R_s and r_s are functions of pressure and temperature, equations (4.16) and (4.17) can be interpreted as equations of state. They can be conveniently written in matrix form, and if we also include the water density this results in

$$
\begin{bmatrix} \rho_g \\ \rho_o \\ \rho_w \end{bmatrix} =
\begin{bmatrix} \dfrac{1}{B_g} & \dfrac{r_s}{B_g} & 0 \\ \dfrac{R_s}{B_o} & \dfrac{1}{B_o} & 0 \\ 0 & 0 & 1 \end{bmatrix}
\begin{bmatrix} \rho_{g,sc} \\ \rho_{o,sc} \\ \rho_{w,sc} \end{bmatrix}
\text{ or }
\begin{bmatrix} \rho_{g,sc} \\ \rho_{o,sc} \\ \rho_{w,sc} \end{bmatrix} =
\begin{bmatrix} \dfrac{B_g}{1-R_s r_s} & \dfrac{-B_o r_s}{1-R_s r_s} & 0 \\ \dfrac{-B_g R_s}{1-R_s r_s} & \dfrac{B_o}{1-R_s r_s} & 0 \\ 0 & 0 & 1 \end{bmatrix}
\begin{bmatrix} \rho_g \\ \rho_o \\ \rho_w \end{bmatrix} , \quad (4.18, 4.19)
$$

where we have assumed that $B_w = 1$, which implies that gas solubility, compressibility, and thermal expansion for water are so small that they can be neglected. The inverse relationship (4.19) has been obtained with the aid of Cramer's rule for inversion of a matrix. We can use Figure 4.1 to derive similar matrix expressions for the volume flow rates, resulting in

$$
\begin{bmatrix} q_{g,sc} \\ q_{o,sc} \\ q_{w,sc} \end{bmatrix} =
\begin{bmatrix} \dfrac{1}{B_g} & \dfrac{R_s}{B_g} & 0 \\ \dfrac{r_s}{B_o} & \dfrac{1}{B_o} & 0 \\ 0 & 0 & 1 \end{bmatrix}
\begin{bmatrix} q_g \\ q_o \\ q_w \end{bmatrix}
\text{ or }
\begin{bmatrix} q_g \\ q_o \\ q_w \end{bmatrix} =
\begin{bmatrix} \dfrac{B_g}{1-R_s r_s} & \dfrac{-B_g R_s}{1-R_s r_s} & 0 \\ \dfrac{-B_o r_s}{1-R_s r_s} & \dfrac{B_o}{1-R_s r_s} & 0 \\ 0 & 0 & 1 \end{bmatrix}
\begin{bmatrix} q_{g,sc} \\ q_{o,sc} \\ q_{w,sc} \end{bmatrix} . \quad (4.20, 4.21)
$$

Determination of the values of B_g, B_o, R_s and r_s as a function of pressure and temperature is usually done with the aid of PVT tests and compositional analysis. This is outside the scope of our course, and therefore we will only use an even further simplified model, as described in the following section. Several varieties of the volatile oil model have been developed, sometimes under the name *modified black oil model*; see Whitson and Brulé (2000) for an overview.

4.5.3 Black oil model and black oil correlations

A further simplified model of two-phase hydrocarbon mixture behaviour is the so-called *black oil model*. The black oil model is also a two-component model, which, however, assumes a constant composition of the gas phase and only accounts for compositional variations in the liquid phase. The relevant equations of the model follow directly from those of the volatile oil model by substitution of $r_s = 0$.

During the early development phase of an oil field no fluid samples may be available. In that case it is necessary to fall back on *correlations*, which are relationships for 'typical' oil and gas compositions, based on experimental data. Especially for black oils such correlations can be quite accurate. In addition, production engineering calculations based on correlations require much less computational effort than calculations based on compositional analysis using an EOS. Therefore, *black oil correlations* are widely used. However, to describe the behaviour of volatile oil or gas-condensate systems, correlations are of very limited value, and performance of PVT analyses on fluid samples is essential to allow proper compositional calculations.

The standard reference for black oil correlations is Standing (1952). Many other correlations have been developed over the past half century, and a few have been reproduced in Appendix B of these lecture notes. An extensive overview is given in Appendix B of Brill and Mukherjee (1999), while further information can be found in the references mentioned in Section 4.2 above.

4.6 Exercises

For exercises 4.1 to 4.5, you should use the oil and gas correlations given in Appendix B. The correlations have been programmed in MATLAB routines which are available from Blackboard; see the file 'Fluid properties.zip'. However, the exercises can also be performed by hand calculation.

4.1 An oil reservoir has a pressure of $p_R = 17$ MPa and a temperature of 76 °C. The bubble point pressure of the oil is $p_b = 19.5$ MPa. The gas and oil densities at standard conditions are $\rho_g = 1.11$ kg/m^3 and $\rho_o = 910$ kg/m^3. What is the solution GOR?

4.2 Refer to question 4.1 above. What is the specific gravity of the gas produced at surface? And what is the density of the gas-cap gas just above the GOC in the reservoir?

4.3 Refer to question 4.1 above. What are the oil and gas viscosities if the reservoir pressure is 22 MPa and all other parameters remain the same?

4.4 Refer to question 4.3 above. What is the compressibility coefficient c_o of the oil?

4.5 Consider a well that produces dry oil with a GOR R_{go} of 250 m^3/m^3. The production history shows no indication of free gas production. The density of the gas and oil at standard conditions are given by $\rho_{g,sc} = 1.02$ kg m^{-3} and $\rho_{o,sc} = 805$ kg m^{-3}. What is the oil formation volume factor at the following pressure and temperature combinations: $p = 15$ MPa and $T = 85$ °C, and $p = 30$ MPa and $T = 105$ °C?

5   Single-phase flow in wells and pipelines

5.1   *What will be covered in this chapter?*

- A derivation of the governing equations for single-phase gas and liquid flow.
- The Moody diagram for friction forces in pipe flow.
- Pressure drop analysis of single-phase oil and gas flow with MATLAB.
- Analytical approximations for the pressure drop in wells or pipelines.

5.2   *Governing equations*

5.2.1   Mass balance, momentum balance and equation of state

In this section we will derive the equations for single-phase fluid flow in a pipeline, flowline or wellbore under the assumption that the temperature profile along the conduit is known. For a detailed treatment of the nature of the equations, see e.g. Bird, Stewart and Lightfoot (2002), or Bobok (1993) who also treat the case where the temperature is not known in advance.

Consider a section of an inclined pipeline with constant cross-sectional area; see Figure 5.1. We can write the mass balance per unit time for the section as:

$$\underbrace{A\rho v}_{\text{mass in}} \; - \; \underbrace{A\left(\rho+\frac{\partial\rho}{\partial s}ds\right)\left(v+\frac{\partial v}{\partial s}ds\right)}_{\text{mass out}} \; = \; \underbrace{A\frac{\partial\rho}{\partial t}ds}_{\text{mass accumulated}} \;, \tag{5.1}$$

where

    A is the cross-sectional area of the pipe, m^2,
    ρ is the fluid density, $kg\,m^{-3}$,
    v is the fluid velocity averaged over the cross-section, $m\,s^{-1}$,
    s is the co-ordinate along the pipe, m, and
    t is time, s.

Initially we assume that the fluid velocity is always positive, i.e. that the fluid always flows in the positive co-ordinate direction. The momentum balance can then be written as:

$$\underbrace{A\rho v^2}_{\text{momentum in}} \; - \; \underbrace{A\left(\rho+\frac{\partial\rho}{\partial s}ds\right)\left(v+\frac{\partial v}{\partial s}ds\right)^2}_{\text{momentum out}} \; + \; \underbrace{Ap - A\left(p+\frac{\partial p}{\partial s}ds\right)}_{\text{pressure forces}} \; +$$

$$\underbrace{F_g(\rho,s)ds}_{\text{gravity force}} \; + \; \underbrace{F_f(\rho,\mu,v)ds}_{\text{friction force}} \; = \; \underbrace{A\frac{\partial(\rho v)}{\partial t}ds}_{\text{momentum accumulated}} \;, \tag{5.2}$$

where

    p is the pressure, Pa,
    $F_g(\rho,s)$ is the gravity force per unit length, $N\,m^{-1}$,
    $F_f(\rho,\mu,v)$ is the friction force per unit length, $N\,m^{-1}$, and
    μ is the dynamic viscosity, Pa s.

The nature of the gravity force $F_g(\rho,s)$ and the friction force $F_f(\rho,\mu,v)$ will be discussed in more detail in Sections 5.2.2 and 5.2.3 below. The viscosity μ is a known function of pressure and temperature, where the temperature is a known function of s. A third equation for the remaining unknown variables ρ, v and p is given by the equation of state for the fluid. For

example, if we consider the flow of single-phase gas, we can use equation (4.6) derived in Section 4.4, while for single-phase oil flow we can use equation (4.11). If we expand equations (5.1) and (5.2), drop all terms higher than first order in the differentials, and simplify the results, we can write the three equations as

$$
\left\{
\begin{array}{l}
\dfrac{\partial(\rho v)}{\partial s} = -\dfrac{\partial \rho}{\partial t} \ , \\[3mm]
\dfrac{\partial(\rho v^2)}{\partial s} = -\dfrac{\partial(\rho v)}{\partial t} - \dfrac{\partial p}{\partial s} + \dfrac{F_g}{A} + \dfrac{F_f}{A} \ , \\[3mm]
\rho = \dfrac{Mp}{ZRT_{abs}} \ \text{for gas}, \ \text{or} \\[3mm]
\rho = \rho_{o,ref} \ \exp\!\left[c_o \left(p - p_{ref} \right) \right] \ \text{for oil} ,
\end{array}
\right.
\qquad (5.3, 5.4, 5.5, 5.6)
$$

where the compressibility c_o and the gas deviation factor Z are known functions of p and T, while, as discussed above, T itself (and therefore also T_{abs}) is a known function of s.
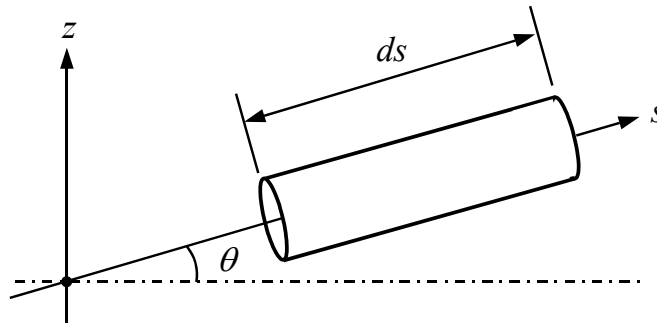
Figure 5.1: Segment of an inclined pipeline.

5.2.2 Gravity force

The gravity force is defined as

$$
F_g \left(\rho, s \right) = -\rho g \sin \theta (s) ds \ , \qquad (5.7)
$$

where

g is the acceleration of gravity, m s^{-2}, and

$\theta(s)$ is the pipeline *inclination*, rad.

In pipeline engineering, the inclination θ is defined as the angle of the pipeline axis with the respect to the horizontal plane. The term $\sin \theta$, which can be positive or negative, is therefore a measure of the change in *elevation* z of the pipeline axis per unit length of *measured distance s*. The inclination is usually known as a function of *s*, either theoretically as one of the design parameters of the pipeline, or actually from measured data obtained during a *pipeline survey*.

In well engineering it is common practice to define the wellbore geometry with a slightly different set of parameters, see Figure 5.2. The inclination α of the well is defined as the angle between the wellbore axis an the vertical direction. The term $\cos \alpha$ is therefore a measure of the change in *true vertical depth z*, which is measured downwards, per unit length of *s*, which is now known as *along hole depth*, or *measured depth*, and naturally is also

positive in downward direction. As a result of the different definition of the inclination, and because s is positive going downwards, the gravity force follows as

$$F_g(\rho, s) = \rho g \cos \alpha(s) ds ,$$ (5.8)

Note that the choice for a downward positive direction of s also implies that wellbore flow to surface has a negative velocity. We will therefore use the sign convention that flow rates related to oil, gas or water production have a negative sign, whereas alll flow rates related to injection are positive. We will use this convention for flow in pipelines, flowlines, wellbores and the near-wellbore area in the reservoir.

5.2.3 Friction force

The frictional loss for single-phase flow in pipes with a circular cross section can be expressed as; see e.g. Brill and Mukherjee (1999):

$$\frac{F_f(\rho, v, s)}{A} = -\frac{\rho}{2d} f(\mu, \rho, v) * v|v| = -\frac{8\rho}{\pi^2 d^5} f(\mu, \rho, v) * q|q| ,$$ (5.9)

where

d is the inside diameter of the pipe, m,
f is the dimensionless Moody (1944) *friction factor*, and
$q = v/A$ is the flow rate, m^3 s^{-1}.

Note the use of the absolute sign in the definition of the friction force: the dependency of the friction force on $-v|v|$ (or $-q|q|$) implies that it is always pointing in a direction opposite to the velocity (or the flow rate). The friction factor f is a function of μ, ρ and v (or q) through its dependence on the Reynolds number N_{Re} which is defined as

$$N_{Re} = \frac{\rho d|v|}{\mu} = \frac{4}{\pi} \frac{\rho|q|}{\mu d} ,$$ (5.10)

where, as discussed before, we assume that μ is a known function of p and $T(s)$. N_{Re} is also a function of the dimensionless pipe roughness ε, defined as
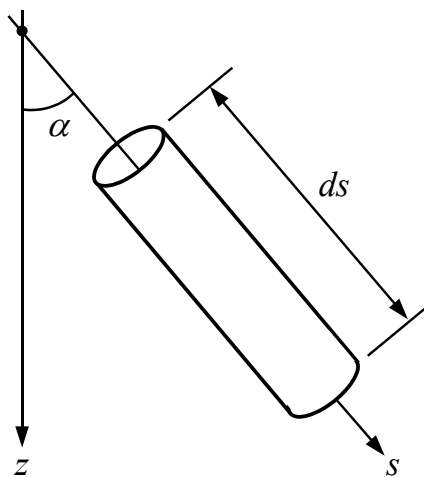
Figure 5.2: Segment of a deviated well.

$$\varepsilon = \frac{e}{d}, \tag{5.11}$$

where e is the pipe roughness expressed in m, which we assume to be a constant. For Reynolds numbers lower than 2000 the flow is laminar, and f is given explicitly by

$$f = \frac{64}{N_{Re}}, \tag{5.12}$$

while for Reynolds numbers larger than 3000 the flow is turbulent and f is given implicitly by the Colebrook (1939) equation:

$$\frac{1}{\sqrt{f}} = 1.74 - 2\log_{10}\left(2\varepsilon + \frac{18.7}{N_{Re}\sqrt{f}}\right). \tag{5.13}$$

Figure 5.3 displays the change of friction factor f with increasing Reynolds number N_{Re} for various values of the dimensionless roughness ε. For flow in the intermediate regime, characterized by Reynolds numbers between 2000 and 3000, we can use a linear interpolation between equations (5.12) and (5.13). The figure has been generated with the aid of the MATLAB file Moody_friction_factor.m.

5.3 Pressure drop analysis

5.3.1 Pressure drop components

Equations (5.3) and (5.4) can be combined and rewritten in terms of pressure drop per unit length $\partial p/\partial s$. If we furthermore restrict the analysis to steady-state flow, in other words if we
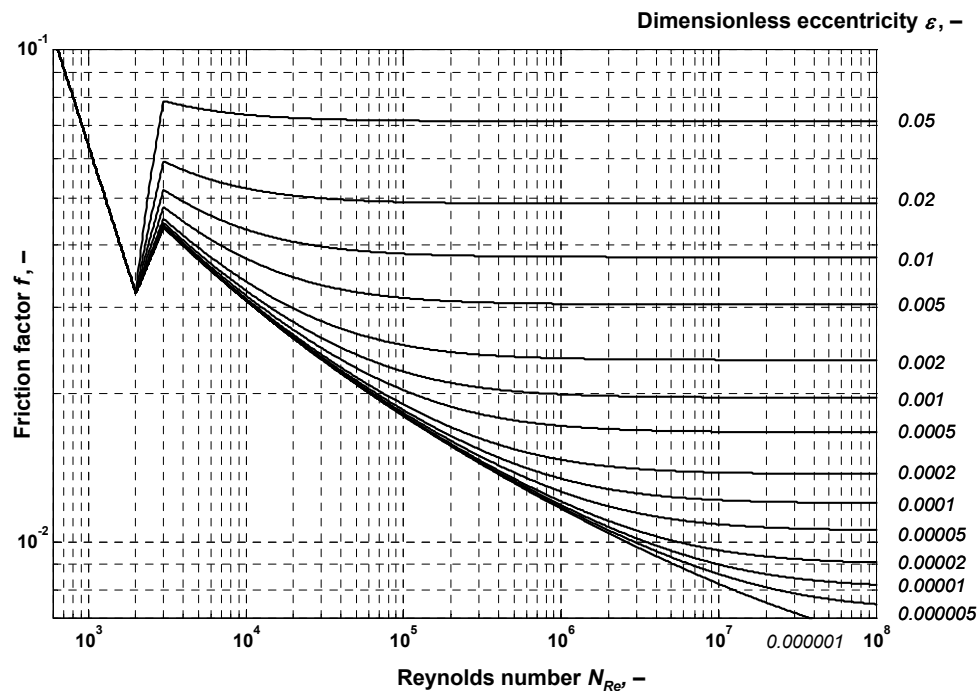
Figure 5.3: Friction factor f as function of Reynolds number N_{Re} for various values of dimensionless roughness ε.

assume that ρ, v and p are only functions of s and not of t, this pressure drop equation can be written as

$$\frac{dp}{ds} = \underbrace{-\rho g \sin\theta}_{\text{head loss}} \; - \; \underbrace{\frac{\rho}{2d} f\, v|v|}_{\text{frictional loss}} \; - \; \underbrace{\rho|v|\frac{dv}{ds}}_{\text{acceleration loss}} \; , \tag{5.14}$$

where we have taken into account the possibility of negative fluid velocities (which, according to our sign convention correspond to production) through the use of the absolute velocity $|v|$.

The *head loss* is the static change in pressure caused by the change in pipeline elevation. In near-horizontal pipelines this component is negligible, but it is usually the most important component in a well. The pressure between surface and bottomhole changes greatly, simply due to the weight of the column of fluid in the well, even if it is not flowing.

The *frictional loss* is caused by the dissipation of energy by viscous forces in the fluid. This term depends strongly on the fluid properties, the flow regime (laminar or turbulent) and the fluid velocity. It is usually the most important component in pipelines.

The *acceleration loss* is caused by the change in momentum when the fluid is accelerated in the well due to expansion. Generally this term is less important, but it can become of significance for very high rate gas wells.

5.3.2 Single-phase oil flow

At steady state conditions, it follows from equation (5.3) that the product ρv remains constant along the pipeline. Therefore we can express v in terms of the constant mass flow w through the line, or, alternatively, in terms of a reference density and reference oil flow rate for which we can choose values at standard conditions:

$$v = \frac{w}{A}\frac{1}{\rho} \quad \text{or} \quad v = \frac{\rho_{o,sc} q_{o,sc}}{A}\frac{1}{\rho} = \frac{B_o q_{o,sc}}{A} \; . \tag{5.15, 5.16}$$

Note that we omit the subscript 'o' in ρ_o to keep the equations more readable. The acceleration term $\rho|v|\, dv/ds$ in equation (5.14) can be rewritten with the aid of the relationship

$$\frac{dv}{ds} = -\left|\frac{dv}{d\rho}\frac{d\rho}{dp}\right|\frac{dp}{ds} = -\left| \underbrace{-\frac{v}{\rho}}_{\frac{dv}{d\rho}} \; \underbrace{c_o \rho}_{\frac{d\rho}{dp}} \right|\frac{dp}{ds} = -c_o|v|\frac{dp}{ds} \; , \tag{5.17}$$

where we made use of equations (5.6) to compute $d\rho/dp$ and (5.15) or (5.16) to compute $dv/d\rho$. Taking due account of the signs of the various terms it follows that

$$\rho|v|\frac{dv}{ds} = -c_o \rho v^2 \frac{dp}{ds} \; . \tag{5.18}$$

However, the compressibility of single-phase oil is usually very small ($c_o \ll 1$), which implies that the density ρ and velocity v can be considered as constants and that the acceleration term can be neglected. If we take the constant oil density as the density at the standard conditions, we can write the governing set of equations for steady-state single-phase oil flow by simplifying equations (5.6), (5.14) and (5.16), resulting in:

$$
\begin{cases}
\dfrac{dp}{ds} = -\rho g \sin\theta - \dfrac{\rho}{2d} f\, v|v| \\[2ex]
v = \dfrac{q_{o,sc}}{A} \\[2ex]
\rho = \rho_{o,sc}
\end{cases}
\qquad (5.19,\ 5.20,\ 5.21)
$$

Equations (5.19) to (5.21) form a set of three differential-algebraic equations for the three unknowns ρ, v and p. The differential equation is of first order, and therefore requires one boundary condition, specifying the pressure p at a certain value of s:

$$
s = \hat{s}: \quad p(\hat{s}) = \hat{p} \ , \qquad (5.22)
$$

where we have used a hat above the variables to indicate that their value is prescribed. The solution to the equation can then be expressed as

$$
p = \hat{p} - \int_{\hat{s}}^{s} \left(\rho g \sin\theta + \frac{\rho}{2d} f * v|v| \right) ds \ . \qquad (5.23)
$$

In the general case, where θ and f are functions of s, it may not be possible to obtain the integral in closed form, in which case it could be obtained numerically with the aid of one of the standard integration routines in MATLAB, see Section C.2 in Appendix C.

Now consider the case of a pipeline with constant inclination θ. If we furthermore assume a constant temperature along the line, the viscosity remains nearly constant and therefore also the friction factor f. Alternatively, we could approximate non-constant inclinations and friction factors with their average values θ_{av} and f_{av}. The integration then becomes trivial, and the pressure p is a linear function of the measured distance s:

$$
p = \hat{p} - \left(\rho g \sin\theta_{av} + \frac{\rho}{2d} f_{av} * v|v| \right)(s - \hat{s}) \ . \qquad (5.24)
$$

5.3.3 Single-phase gas flow

In the case of steady-state single-phase gas flow, we can use equations (5.5) and (5.15) or (5.16) to derive that

$$
\frac{dv}{ds} = -\frac{dv}{d\rho}\left|\frac{d\rho}{dp}\frac{dp}{ds}\right| = -\left| \underbrace{-\frac{v}{\rho}}_{\frac{dv}{d\rho}} \underbrace{\left(\frac{\rho}{p} + \frac{\rho}{Z}\frac{dZ}{dp} \right)}_{\frac{d\rho}{dp}} \right| \frac{dp}{ds} = -|v|\left(\frac{1}{p} + \frac{1}{Z}\frac{dZ}{dp} \right)\frac{dp}{ds} \ , \qquad (5.25)
$$

and therefore that

$$
\rho|v|\frac{dv}{ds} = -\rho v^2 \left(\frac{1}{p} + \frac{1}{Z}\frac{dZ}{dp} \right)\frac{dp}{ds} \ . \qquad (5.26)
$$

The governing set of equations for steady-state single-phase gas flow through a pipeline then follows by combining equations (5.5), (5.14), (5.16) and (5.26), modifying them where necessary to be applicable to gas:

$$\begin{cases} \dfrac{dp}{ds} = \left[1 - \rho v^2 \left(\dfrac{1}{p} + \dfrac{1}{Z}\dfrac{dZ}{dp}\right)\right]^{-1} \left[-\rho g \sin\theta - \dfrac{\rho}{2d} f * v|v|\right], \\[2em] v = \dfrac{\rho_{g,sc} q_{g,sc}}{A} \dfrac{1}{\rho}, \\[2em] \rho = \dfrac{Mp}{ZRT_{abs}}. \end{cases} \qquad (5.27,\ 5.28,\ 5.29)$$

In line with the discussion on single-phase oil flow, the set of equations (5.27) to (5.29) requires a single initial condition and can then be solved numerically with the aid of MATLAB.

It follows from equation (5.27) that the pressure drop dp/ds approaches infinity when the first term at the right-hand side approaches zero. This happens when the absolute value of the velocity approaches

$$v_s = \sqrt{\left[\rho\left(\frac{1}{p} + \frac{1}{Z}\frac{dZ}{dp}\right)\right]^{-1}} = \sqrt{\frac{dp}{d\rho}}, \qquad (5.30)$$

which can be interpreted as the *sonic velocity* for gas under isothermal conditions. The ratio $|v|/v_s$ is therefore a measure for the importance of acceleration losses. Generally, they can be neglected. Only in very high-rate gas wells, or in a situation of uncontrolled gas flow, such as a wellbore *blow-out*, the gas velocity in a well may approach the sonic velocity.

An approximate analytical solution can be obtained by assuming that the acceleration losses may be neglected, i.e. that $|v| \ll v_s$, and that f, T_{abs}, θ and Z may be taken as constant 'average' values f_{av}, $T_{av,abs}$, θ_{av}, and Z_{av} over the length of the pipeline. In that case the set of equations reduces to a single differential equation in p:

$$\frac{dp}{ds} = k_1 p + \frac{k_2}{p} \qquad (5.31)$$

where the coefficients k_1 and k_2 are given by

$$k_1 = -\frac{Mg\sin\theta_{av}}{Z_{av}RT_{av,abs}} \quad \text{and} \quad k_2 = -\frac{8Z_{av}RT_{av,abs}f_{av}\rho_{g,sc}^2 q_{g,sc}|q_{g,sc}|}{\pi^2 d^5 M}, \qquad (5.32,\ 5.33)$$

and where we used the relationship $A = \pi d^2/4$. Equation (5.31) can be rewritten as

$$2p\frac{dp}{ds} = 2k_1 p^2 + 2k_2 \quad \text{and therefore as} \quad \frac{d(p^2)}{ds} = 2k_1 p^2 + 2k_2, \qquad (5.34,\ 5.35)$$

which has as solution

$$p^2 = C\exp(2k_1 s) - \frac{k_2}{k_1}. \qquad (5.36)$$

If we use boundary condition (5.22) to solve for the integration constant C we arrive at

$$p = \sqrt{\left(\hat{p}^2 + \frac{k_2}{k_1}\right)\exp\left[2k_1(s - \hat{s})\right] - \frac{k_2}{k_1}}. \qquad (5.37)$$

Usually it will be necessary to perform one or more iterations to obtain the average values f_{av}, $T_{av,abs}$, θ_{av}, and Z_{av} because they depend on the unknown pressure $p(s)$. For further analytical solutions of the single-phase gas flow equation, in particular for wells, we refer to Hagoort (1988).

5.3.4 Element equations

Referring back to Chapter 2, we can now determine the *element equations* for single phase well or pipeline flow that were already specified in concise form in equation (2.4) as

$$p_{out} = f_3\left(p_{in}, q_{sc}\right). \tag{5.38}$$

If we choose the boundary condition at the inflow-end of the element, i.e. $\hat{p} = p_{in}$, we can compute the pressure p_{out} at the outflow-end through numerical integration of the systems of equations (5.27) to (5.29), or directly from the analytical expressions (5.24) or (5.37), depending on the assumptions and the required accuracy. The velocity v appearing in all these expressions can be related to q_{sc} with the aid of equation (5.16) or its equivalent for gas, keeping in mind that negative values of q and v indicate flow in a production situation.

The MATLAB file `well_p_tf.m` provides an element equation according to expression (5.38), that can be used to compute the THP (output pressure) p_{tf} of a single-phase liquid or gas well for a known BHP (input pressure) p_{wf}; i.e. a pressure drop calculation. A file to compute p_{wf} for a known p_{tf}, i.e. an operating point calculation, is `well_p_wf.m`. Similarly the files `flowline_p_mf.m` and `flowline_p_fl.m` can be used for flowlines to compute the manifold pressure for a given flowline pressure and vice versa. Examples of how to use these files are provided by the MATLAB script files `example_flowline` and `example_wellbore`. The files can be downloaded from Blackboard; see the file 'Fluid forces.zip'.

With the aid of these files it is possible to create plots of the wellbore pressure p as a function of measured depth s. Such plots are often referred to as *traverses*, and an example of how to create them with the MATLAB files listed above is given in the script file `example_traverse.m`. It is also possible to repeat the computation of the BHP, at a fixed THP, for a large number of flow rates. This results in a so called *tubing intake curve* or *intake pressure curve* which depicts the BHP as a function of flow rate; see the script file `example_intake_curve.m`.

Figures 5.4 and 5.5 depict traverses for a dry gas well with parameters given in Table 5.1. They were both computed for the same BHP, but different flow rates and therefore different THPs. Figure 5.4 corresponds to a relatively low rate, where gravity losses dominate the pressure drop over the well. Figure 5.5 corresponds to twice the rate, and it can be seen that friction losses play a much larger role. Acceleration losses are of no significance, and only in Figure 5.5 they can be noticed, for very low pressures close to the surface. Going from the bottom of the well to the surface, the gravity losses gradually decrease because the density of the gas decreases, as can be clearly observed in Figure 5.5. Because the mass flow rate remains the same, the reduction in density with elevation also causes an increase in volume flow rate and therefore in gas velocity. The increased velocity, in turn, results in an increase of the friction losses, which is also clearly visible in Figure 5.5.
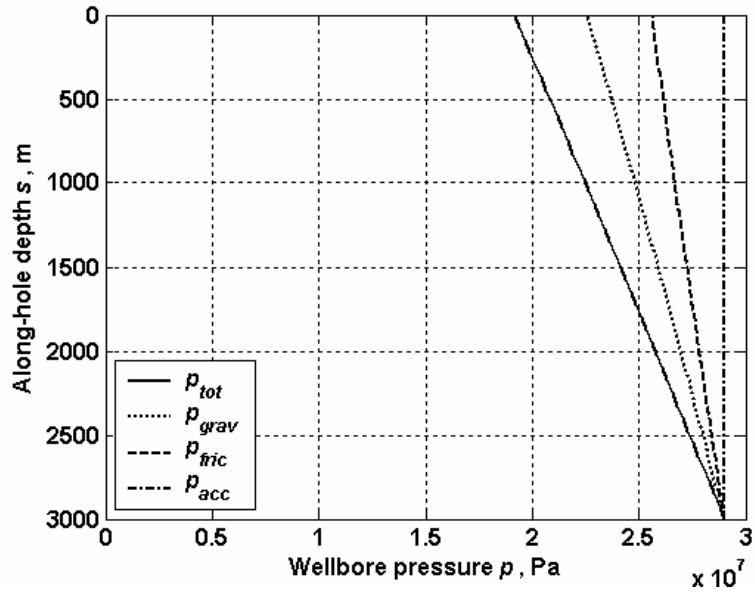
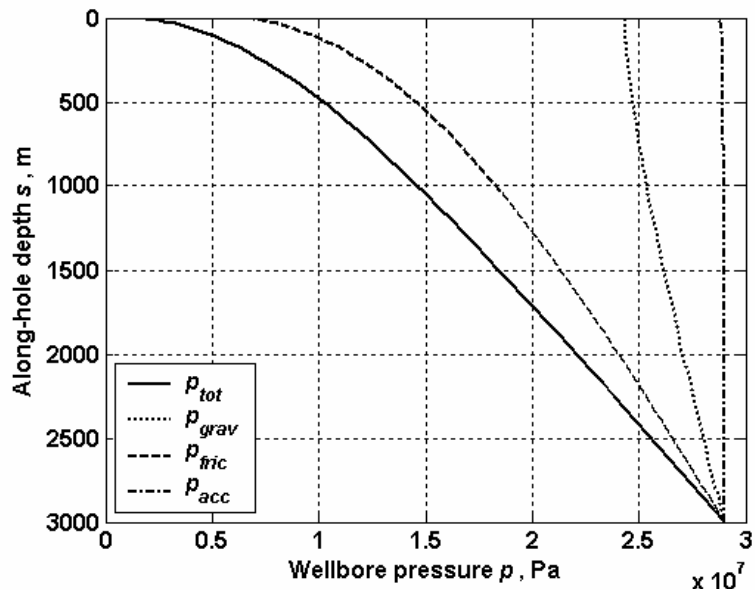*Figure 5.4: Traverse for a low-rate single-phase gas well.*

Figure 5.5: Traverse for the same well as in Figure 5.4 but at a higher rate.

Table 5.1: Parameter values for Figures 5.4 and 5.5.					
Parameter		SI units		Field units	
Inclination	α	0	rad	0	deg.
Diameter	d	$62.3 * 10^{-3}$	m	2.453	in
Roughness	e	$30 * 10^{-6}$	m	0.0012	in
FBHP	p_{wf}	$29.0 * 10^{6}$	Pa	4206	psi
FTHP Fig. 5.4	p_{tf}	$19.2 * 10^{6}$	Pa	2785	psi
FTHP Fig. 5.5	p_{tf}	$1.5 * 10^{6}.$	Pa	218	psi
Rate Fig. 5.4	$q_{g,sc}$	−4.31	m^3/s	$-13.15 * 10^{6}$	ft^3/d
Rate Fig. 5.5	$q_{g,sc}$	−8.62	m^3/s	$-26.30 * 10^{6}$	ft^3/d
Dens./gravity	$\rho_{g,sc}$ / γ_g	0.95	kg/m^3	0.77	-
FBHT	T_{wf}	120	°C	248	°F
FTHT	T_{tf}	30	°C	86	°F
Well depth	z_{tot}	3000	m	9843	ft
Viscosity	μ_g	Carr, Kobayashi and Burrows (1954) correlation			

5.4 Exercises

Exercises 5.1 and 5.3 can be performed by hand calculation. The other two require the use of MATLAB. Some guidance on the use of the required numerical integration routines is given in C.2 of Appendix C. The worked-out MATLAB exercises can be downloaded from Blackboard, see the file 'Exercises.zip'

5.1 Single-phase oil is pumped uphill through a pipeline under a 1.5 degree angle over a length of 3 km. The oil has a density of 850 kg/m^3, the pipeline has an inside diameter of 232 mm and a roughness of 0.003 mm, the ambient temperature is 45 °C, and the pipeline pressure at the inlet is 10 bar. What is the outlet pressure for a flow rate q_o = −5000 m^3/d? Hint: Use the Dempsey dead-oil correlation (B. 119) to compute the viscosity and equation (5.24) to compute the pressure drop. Choose the origin at the outlet of the pipeline.

5.2 Compare the results of question 5.1 with the results from using the MATLAB m-file `flowline_p_mf`. You may want to inspect the file `example_flowline.m` to get started.

5.3 The gas well of Figure 5.5 has friction and Z factors that change only slightly over the height of the well. Their average values are Z_{av} = 0.96 and f_{av} = 0.0166. Verify the numerical results of Figure 5.5 with the aid of the approximate analytical solution described in Section 5.3.3.

5.4 Refer to the last paragraph of Section C.2.2 in Appendix C. Use MATLAB file `example_flowline.m` as a template and write a script file to check the absolute and relative errors in the BHP for the example of Figure 5.5.

6 Multi-phase flow in wells, pipelines and chokes

6.1 What will be covered in this chapter?

- Some introductory aspects of two-phase gas-liquid flow in wells and pipelines.
- Pressure gradient curves for a well.
- Tubing performance description with intake pressure curves.
- Multi-phase flow through chokes.

Multi-phase flow will not be treated in detail in these lecture notes, since the majority of the material is covered in the SPE Monograph *Multi-phase flow in wells* by Brill and Mukherjee (1999) of which several sections form obligatory material for this course; see Section 1.3.2. Furthermore, several aspects have already been covered in ta3470 *Flow and heat transport*. A fundamental treatment of two-phase flow is given in the course tn3782 *Applied multi-phase flows*; see Oliemans (1998). Other usefull reference texts are Wallis (1969), Bobok (1993) and Hasan and Kabir (2002).

6.2 Flow regimes

A typical feature of multi-phase (gas-liquid) flow is the occurrence of radically different *flow regimes* depending on the gas-liquid ratio and the gas and liquid velocities. The flow regimes for gas-liquid flow in horizontal pipelines are shown in Figure 6.1. They are generally known as follows, although some authors use a classification with more categories:

- Single-phase liquid flow.
- Bubble flow.
- Slug flow.
- Stratified flow.
- Annular flow.
- Mist flow (fully dispersed liquid mist).

For vertical flow in a well, a similar flow pattern classification can be made. This is shown in Figure 6.2. The flow regimes are the same as those in horizontal flow except for the absence of stratified flow and the occurrence of *churn flow* as an intermediate regime between slug
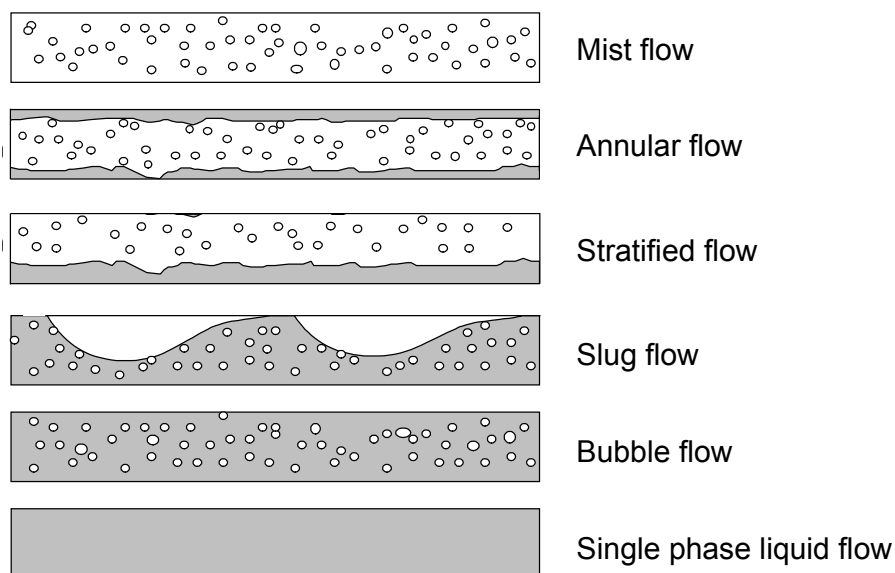
Figure6.1: Flow regimes in horizontal two-phase flow.

| Single phase liquid flow | Bubble flow | Slug flow | Churn flow | Annular flow | Mist flow |
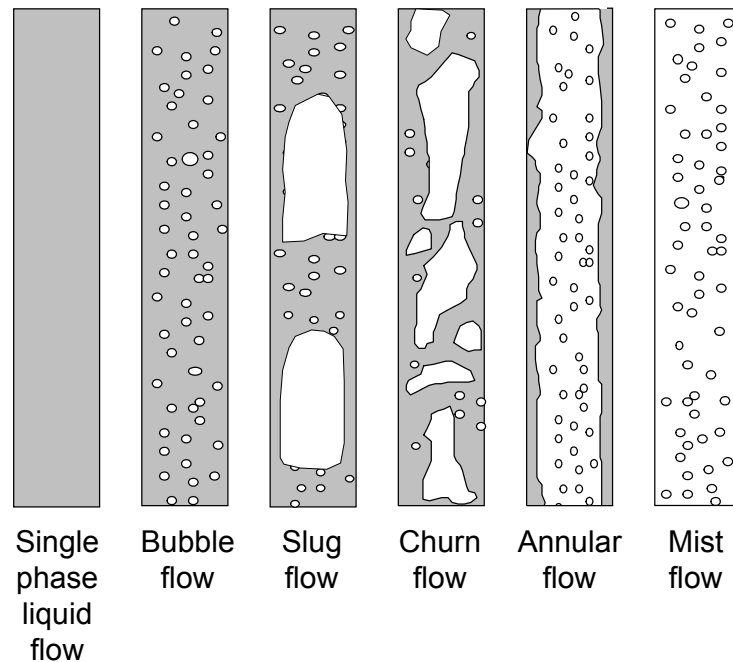
Figure 6.2: Flow regimes in two-phase vertical flow.

and annular flow. Furthermore, the slug flow regime is now somewhat different, and displays bullet-shaped slugs that remain more or less centred in the wellbore.

To describe flow in real pipelines or wells the inclination of the pipe has to be taken into account to give a full map of multi-phase effects. For an in-depth treatment of omni-angle *flow maps* based on physical principles, see Oliemans (1998) and Hasan and Kabir (2002). Several simpler, but less accurate, approaches based on empirical correlations are discussed in Brill and Mukherjee (1999). In a vertical oil well, the pressure decreases as the oil flows from bottom to top of the well. Thus, all of the flow patterns shown in Figure 6.2 may arise. Generally, however, over most of their length, most oil wells operate in the bubble flow and slug flow regimes, while most gas wells operate in the annular flow regime. It is a formidable task to try to solve the equations, based on the laws of physics, which govern these types of flow. There are numerical simulators which attempt this for sensitive industrial processes that need very careful modelling. Within the oil industry, a simpler approach is often adopted. Empirical correlations have been developed, based on extensive experiments. Some of these correlations have been published, others remain proprietary to oil companies or service companies. These correlations differ in complexity. Some are proposed as valid for all flow regimes, while others have separate correlations for each different regime. Some methods try to include some basic physics, such as modelling the behaviour of gas-liquid interfaces, while others rely on a purely empirical approach. For an overview we refer again to Brill and Mukherjee (1999) and for an in-depth treatment to Oliemans (1998) and Hasan and Kabir (2002). Many of these correlations are usually built into modern well simulators. Care needs to be taken because correlations are often suitable for only certain types of well. Note that, as discussed in Chapter 3, the correlations used for the oil properties will affect the results, and may contribute to the inaccuracy.

6.3 Slip and hold-up

One of the complicating factors in the description of multiphase flow is the difference in velocity between the phases. It is generally assumed that water and oil travel at the same

speed, known as the liquid velocity, although in reality this is not always the case, in particular for stratified flow. However, most computational methods do take into account the difference between the liquid velocity and the gas velocity which is known as *slip* between the two phases. But before considering phase velocities, it is useful to address phase flow rates. The ratio of the local oil flow rate q_o and the local total liquid flow rate $q_l = q_o + q_w$ is known as the oil *fraction*, while a similar definition holds for the water fraction:

$$f_o = \frac{q_o}{q_l} = \frac{q_o}{q_o + q_w} \; , \;\; f_w = \frac{q_w}{q_l} = \frac{q_w}{q_o + q_w} \; . \tag{6.1, 6.2}$$

Here we use the word "local" to refer to local pressure and temperature conditions. To obtain the expressions in terms of flow rates at standard conditions, the appropriate formation volume factors and solution ratios need to be introduced according to equations (4.21). However, we do *not* imply that "local" refers to a very small length scale, i.e. we are not interested in fluctuations in flowrates or velocities as a result of small-scale flow features such as slugs or bubbles. Instead, all quantities should be interpreted as averaged over a distance much larger than the small-scale features, i.e. in the order of meters. Note that from equations (6.1) and (6.2) it follows that $f_o + f_w = 1$. The gas fraction and the liquid fraction are defined in the same fashion, although we will indicate them with a λ instead of an *f*:

$$\lambda_g = \frac{q_g}{q_m} = \frac{q_g}{q_g + q_l} \; , \;\; \lambda_l = \frac{q_l}{q_m} = \frac{q_l}{q_g + q_l} \; , \tag{6.3, 6.4}$$

where the quantity $q_m = q_g + g_l = q_g + q_o + q_w$ is known as the *mixture* flow rate. Note that also $\lambda_g + \lambda_l = 1$. Because of slip the fractions of a unit volume of pipe that are occupied by gas and liquid are generally not equal to the gas and liquid fractions as given in equations (6.3) and (6.4). In upward flow, as occurs in a production well or an up-hill pipeline, the gas usually travels faster than the liquid, and liquid *hold-up* occurs. In downward flow, as occurs in a down-hill pipeline, the liquid may travel faster than the gas, in which case the gas is held up. The expression "hold-up" is also often used in the oil industry to indicate the volume fractions occupied by gas and liquid, although in upward flow the gas is not actually held up, but to the contrary is speeded up. The gas and liquid hold-ups H_g and H_l are defined as

$$H_g = \frac{V_g}{V} = \frac{A_g}{A} \; , \;\; H_l = \frac{V_l}{V} = \frac{A_l}{A} \; , \tag{6.5, 6.6}$$

where V_g and V_l are the fractions of a reference volume of pipe that are being occupied by gas and liquid and $V = V_g + V_l$ is the total reference volume. Similarly, A_g and A_l are the parts of the pipe's cross-sectional area occupied by the gas and the liquid respectively, and $A = A_g + A_l$ is the total cross-sectional area. Note that volumes and areas should be interpreted as quantities averaged over a length that is suffuciently large to suppress the effect of small scale flow features. Just as was the case for fractions, $H_g + H_l = 1$. An alternative way to express the equations for phase fractions (6.3) and (6.4) and phase hold-ups (6.5) and (6.6) makes use of variables known as the local or in-situ phase velocities

$$v_g = \frac{q_g}{A_g} \; , \;\; v_l = \frac{q_l}{A_l} \; , \tag{6.7, 6.8}$$

the *superficial* phase velocities

$$v_{sg} = \frac{q_g}{A}, \quad v_{sl} = \frac{q_l}{A}, \tag{6.9, 6.10}$$

and the mixture velocity

$$v_m = v_{sg} + v_{sl} = \frac{q_g + q_l}{A}. \tag{6.11}$$

Substitution of these expressions in equations (6.3) and (6.4) results in

$$\lambda_g = \frac{v_{sg}}{v_m}, \quad \lambda_l = \frac{v_{sl}}{v_m}, \tag{6.12, 6.13}$$

while substitution in equations (6.5) and (6.6) gives

$$H_g = \frac{v_{sg}}{v_g}, \quad H_l = \frac{v_{sl}}{v_l}. \tag{6.14, 6.15}$$

Most computational methods for multi-phase flow simulation make use of experimental correlations for the liquid hold-up expressed as functions of fluid properties, flow rates, pipe diameter and inclination. Equations (6.9), (6.10), (6.14) and (6.15) can then be used to compute the gas and liquid velocities for given flow rates according to

$$v_g = \frac{q_g}{\left(1 - H_l\right) A}, \quad v_l = \frac{q_l}{H_l A}. \tag{6.16, 6.17}$$

If there is no slip, the local phase velocities v_g and v_l are both identical to the mixture velocity v_m and therefore the hold-ups as expressed in equations (6.14) and (6.15) become identical to the phase fractions as expressed in equations (6.12) and (6.13). Other names for phase fraction are therefore *no-slip hold-up,* or *no-slip volume fraction*. Alternatively, the expressions *phase content* or *input fraction* are being used in some publications to identify what we call phase fraction. Another name for hold-up is *in-situ volume fraction*, while for gas also the term *void fraction* is found. In analogy to porous-media flow the term *saturation* could also be applied. However, we will stick to the oil industry convention and speak of gas and liquid hold-ups. Other multi-phase flow concepts used in litterature are the *slip velocity* defined as $v_s = v_g - v_l$, and the gas and liquid *mass fractions* x_g and x_l defined as

$$x_g = \frac{w_g}{w_g + w_l} = \frac{q_g \rho_g}{q_g \rho_g + q_l \rho_l}, \quad x_l = \frac{w_l}{w_g + w_l} = \frac{q_l \rho_l}{q_g \rho_g + q_l \rho_l}, \tag{6.18, 6.19}$$

where w_g and w_l are the gas and liquid mass flow rates, and where x_g is also known as the *quality* of the gas-liquid mixture. To illustrate the effect of slip on the liquid fraction and the liquid hold-up Figure 6.3 gives an example of stratified flow where the liquid flow rate equals one-third of the gas flow rate. In case of no slip between the phases the liquid hold-up is equal to the liquid fraction and 25% of the pipe's cross-sectional area is occupied by liquid. However, if the gas flows twice as fast as the liquid, the liquid fraction remains the same but the liquid hold-up increases such that 40% of the area is occupied by liquid.
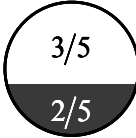
$$\text{no slip:} \quad \left. \begin{array}{l} q_l = \frac{1}{3}q_g \\[2mm] v_l = v_g \end{array} \right\} A_l = \frac{q_l}{v_l} = \frac{\frac{1}{3}q_g}{v_g} = \frac{1}{3}A_g$$

$$\lambda_l = \frac{q_l}{q_g + q_l} = \frac{\frac{1}{3}}{1+\frac{1}{3}} = \frac{1}{4} \qquad H_l = \frac{A_l}{A_g + A_l} = \frac{\frac{1}{3}}{1+\frac{1}{3}} = \frac{1}{4}$$

$$\text{slip:} \quad \left. \begin{array}{l} q_l = \frac{1}{3}q_g \\[2mm] v_l = \frac{1}{2}v_g \end{array} \right\} A_l = \frac{q_l}{v_l} = \frac{\frac{1}{3}q_g}{\frac{1}{2}v_g} = \frac{2}{3}A_g$$

$$\lambda_l = \frac{q_l}{q_g + q_l} = \frac{\frac{1}{3}}{1+\frac{1}{3}} = \frac{1}{4} \qquad H_l = \frac{A_l}{A_g + A_l} = \frac{\frac{2}{3}}{1+\frac{2}{3}} = \frac{2}{5}$$

Figure 6.3: Illustration of the effect of slip between the gas and liquid phases on the liquid fraction λ_l (no effect) and the liquid hold-up H_l (increases for increasing slip velocity).

6.4 Gradient curves

Before the advent of modern computers, the practice was to present empirical correlations for wellbore pressure drop in the form of *gradient curves*. Although these curves are nowadays hardly used, they give some insight into the effect of the various parameters. The gradient curve graphs are valid only for vertical wells. Their vertical axis represents the difference in vertical depth between two points in the wellbore, the horizontal axis the corresponding pressure difference. An example is given in Figure 6.4, which was generated with the aid of the Duns-Ros correlation for 3000 bpd flow with a GLR of 2000 scf/stb and zero watercut in a 4½″ tubing; see Duns and Ros (1963).

Note that the vertical axis represents the difference in depth. The absolute depth is not relevant. The slope of the gradient curves reduces with depth. This is a result of the gas being compressed, the average density increasing, and the pressure gradient increasing, while the other frictional effects on the pressure drop remain roughly constant. For very low pressures, the pressure gradient starts to increase again. This is a result of increasing importance of the frictional effects at high production rates, low pressures and high gas-oil ratios.

How are gradient curves used? Consider Figure 6.5. Suppose the pressure at depth 4000 ft is known to be 3800 psia, and we wish to determine the pressure at 1500 ft. As shown in Figure 6.5, we select the point on the curve at pressure 3800 psia. We go horizontally across to the vertical axis and go up by the depth difference of 2500 ft. Going back to the gradient curve, we read off the pressure at 1500 ft as 300 psia. In this way we can read off the pressure drop over any portion of the tubing if we know the pressure at one of these two depths. An extensive collection of gradient curves is presented in Beggs (1991).
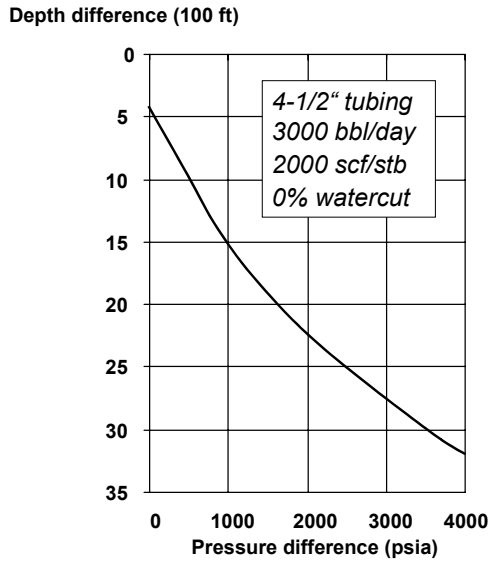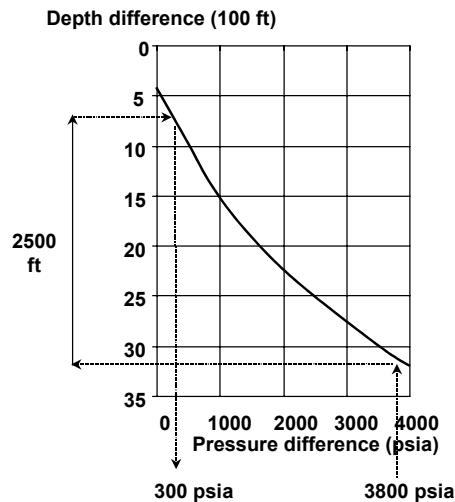
Figure 6.4: Example of a gradient curve.

Figure 6.5: How to use a gradient curve.

6.5   *Intake pressure curves for describing tubing performance*

As discussed in Section 2.3.3 of Chapter 2, the multi-phase flow equations for a wellbore element specify a relation between the oil and gas flow rates $q_{o,sc}$ and $q_{g,sc}$ and the wellbore pressure drop $\Delta p = p_{in} - p_{out}$; see equation (2.7). If we know the gas-oil ratio R_{go}, we can also determine the flow rates from the pressure drop, although in an iterative fashion. However, usually it is one of the pressures which is unknown. If the flowing wellbore pressure p_{wf} is specified, then the THP p_{tf} can be calculated with a pressure drop calculation. Usually, however, the p_{tf} is determined by the operating conditions, and p_{wf} is calculated with an operating point calculation. By performing successive operating point calculations, while varying one of the process variables, we can generate what are called *tubing intake curves* or *intake pressure curves* since they give the intake pressure p_{wf} at the bottom of the tubing

required to flow the well against a given surface *back-pressure*. Typical examples are shown in Figures 6.6, 6.7 and 6.8 below.
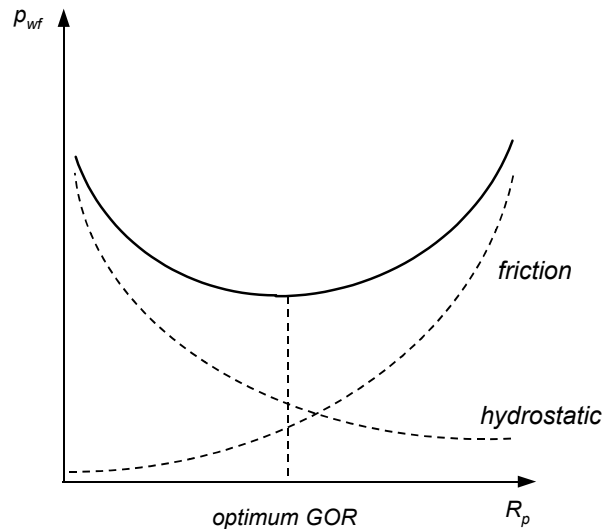
Figure 6.6: Intake pressure curve for varying gas-oil ratios.

Figure 6.6 shows the intake pressure curve which is generated if the oil production rate $q_{o,sc}$ is held constant while the GOR R_{go} is varied. This curve illustrates some of the peculiarities of two-phase flow. At zero GOR, the well is producing only liquid. Since the production rate is low, the friction is low, and the intake pressure is close to the hydrostatic pressure of the fluid column. If gas is introduced, the liquid column gets lighter, and hence the hydrostatic pressure decreases, and the intake pressure decreases. This effect continues as the GOR increases, but at the same time the frictional pressure drop slowly increases, because of the increased total mass flow of oil and gas. At a certain point, the friction pressure drop starts to dominate, and the intake pressure starts to increase again. The minimum intake pressure corresponds to an optimum GOR. At this point the gas is most effective in lifting the liquid. Therefore for a well flowing a given volume of liquid, there is an optimum GOR which will minimize the pressure drop over the tubing. This effect plays an important role in gas-lift optimisation.

In wells which are naturally flowing, without gas lift, Figure 6.6 is not of much interest, since the GOR is fixed. Instead, the intake pressure curve as a function of tubing diameter (Figure 6.7) or as a function of production rate (Figure 6.8) are used. In Figure 6.7 it is seen that there is an optimum tubing size (for a fixed production rate). As expected, below this optimum, the pressure decreases as the tubing diameter increases, since it is easier to flow the fluid through a wider tube. But above the optimum diameter, multi-phase effects start to play a role. With a wider tubing size it becomes easier for the gas to slip past the liquid and the lifting is less efficient. The downhole pressure required to maintain the flow rate therefore rises.

In Figure 6.8 it is seen that the downhole pressure may also decrease as the flow rate increases, all other parameters being held constant. This is due to changes in flow regime as the flow rate increases, for fixed GLR. We shall see in Chapter 8 that this surprising result has consequences for well flow stability.
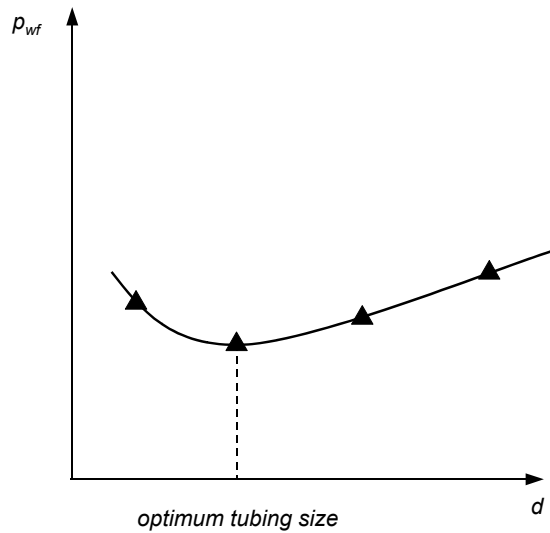
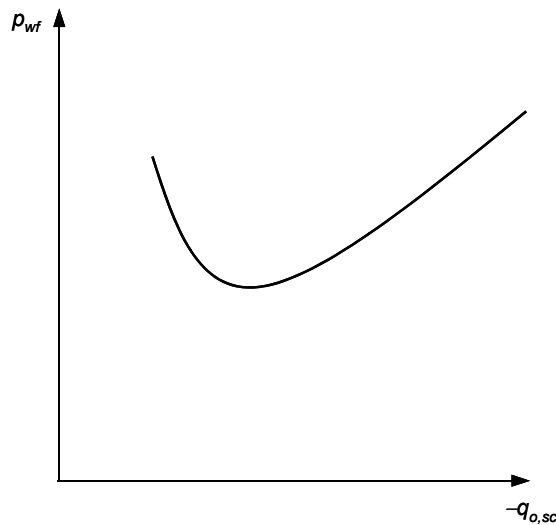*Figure 6.7: Intake pressure curve for varying tubing diameter.*

Figure 6.8: Intake pressure curve for varying production rate.

6.6 Multi-phase flow through chokes

The production rate of a well is usually controlled by adjusting the *choke* at the surface wellhead or the flow station manifold. The choke is also called a *bean*. Essentially the choke is an adjustable valve, with a calibrated restricted area through which the fluids flow.

There are different types of chokes – fixed (also called positive), needle and seat, plug and cage or adjustable. But they all work on the same principle of dissipating large amounts of potential energy over a short distance. This is done by causing the fluids to pass through a short rapid contraction. This restriction has the effect of forcing the fluids into a narrow jet, creating eddies on both the inlet and exit side of the choke and increasing the turbulence of the flow, thus dissipating energy and reducing the flow rate. There is a large pressure drop over the choke. We define the following variables:

$q_{l,sc}$ is the liquid flow-rate through the choke, m^3s^{-1} (bpd),
p_1 is the pressure upstream of the choke, Pa (psi), and

p_2 is the pressure downstream of the choke, Pa (psi).

Experimentally it is found that for a given value of the upstream pressure p_1 there is a critical pressure ratio $(p_1/p_2)_{crit}$. If $p_1/p_2 < (p_1/p_2)_{crit}$, then $|q_{l,sc}|$ increases as the pressure drop p_1-p_2 increases, reaching the maximum rate $q_{l,crit}$ at $(p_1/p_2)_{crit}$. This is as expected; the larger the pressure drop, the faster the flow. However, if $p_1/p_2 > (p_1/p_2)_{crit}$, then $q_{l,sc}$ remains constant at $q_{l,crit}$. This phenomenon is called critical flow. Critical flow is reached when the velocity in the contraction of the choke reaches sonic velocity. Pressure disturbances downstream can no longer propagate through the choke to the upstream side. Hence the flow behaviour becomes independent of the downstream pressure p_2.

There are advantages in operating the choke above the critical pressure ratio. The pressure p_1 at the wellhead is then independent of fluctuations in p_2, the pressure on the downstream side of the choke. The pressure p_2 may vary for many reasons: there may be more wells entering the same manifold, and one of these may be shut in; there may be fluctuations in the processing system; the operating staff may vary valves in the downstream system. These effects will not change the production rate of the well if the choke is operating above critical conditions.

Several expressions exist to predict the occurrence of critical flow through a choke; see e.g. Chapter 5 of Brill and Mukherjee (1999). As a rule of thumb, critical flow occurs when

$$p_1 / p_2 > 1.7 \; . \tag{6.20}$$

Below critical conditions, the flow rate of a gas-liquid mixture through a choke depends on the specific type of choke, the properties of the multi-phase mixture etc., and there is no simple pressure drop/flow rate relationship. Above critical conditions, there are a number of empirical correlations, proposed see e.g. Gilbert (1954), Ros (1960). Other correlations are connected to the names of Baxendell and Achong; see Brill and Mukherjee (1999). They all have the form:

$$p_1 = -Aq_{l,sc} \frac{\left(E * R_{gl}\right)^B}{\left(F * d_{ch}\right)^C} + D \;, \tag{6.21}$$

where,

R_{gl} is the gas-liquid ratio, m^3/m^3 (scf stb^{-1}),
d_{ch} is the choke diameter, m (1/64th inch),
A, B, C, and D are experimentally-determined constants given in Table 6.1,

and where we have assumed that $q_{l,sc}$ has a negative value in line with our convention that flowrates in production wells are negative. Note that in field units the diameter is specified in 1/64th of an inch. For a given choke size, the flow rate-pressure relationship is a straight line. This is called the choke performance curve; see Figure 6.9. For fixed pressure, the flow rate is approximately equal to the square of the choke diameter, i.e. the cross-sectional area, as might be expected. For pressures below about 1.7 times the manifold or flowline pressure p_2, these curves are of course invalid, since this is the non-critical region. The four critical choke models have been programmed in MATLAB file `choke_critical_p_tf`, assuming that the upstream choke pressure p_1 is equal to the flowing THP p_{tf}.

Table 6.1: Coefficients for different choke models.						
Correlation	SI units					
	A	B	C	D	E	F
Gilbert	$3.75 * 10^{10}$	0.546	1.89	$1.01 * 10^5$	5.61	$2.52 * 10^3$
Ros	$6.52 * 10^{10}$	0.500	2.00	$1.01 * 10^5$	5.61	$2.52 * 10^3$
Baxendell	$3.58 * 10^{10}$	0.546	1.93	$1.01 * 10^5$	5.61	$2.52 * 10^3$
Achong	$1.43 * 10^{10}$	0.650	1.88	$1.01 * 10^5$	5.61	$2.52 * 10^3$
Correlation	field units					
	A	B	C	D	E	F
Gilbert	10.0	0.546	1.89	14.7	1.00	1.00
Ros	17.4	0.500	2.00	14.7	1.00	1.00
Baxendell	9.56	0.546	1.93	14.7	1.00	1.00
Achong	3.82	0.650	1.88	14.7	1.00	1.00

In the non-critical regime the pressure drop over the choke is usually assumed to behave as a quadratic function of the local flow rate or velocity:

$$p_1 - p_2 = \frac{v_m^2}{2\rho_n C_{ch}^2} = \frac{\left(q_g + q_l\right)^2}{2\left(\lambda_g \rho_g + \lambda_l \rho_l\right) A_{ch}^2 C_{ch}^2} \,, \tag{6.22}$$

where C_{ch} is a dimensionless drag coefficient that accounts for the energy losses in the choke and that needs to be determined experimentally. A pragmatic choice for the drag coefficient is such that the curves for critical and non-critical flow are continuous at the transition point.
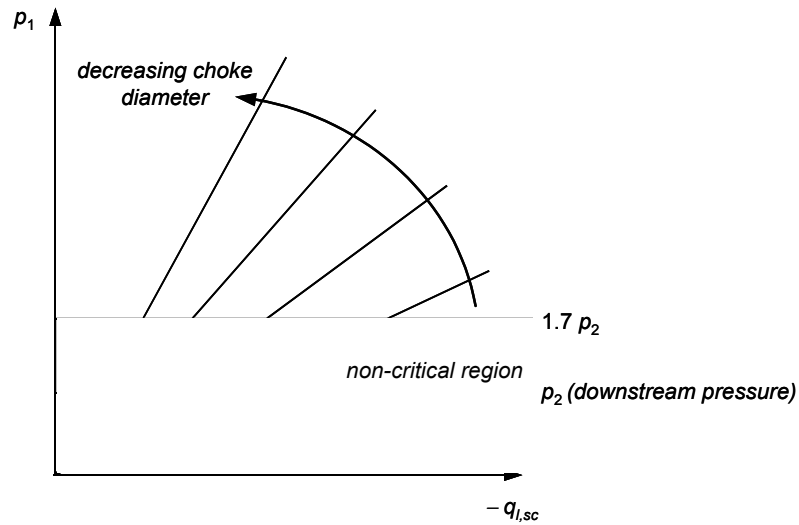
Figure 6.9: Choke performance curves.

6.7 Exercises

6.1 Consider a gas-liquid mixture with $q_l = 0.3 * q_g$, and $v_g = 1.2 * v_l$. What are the liquid fraction and the liquid hold-up?

6.2 A well is completed with a 0.122 m ID tubing and produces a gas-oil-water mixture with the following properties: $q_{o,sc} = 18.4*10^{-3}$ m³/s, $R_{go} = R_p = 238$ m³/m³, $f_{w,sc} = 0.23$. We know that we are dealing with a black oil and that at depth of 400 m the formation volume factors and the solution GOR are given by $B_g = 0.05$, $B_o = 1.15$, $B_w = 1.00$, and $R_s = 10.1$, all expressed in m³/m³. Furthermore we know that the liquid hold-up is about 5% higher than the liquid volume fraction. What are the superficial and local gas and liquid velocities?

7 Inflow performance

7.1 What will be covered in this chapter?

- Linear inflow performance of single-phase oil wells, as described by the Productivity Index (PI).
- The causes of formation damage (impairment) and the definition of 'skin'.
- Non-linear inflow performance relationships (IPRs) for gas wells and multi-phase (gas-oil-water) wells.

7.2 The importance of inflow performance

In this section we will discuss the relationship between flow rate and pressure in the near-wellbore area. The difference between the reservoir pressure and the BHP of a well is the driving force for *inflow* into the wellbore. Resistance to well inflow depends on reservoir rock properties, fluid properties, details of the completion of the well, and sometimes the late effects of drilling and workover activities. In combination, these factors determine the *inflow performance* of the well. Because all fluids entering the wellbore have to pass through the narrow area around the wellbore, the highest flow rates in the reservoir occur just there and any increased resistance to flow has a large effect on the well performance.

Because inflow performance plays such an important role, it should be regularly measured through *production testing*, i.e. by flowing the well through a test separator and determining the gas, oil, and water flow rates as function of wellbore pressure. The pressure should preferably be measured at the bottomhole with either a *permanent downhole gauge* (PDG) or a dedicated wire line tool. This regular testing will give an indication when a well is producing less than expected due to *impairment*, i.e. blockage of the pores in the near-wellbore area. Remedial measures, such as *hydraulic fracturing* of the formation through pumping of high-pressure liquids, or *stimulation* with acids, can then be taken. The results of the well tests can be incorporated in one of the models for inflow performance given below. It is important to realize that these are only models, and the actual downhole well data must be respected. For details of inflow performance measurement, see e.g. Golan and Whitson (1991) and Economides et al. (1994).

As an example of general nature of a well's inflow performance, consider a vertical oil well, with either an open-hole producing zone or a perforated zone. The production performance of this zone is usually described by an *Inflow Performance Relationship* (IPR) between the oil flow rate $q_{o,sc}$ and the BHP p_{wf}. In practice, it is found that the IPR is an almost-linear relationship between p_{wf} and $q_{o,sc}$, as long as p_{wf} is above the bubble point pressure p_b. In that case the IPR can be expressed as a *Productivity Index* (PI) J defined as the ratio between $q_{o,sc}$ and the *drawdown* Δp, which is the difference between the *static* or *closed-in* BHP p_{ws} and the *dynamic* or *flowing* BHP p_{wf}, both measured at the middle of the zone or at the middle of the perforations. If we assume that the static BHP equals the *reservoir pressure p_R*, we can write

$$ J = \frac{-q_{o,sc}}{p_R - p_{wf}} \quad , \tag{7.1} $$

where we adopt the convention that a positive flow rate $q_{o,sc}$ implies injection into the reservoir, and a negative flow rate production into the well. The units of the PI are $\mathrm{m^3\,s^{-1}\,Pa^{-1}}$ ('strict' SI units), $\mathrm{m^3\,d^{-1}\,kPa^{-1}}$ ('allowable' SI units) or $\mathrm{bpd\,psi^{-1}}$ (field units). The reservoir pressure is the pressure at the boundary of the *drainage area* of the well. Alternatively, the PI can be defined in terms of the *average reservoir pressure $p_{R,av}$* in the drainage area of the

well, which results in a higher value of the PI for the same flow rate. For injection wells it is customary to use the *Injectivity Index* (II) as an indication of the injection performance. The definition of the II is completely analogous to that of the PI. Figure 7.1 depicts the linear IPR for a single-phase oil well. At a flow rate $q_{o,sc} = 0$ the BHP p_{wf} equals the static BHP p_R. In the theoretical case of a zero pressure at the bottomhole, the flow rate would reach a value known as the *absolute open flowing potential* (AOFP) of the well.

For gas wells, or oil wells producing from a reservoir below bubble point pressure, the IPR is a non-linear function of the flow rate and cannot be represented with a straight-line PI anymore. In the following sections we will consider in some detail the nature of the IPR for single-phase production, and briefly discuss the effects of multi-phase flow.

7.3 Governing equations

7.3.1 Mass balance, momentum balance and equation of state

In this section we will derive the equations for single-phase fluid flow in the near-wellbore area, using the same approach as we used to describe pipe flow in Chapter 5. Consider the classic text-book case of a single vertical well, either open-hole or perforated over the entire reservoir height, producing from a circular reservoir; see Figure 7.2. Using cylindrical co-ordinates we can write the mass balance per unit time through a control volume as:

$$\underbrace{A\rho v}_{\text{mass in}} - \underbrace{\left(A + \frac{\partial A}{\partial r}dr\right)\left(\rho + \frac{\partial \rho}{\partial r}dr\right)\left(v + \frac{\partial v}{\partial r}dr\right)}_{\text{mass out}} = \underbrace{A\phi\frac{\partial \rho}{\partial t}dr}_{\text{mass accumulated}} \quad , \qquad (7.2)$$

where $A = h\,r\,d\psi$ is the cross-sectional area of the control volume in radial direction, m^2,

  h is the reservoir height, m,
  r is the radial co-ordinate, m,
  ψ is the tangential co-ordinate, rad,
  ρ is the fluid density, kg m^{-3},
  $v = q/A$ is the superficial radial fluid velocity, m s^{-1},
  q is the radial flow rate, m^{3}s^{-1},
  ϕ is the porosity, -, and
  t is time, s.
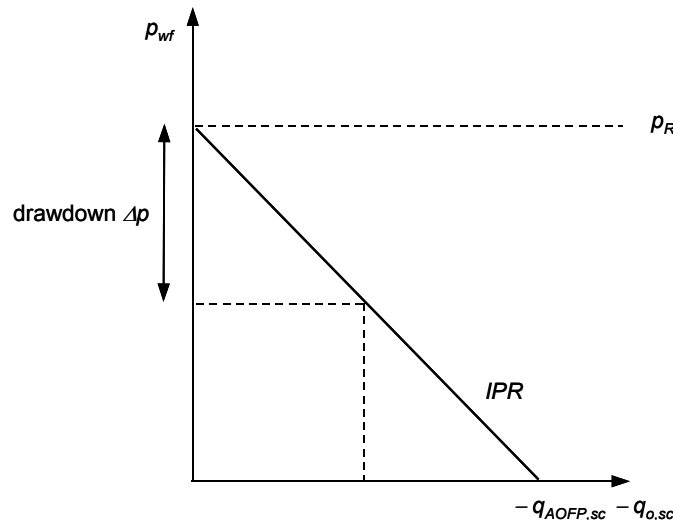
Figure 7.1: Straight-line inflow performance relationship.
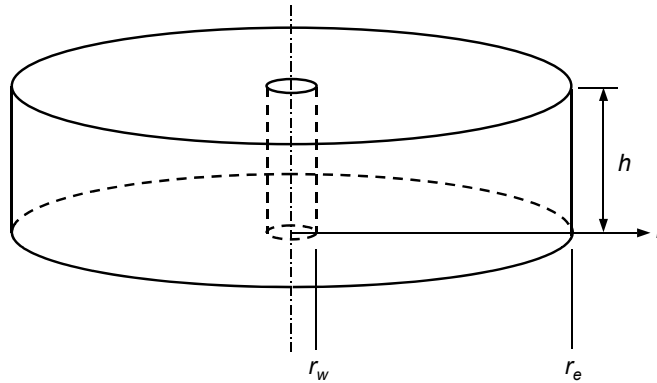
Figure 7.2: Well in a circular reservoir.

Note that a positive velocity implies flow in the positive co-ordinate direction, and therefore corresponds to injection from the well into the reservoir. Maintaining the analogy with pipe flow, the momentum balance can formally be written as:

$$
\underbrace{A\rho v^2}_{\text{momentum in}} - \underbrace{\left(A + \frac{\partial A}{\partial r}dr\right)\left(\rho + \frac{\partial \rho}{\partial r}dr\right)\left(v + \frac{\partial v}{\partial r}dr\right)^2}_{\text{momentum out}} +
$$

$$
\underbrace{Ap + 2h\left(p + \frac{\partial p}{\partial r}\frac{dr}{2}\right)dr\sin\frac{d\psi}{2} - \left(A + \frac{\partial A}{\partial r}dr\right)\left(p + \frac{\partial p}{\partial r}dr\right)}_{\text{pressure forces}} + \tag{7.3}
$$

$$
\underbrace{F_g(\rho,r)ds}_{\text{gravity force}} + \underbrace{F_f(\rho,\mu,v)dr}_{\text{friction force}} = \underbrace{A\phi\frac{\partial(\rho v)}{\partial t}dr}_{\text{momentum accumulated}} ,
$$

where the components of the pressure term have been illustrated in Figure 7.3, and where

p is the pressure, Pa,
$F_g(\rho,s)$ is the gravity force per unit length, N m^{-1},
$F_f(\rho,\mu,v)$ is the friction force per unit length, N m^{-1}, and
μ is the dynamic viscosity, Pa s.

However, in flow through porous media the velocities v are usually so small that the momentum terms at the left-hand side, which depend on v^2, play no role. Furthermore, it can be shown that also the momentum term at the right hand side is negligible, and therefore only the pressure, gravity and friction terms need to be taken into account; see Bear (1972). In our case, we can furthermore disregard the gravity term because we consider horizontal flow only. The nature of the friction force $F_f(\rho,\mu,v)$ will be discussed in more detail in Section 7.3.2 below. Just as in the case of pipe flow we can complete the set of governing equations with the aid of the equation of state for the fluid, i.e. equation (4.6) for single-phase gas or equation (4.11) for single-phase oil. If we expand equations (7.2) and (7.3), substitute $A = h\,r\,d\psi$, disregard the momentum and the gravity terms, drop all terms higher than first order in the differentials, and simplify the results, we can write the three equations as

$$\begin{cases} \dfrac{\partial(\rho v r)}{\partial r} = -\phi r \dfrac{\partial \rho}{\partial t} \ , \\[2ex] \dfrac{\partial p}{\partial r} = \dfrac{F_f}{2\pi h r} \ , \\[2ex] \rho = \dfrac{Mp}{ZRT_{abs}} \ \text{for gas}\ , \ \text{or} \\[2ex] \rho = \rho_{o,ref} \exp\!\left[c_o\!\left(p - p_{ref}\right)\right] \text{for oil} \ , \end{cases} \qquad (7.4,\ 7.5,\ 7.6,\ 7.7)$$

where the compressibility c_o is a known function of pressure p and temperature T, and the gas deviation factor Z is a known function of p. The temperature T (and therefore also T_{abs}) can generally be taken as constant because the large *heat capacity* of the reservoir is usually sufficient to guarantee *iso-thermal conditions*. Only in high-rate gas wells, some cooling due to expansion of the gas may occur in the near-wellbore area, an effect known as the *Joule-Thomson cooling*; see e.g. Moran and Shapiro (1998).

7.3.2 Friction force – Darcy's law and Forcheimer's coefficient

The frictional loss for single-phase liquid flow in porous media is described by the experimental relationship known as *Darcy's law*, which can be written in polar co-ordinates as:

$$\frac{F_f}{2\pi h r} = -\frac{\mu}{k} v \ . \qquad (7.8)$$

For iso-thermal liquid flow and a homogeneous reservoir, μ and k can be considered constants. For gas flow, we can use the same relationship except for very high velocities such as occur in the near-wellbore area of high-rate gas wells. In that case we have to replace Darcy's law with

$$\frac{F_f}{2\pi h r} = -\frac{\mu}{k} v - \beta \rho v^2 \ , \qquad (7.9)$$

where β is *Forcheimer's coefficient* with dimension L^{-1}. It represents the inertia effects experienced by the gas when it is accelerated and decelerated during its flow through the pore
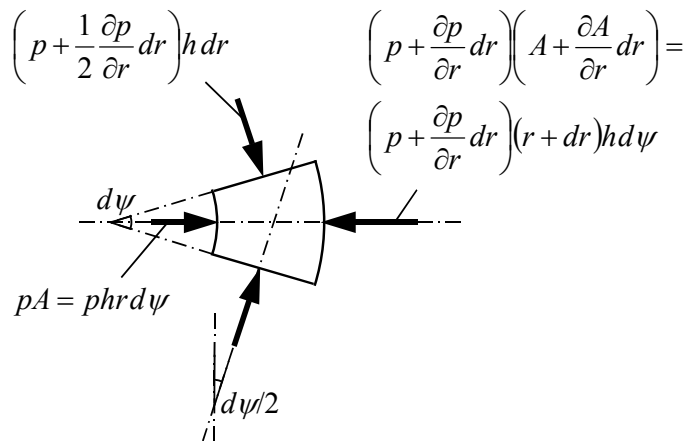
Figure 7.3: Control volume and pressure forces in cylindrical co-ordinates.

throats. It is also referred to as *inertia coefficient* or *turbulence coefficient*. The latter name is not entirely correct because the inertia effect can be noticed at much lower velocities than the velocity that corresponds to the onset of turbulence in the pores; see Bear (1972). The values of k and β should be determined experimentally, either directly through measurements on cores, or indirectly from well tests. The relationship between β and k is typically of the form

$$\beta = A k_g^{-B} \ . \tag{7.10}$$

Dake (1978) gives an example with values of the constants determined as $A = 2.4 * 10^{-6}$ and $B = 1.1$, with k expressed in m^2 and β in m^{-1}.

7.4 Inflow performance relationships

7.4.1 Single-phase oil flow – steady state

At steady state conditions, the right-hand side of the mass conservation equation (7.4) vanishes. Furthermore, we can assume that the compressibility of single-phase oil is small enough to take the density as constant in the drainage area of the well, which reduces (7.4) equation further to

$$\frac{\partial(vr)}{\partial r} = 0 \ . \tag{7.11}$$

This is a first-order differential equation, albeit a trivial one, that therefore requires one boundary condition which can be obtained from the known velocity at the wellbore radius:

$$v\big|_{r=r_w} = \frac{q_o}{A} = \frac{q_o}{2\pi h r_w} = \frac{B_o q_{o,sc}}{2\pi h r_w} \ , \tag{7.12}$$

where we have used the oil-formation volume factor B_o to relate the downhole flow rate q_o to the surface flow rate at standard conditions $q_{o,sc}$. Integrating equation (7.11) and solving for the integration constant with the aid of boundary condition (7.12) results in:

$$vr = \frac{B_o q_{o,sc}}{2\pi h} \ , \tag{7.13}$$

Next, equations (7.5), (7.8) and (7.13) can be combined to give the classic differential equation for steady-state radial flow:

$$\frac{dp}{dr} = -\frac{\mu B_o q_{o,sc}}{2\pi k h r} \ . \tag{7.14}$$

Equation (7.14) is also of first order and the boundary condition can now be specified as

$$p\big|_{r=r_e} = p_R \ , \tag{7.15}$$

which represents a constant pressure p_R at the external boundary of the circular drainage area. This situation can, with some imagination, be interpreted as a reservoir with constant pressure support in the form of a strong aquifer. If we assume that the k, μ and B_o are constants, equation (7.14) can be integrated to give

$$p = -\frac{\mu B_o q_{o,sc}}{2\pi k h} \ln r + C \ . \tag{7.16}$$

The value of the unknown integration constant C can be found with the aid of boundary condition (7.15), and substitution in equation (7.16) then gives us the expression for p as a function of r under steady-state flow conditions:

$$p = p_R + \frac{\mu B_o q_{o,sc}}{2\pi kh} \ln\left(\frac{r_e}{r}\right) . \quad (7.17)$$

In particular, we can now define the IPR between the flowing bottomhole pressure p_{wf} and the flow rate $q_{o,sc}$ as:

$$p_R - p_{wf} = -\frac{\mu B_o q_{o,sc}}{2\pi kh} \ln\left(\frac{r_e}{r_w}\right) . \quad (7.18)$$

Note that because of our definition of the positive flow direction, a positive drawdown corresponds to a negative flow rate, i.e. to flow towards the well as occurs in a production well.

Alternatively, we may want to express the IPR in terms of the volume-averaged reservoir pressure $p_{R,av}$ defined as

$$p_{R,av} = \frac{2\pi h\phi \int\limits_{r_w}^{r_e} pr\,dr}{2\pi h\phi \int\limits_{r_w}^{r_e} r\,dr} = \frac{2\int\limits_{r_w}^{r_e} pr\,dr}{r_e^2 - r_w^2} . \quad (7.19)$$

Substitution of equation (7.17) in equation (7.19) gives

$$p_{R,av} = \frac{2}{r_e^2 - r_w^2} \int\limits_{r_w}^{r_e}\left[p_R + \frac{\mu B_o q_{o,sc}}{2\pi kh} \ln\left(\frac{r_e}{r}\right)\right] r\,dr = p_R + \frac{\mu B_o q_{o,sc}}{\pi kh\left(r_e^2 - r_w^2\right)} \int\limits_{r_w}^{r_e} r\ln\left(\frac{r_e}{r}\right) dr ,\quad(7.20)$$

where the integral can be solved through integration by parts as follows:

$$\int\limits_{r_w}^{r_e} r\ln\left(\frac{r_e}{r}\right) dr = -\int\limits_{r_w}^{r_e} r\ln\left(\frac{r}{r_e}\right) dr = -\frac{1}{2}r^2\ln\left(\frac{r}{r_e}\right)\Bigg|_{r_w}^{r_e} + \int\limits_{r_w}^{r_e}\frac{1}{2}r^2\frac{1}{r}dr = \frac{1}{4}\left(r_e^2 - r_w^2\right) - \frac{1}{2}r_w^2\ln\left(\frac{r_w}{r_e}\right) .\quad(7.21)$$

Substitution of this result in equation (7.20), solving for p_R, substitution in equation (7.18) and rearranging the result gives us the required expression for p_{wf} in terms of $p_{R,av}$ for steady-state flow:

$$p_{R,av} - p_{wf} = -\frac{\mu B_o q_{o,sc}}{2\pi kh}\left[\frac{1}{1 - r_w^2/r_e^2}\ln\left(\frac{r_e}{r_w}\right) - \frac{1}{2}\right] \approx -\frac{\mu B_o q_{o,sc}}{2\pi kh}\left[\ln\left(\frac{r_e}{r_w}\right) - \frac{1}{2}\right] . \quad (7.22)$$

where the approximation holds for $r_w \ll r_e$ which is the usual situation.

7.4.2 Single-phase oil flow – semi-steady state

Often we encounter a situation where pressure support in a reservoir is not sufficient to maintain a constant pressure, and where the pressure gradually drops over time. Such a gradual pressure depletion scenario can be schematically represented by circular reservoir with a boundary condition

$$\left.\frac{dp}{dr}\right|_{r=r_e} = 0 \ , \tag{7.23}$$

which implies that there is no pressure gradient and therefore no driving force for flow at the external boundary. This type of *no-flow condition* typically occurs when a large number of vertical wells producing at equal rates is used to drain a reservoir in a regular pattern. The drainage areas can then reasonably well be approximated by circular cylindrical volumes. A refined approximation can be obtained with the aid of *shape factors* to account for the fact that the drainage areas are not exactly circular, see Dietz (1965). As a consequence of the absence of flow through the outer boundary and of a constant production q_o from the wells, the pressure in the reservoir will steadily decrease, a situation known as *semi steady-state*. To analyse this situation, we can start from the mass balance equation (7.5) which can be rewritten with the aid of the equation of state (7.7) as follows:

$$\frac{\partial(\rho v r)}{\partial r} = -\phi r \frac{\partial \rho}{\partial p} \frac{\partial p}{\partial t} = -\phi c_o \rho r \frac{\partial p}{\partial t} \ . \tag{7.24}$$

where c_o is the iso-thermal compressibility for oil; see also Section 4.4.3. Under steady-state conditions the pressure derivative $\partial p/\partial t$ should remain constant, say equal to an unknown constant C_1. As before, we can assume that ρ is constant for single-phase oil, and the mass balance equation therefore reduces to

$$\frac{d(vr)}{dr} = -C_1 \phi c_o r \ . \tag{7.25}$$

This is again a first-order differential equation that can be integrated to give

$$vr = -\frac{1}{2} C_1 \phi c_o r^2 + C_2 \ . \tag{7.26}$$

With the aid of boundary condition (7.12) that was also used for the steady-state solution, we can solve for the integration constant C_2. In addition, we know that $v = 0$ at $r = r_e$, which allows us to solve for C_1. After substitution in equation (7.26) and reorganization of the result we find

$$vr = \frac{B_o q_{o,sc}}{2\pi h}\left(1 - \frac{r^2 - r_w^2}{r_e^2 - r_w^2}\right) \approx \frac{B_o q_{o,sc}}{2\pi h}\left(1 - \frac{r^2}{r_e^2}\right) \ . \tag{7.27}$$

Similarly to what we did in the steady-state situation, we can now combine equations (7.5), (7.8) and (7.27) to arrive at the differential equation for semi steady-state radial flow:

$$\frac{dp}{dr} = -\frac{\mu B_o q_{o,sc}}{2\pi k h}\left(\frac{1}{r} - \frac{r}{r_e^2}\right) \ . \tag{7.28}$$

Integration of the equation results in

$$p = -\frac{\mu B_o q_{o,sc}}{2\pi k h}\left(\ln r - \frac{1}{2}\frac{r^2}{r_e^2}\right) + C_3 \ . \tag{7.29}$$

Using boundary condition (7.15) to solve for the integration constant C_3 and substitution of the result in equation (7.29) gives us an expression for p as a function of r under semi steady-state flow conditions:

$$p = p_R + \frac{\mu B_o q_{o,sc}}{2\pi k h} \left[\ln\left(\frac{r_e}{r}\right) - \frac{1}{2}\left(1 - \frac{r^2}{r_e^2}\right) \right] . \tag{7.30}$$

In particular, the IPR for semi steady-state flow can now be written as:

$$p_R - p_{wf} \approx -\frac{\mu B_o q_{o,sc}}{2\pi k h} \left[\ln\left(\frac{r_e}{r_w}\right) - \frac{1}{2} \right] . \tag{7.31}$$

The difficulty with expressions (7.30) and (7.31) is that the pressure p_R at the external boundary, which is gradually decreasing just like the pressure in any point of the reservoir, can usually not be determined. However, the average pressure $p_{R,av}$ can often be determined from the pressure response in a well after shut-in, a procedure known as *pressure transient analysis* or *well testing*; see e.g. Dake (1978). To express equation (7.31) in terms of the average reservoir pressure, we can proceed along the same lines as we did for steady-state flow above, which results in

$$p_{R,av} - p_{wf} \approx -\frac{\mu B_o q_{o,sc}}{2\pi k h} \left[\ln\left(\frac{r_e}{r_w}\right) - \frac{3}{4} \right] . \tag{7.32}$$

7.4.3   Single-phase gas flow

In the case of single-phase gas flow we can no longer justify the assumption of constant density in the near-wellbore area that as we did for single-phase oil. Therefore, the mass conservation equation (7.4) should now be written, for steady-state conditions, as

$$\frac{\partial(v\rho r)}{\partial r} = 0 \ . \tag{7.33}$$

The corresponding boundary condition at the wellbore radius becomes:

$$v\rho\big|_{r=r_w} = \frac{q_g \rho}{2\pi h r_w}\bigg|_{r=r_w} = \frac{q_{g,sc}\rho_{g,sc}}{2\pi h r_w} \ , \tag{7.34}$$

where we have used the fact that the mass flow rate at surface and downhole are identical under steady-state conditions. We can now solve equation (7.33) and determine the integration constant with the aid of boundary condition (7.34) in the usual fashion. Next we can combine equations (7.5) and (7.9), and together with the equation of state for gas (7.7), we then arrive at the following set of equations to describe single-phase gas flow in the near well-bore area:

$$\begin{cases} \dfrac{dp}{ds} = -\dfrac{\mu}{k}v - \beta\rho v^2, \\[2mm] v = \dfrac{\rho_{g,sc}q_{g,sc}}{2\pi h}\dfrac{1}{\rho r} \ , \\[2mm] \rho = \dfrac{Mp}{ZRT_{abs}} \ . \end{cases} \tag{7.35, 7.36, 7.37}$$

This set of equations strongly resembles equations (5.27) to (5.29) as defined in Chapter 5 to describe the flow of gas in pipes. The equations are non-linear because ρ, μ and Z are functions of the unknown pressure p. The differential equation (7.35) requires one boundary

condition, for which we can use equation (7.15). Just as was done for pipe flow, the equations can be solved with the aid of a standard numerical integration routine in MATLAB.

Alternatively, the equations can be linearized through the use of a *real-gas pseudo-pressure* defined as:

$$m(p) = \left.\frac{\mu}{\rho}\right|_{p=p_{ref}} * \int_{p_{ref}}^{p} \frac{\rho}{\mu} dp = \left.\frac{\mu Z}{p}\right|_{p=p_{ref}} * \int_{p_{ref}}^{p} \frac{p}{\mu Z} dp \ , \tag{7.38}$$

where p_{ref} is an arbitrary reference pressure expressed in Pa; see Hagoort (1988). For a given gas composition, and corresponding relationships for μ and Z as function of p, we can determine a one-to-one relationship between p and $m(p)$, through numerically integrating equation (7.38). If we disregard the inertia coefficient β, we can now simply use all the results that were obtained for single-phase oil flow, by replacing p with $m(p)$, and by changing the oil properties μ_o, k_o, B_o and $q_{o,sc}$ to gas properties μ_g, k_g, B_g and $q_{g,sc}$. The value of the arbitrary reference pressure p_{ref}, is not relevant because we are only interested in pressure differences, and not in absolute pressures. We will not further consider the use of pseudo-pressures in this course, and refer to Hagoort (1988) for details.

If the difference between the average reservoir pressure $p_{R,av}$ and the flowing BHP p_{wf} is not too large we can use constant average values μ_{av} and Z_{av} in the definition of the pseudo-pressure. In this case, integration shows that the pseudo-pressure can be approximated by

$$m(p) = \frac{p^2 - p_{ref}^2}{p_{ref}} \ . \tag{7.39}$$

Expression (7.39) can now be used to convert any of the IPRs for single-phase oil flow for use in single-phase gas flow analysis. For example, substitution in the semi-steady state IPR (7.32) and making the necessary changes from oil to gas properties results in:

$$p_{R,av}^2 - p_{wf}^2 \approx -\frac{\mu_{av} B_{g,av} q_{g,sc}}{2\pi k_g h} \left[\ln\left(\frac{r_e}{r_w}\right) - \frac{3}{4} \right] \ . \tag{7.40}$$

The form of this quadratic inflow performance relationship is shown in Figure 7.4. We will not consider the effects of the inertia coefficient β, and refer to Dake (1978) or Hagoort (1988) for further information.

7.4.4 Multi-phase flow

The straight line IPR for single-phase oil flow needs modification if the pressure drops below bubble-point pressure and the oil becomes saturated. There are two modifications in use, proposed by Vogel (1968) and Fetkovich (1973):
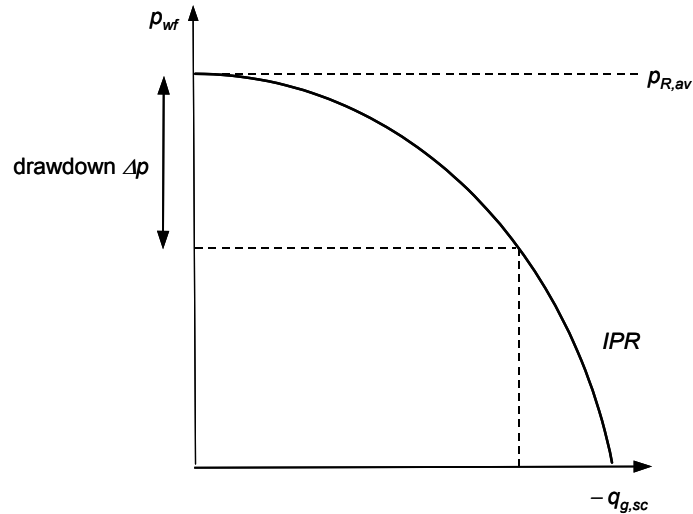
Figure 7.4: Non-linear inflow performance relationship for a gas well.

$$\text{Vogel:} \quad \frac{q_{o,sc}}{q_{o,sc,max}} = 1 - \alpha\left(\frac{p_{wf}}{p_R}\right) - (1-\alpha)\left(\frac{p_{wf}}{p_R}\right)^2 \text{ , with } \alpha = 0.2 \text{ ,} \qquad (7.41)$$

$$\text{Fetkovitch:} \quad \frac{q_{o,sc}}{q_{o,sc,max}} = \left[1 - \left(\frac{p_{wf}}{p_R}\right)^2\right]^n \text{ ,} \qquad (7.42)$$

where $q_{o,sc,max}$ is the AOFP, i.e. the value of $q_{o,sc}$ when p_{wf} is zero. Note that this zero pressure will not actually be achievable in practice. Vogel's IPR curve resulted from carrying out a large number of numerical simulations and looking for a best fit. By choosing the value of n, Fetkovich's IPR curve can fit field data reasonably well.

7.5 Formation damage and skin

The IPRs derived above assume that the radial permeability is everywhere constant. In practice, this is not the case. In addition to geological variations (which we ignore, assuming they average out in some sense), the well may be impaired. During the drilling of the well there is penetration of alien fluids into the reservoir rock, which may reduce the permeability of the rock around the well and therefore reduce the rate of oil inflow. This reduction in permeability is called formation damage or impairment.

We currently have a good understanding of the fundamental causes of formation damage, thanks to experimental and theoretical research over the past years. For an extensive overview, see Civan (2000). From the moment the drill bit first penetrates the reservoir section until the well is put on production, the reservoir rock is exposed to a series of operations that can cause damage:

- *Mechanical*
  The drilling itself can create mechanical damage, with pore collapse and particle re-arrangement.
- *Solids*
  Solids come into contact with the rock formation, such as drilled rock, solid material

added to the drilling mud or metal debris. If small enough, the solids can be swept into the formation and block the pores. If larger, the solid particles cannot enter into the rock pores, but are deposited on the surface of the rock. Some of these solids will be swept away again when the well is put on production, but not all, as shown in Figure 7.5, showing a thin layer of residual mud solids.

- *Fluids*
  Fluids used in well construction can also cause formation damage. Such fluids are composed of water, oils, salts, acids, surfactants and many other chemicals. These may interact with the reservoir rock and fluids, causing detachment of fine particles, flocculation, wettability change, precipitation, emulsion formation or fluid saturation changes. In particular, the pores may be lined with clay which may swell disastrously, completely blocking the pore.

- *Phase changes*
  Changes in pressure and temperature in the oil and water may result in phase changes, with precipitation of waxes, asphaltenes, or scale which deposit themselves in the pores.

- *Microbial*
  Lastly, microbes introduced into the well, or possibly indigenous in the reservoir in a dormant state, may multiply forming deposits in the pores.

- The effect of all these damage mechanisms is to reduce the permeability of the reservoir rock over a relatively small region around the wellbore. This small damaged region is called the 'skin' of the well. This skin gives rise to an additional pressure drop, as shown in Figure 7.6, so that the well produces less than expected.

The additional pressure drop can be taken into account in the IPR as follows. For example, the semi steady-state solution (7.32) can now be modified to give

$$p_{R,av} - p_{wf} - \Delta p_{skin} = -\frac{\mu B_o q_{o,sc}}{2\pi kh}\left[\ln\left(\frac{r_e}{r_w}\right) - \frac{3}{4}\right] . \tag{7.43}$$
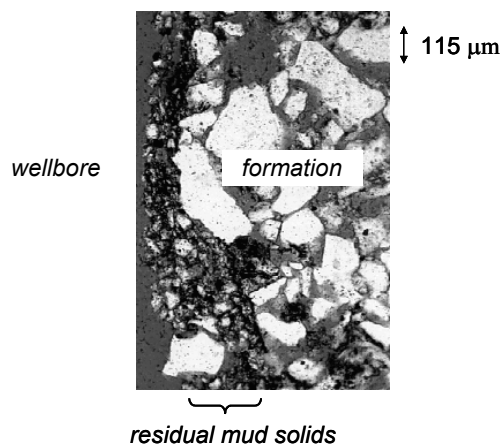
Figure 7.5: Residual mud solids.
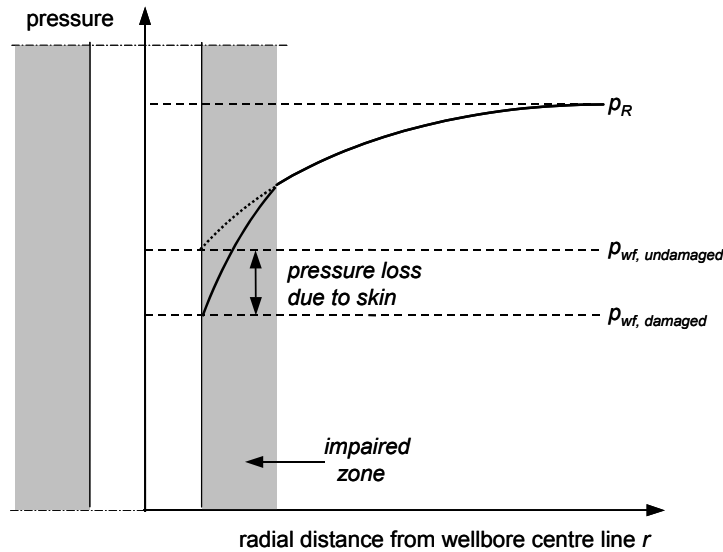
Figure 7.6: The extra pressure drop caused by skin, at a given flow rate.

Introducing the dimensionless skin factor S defined by

$$\Delta p_{skin} = \frac{\mu B_o q_{o,sc} S}{2\pi kh} \ ,$$ (7.44)

we can rewrite the steady state solution as

$$p_{R,av} - p_{wf} = -\frac{\mu B_o q_{o,sc}}{2\pi kh}\left[\ln\left(\frac{r_e}{r_w}\right) - \frac{3}{4} + S\right] .$$ (7.45)

Accordingly, the formula for the PI becomes

$$J = \frac{-q_{o,sc}}{\overline{p} - p_{wf}} = -\frac{2\pi kh}{\mu B_o\left[\ln\left(\dfrac{r_e}{r_w}\right) - \dfrac{3}{4} + S\right]} \ .$$ (7.46)

Note the minus sign because we have assumed a positive flow direction from the well into the reservoir. The value of the skin S can be determined from transient well tests; see e.g. Dake (1978) or Economides et al. (1994). If the skin is high, then remedial measures may be required e.g. stimulating the well with acid to remove the damage.

If a well is tested, it may appear that the skin S is non-zero. But this may not be due to formation damage. It may be due to the completion. If the well is gravel-packed, the permeability of the gravel will be different from that of the reservoir rock. Thus the gravel pack may give less pressure drop, resulting in negative skin. On the other hand, the gravel pack itself can be heavily impaired during installation or subsequent production. So, positive skin could result from the gravel pack. Perforations can give rise to negative skin, if they provide a very effective path for the oil to flow into the well. Often, they contain debris from the shooting of the perforations, and have a crushed zone of rock around them, both effects contributing to positive skin. Fractures, whether natural or produced by hydraulic fracturing will result in easier inflow, and thus negative skin.

7.6 Multi-layer inflow performance

If a well is completed on more than one layer, with different reservoir properties and different reservoir pressures, then the combined inflow performance can be readily calculated, provided the individual IPRs are both linear.

As shown in Figure 7.7, for a given value of p_{wf}, the total production rate $q_{o,sc}$ can be calculated by calculating the individual contributions $q_{o,sc,1}$ and $q_{o,sc,2}$, and adding them:

$$q_{o,sc,1} = -J_1\left(p_{R,1} - p_{wf}\right), \quad q_{o,sc,2} = -J_2\left(p_{R,2} - p_{wf}\right),$$
$$q_{o,sc} = q_{o,sc,1} + q_{o,sc,2} = -J_1 p_{R,1} - J_2 p_{R,2} + \left(J_1 + J_2\right) p_{wf} .$$

$$(7.47)$$

Thus the production rate still varies linearly with p_{wf}. Note however that this formula applies only for values of p_{wf} lower than the lower of the two zone pressure. Above this pressure, part of the production from one zone will be injected into the other zone. This phenomenon, which is often referred to as *cross flow,* is illustrated in Figure 7.8. If the well is closed-in at surface, a steady-state situation will develop in which equal amounts are produced from and injected into the respective reservoir units. Cross-flow can seriously impair the reservoir into which the injection takes place.
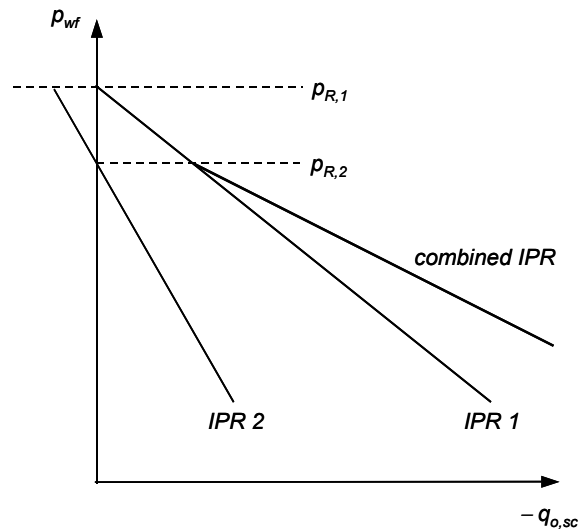
Figure 7.7: Two-layer inflow performance.
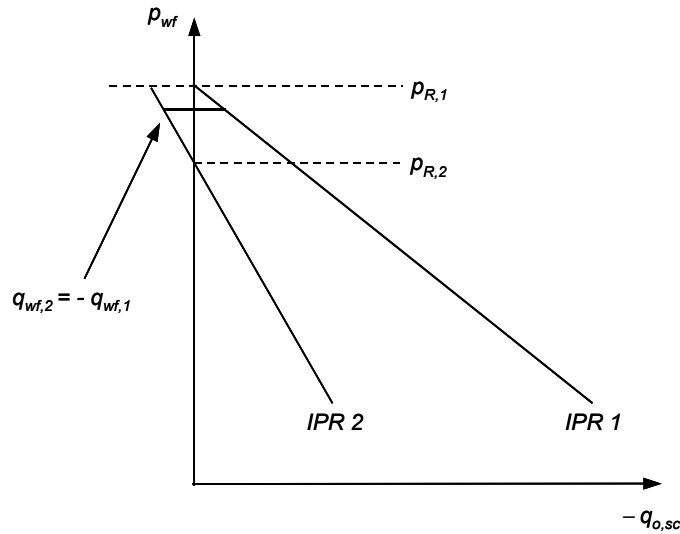
Figure 7.8: Cross-flow between two reservoir units in a closed-in well.

7.7   Related topics that have not been considered in this chapter

- For all wells, a number of near wellbore factors have not been considered at all, such as the effect of on inflow performance of well deviation, permeability anisotropy, fractures, perforation pattern, washed out well sections, gravel packs and slotted liners, fractures.
- In horizontal wells the above considerations must be applied 'locally'. At any point in the well, the inflow will be proportional to the local drawdown. But as we move along the well, the drawdown will change, being influenced by the flow in the well itself. In a long horizontal well (say more than 500 m) these effects can be substantial; see Dikken (1990). For a discussion and further references on horizontal well inflow performance, see Joshi (1991) and Economides et al. (1998).

For further reading on the topic of inflow performance, we refer to the textbooks of Brown (1984), Beggs (1991), Golan and Whitson (1991), Economides et al. (1994), and Economides et al. (1998).

8 Oil well productivity

8.1 What will be covered in this chapter?

- Methods of analysing the production from an oil well; the intake pressure curve for analysing situations in which inflow performance from the reservoir is important; the tubing response curve for analysing situations in which well or surface conditions are changed.
- The role of well productivity analysis in field development planning and field management.
- Short-term and long term optimisation of well performance.

8.2 Optimising well productivity

To optimise the productivity from an oil well, we need tools to predict its flow behaviour. For example, in designing a completion for a new well, we need to assess the effect of the tubing size on well productivity, and predict the productivity change as the reservoir pressure declines. Similarly, in a producing well, we need to decide when it makes economic sense to carry out operations to increase the productivity, for example whether the skin is significantly affecting production and the well needs stimulating, or when we should change out the tubing.

8.3 Oil well completions

A typical completion for a traditional vertical or deviated oil well was shown schematically in Figure 2.1. The total pressure drop between the reservoir and the wellhead is made up of the drawdown associated with the inflow from the reservoir and the vertical flow pressure drop. Typically, the vertical pressure drop makes up 75% of the total pressure drop. In Figure 2.2, a horizontal well completion is shown schematically. In this case the total pressure drop is made up of the inflow pressure drop, the pressure drop along the horizontal well and the vertical flow pressure drop.

These figures are only schematic. We note the following points:

- The dimensions are not correct in the schematic diagrams. The vertical depth of the wells is usually between 1500 and 5000 m, the completed interval for a vertical well is usually between 10 and 200 m, and the length of a horizontal well can vary from 20 - 1000 m.
- 'Vertical wells' are never vertical. They are deviated, and often highly deviated. However, the section over the reservoir is usually vertical or near vertical.
- Vertical wells are usually cased and perforated.
- Horizontal wells are usually completed as open holes, with a slotted liner or wire-wrapped screen lining the borehole. This is reverting to technology which was abandoned earlier for vertical wells, because it gave little control, and the screens were prone to impairment. But for horizontal wells, it is difficult to complete as cased hole, although it is sometimes done.

In this course we consider mainly vertical wells, concentrating on inflow and vertical flow.

8.4 Production rate of a vertical well operating at given tubing head pressure

A vertical well is being operated at a fixed THP p_{tf}. What is the production rate? The flow system between the reservoir and the tubing head can be broken down into

- the inflow into the well, and
- the flow up the tubing to the tubing head.

As we have seen in Chapter 7, the inflow into the well is affected by

- the reservoir pressure,
- the reservoir properties,
- the skin, including 'skin' due to the completion, and
- the properties of the reservoir fluids.

However, as we have seen, all these effects can be brought into a single relationship, the inflow performance of the well. Assuming that we have a linear inflow performance, with productivity index J, then

$$p_{wf} = p_R + \frac{q_{o,sc}}{J} \, , \tag{8.1}$$

where a positive value of $q_{o,sc}$ implies injection and a negative value production. Similarly, the flow up the tubing is affected by

- the tubing size and other completion parameters,
- the flow regime in which the well operates, and
- the fluid properties.

These effects cannot be brought into a single relationship which predicts the pressure drop over tubing. However, as we saw in Chapter 8, if the THP is specified, and all other factors such as tubing diameter are held constant, then we can construct an *intake pressure curve*, which shows the dependence of the BHP on flow rate $q_{o,sc}$.

$$p_{wf} = F_{ip}(q_{o,sc}) \, , \tag{8.2}$$

where F_{ip} is the intake pressure curve function. The actual form of F_{ip} depends on the other parameters such as THP, tubing diameter, GLR and watercut.
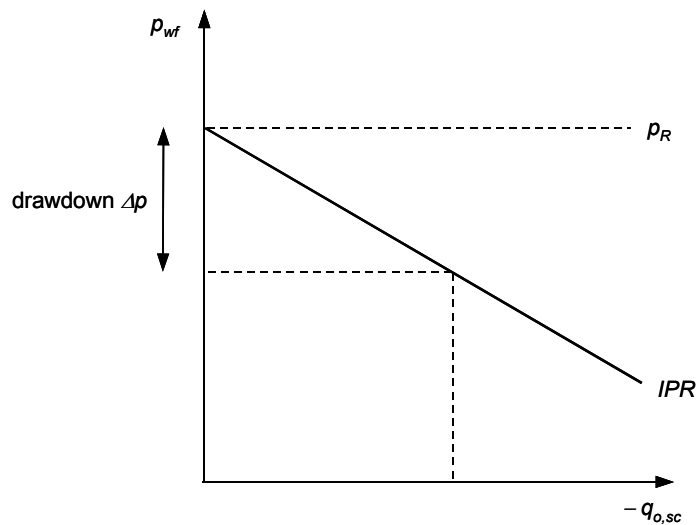
Figure 8.9: Inflow performance curve for constant PI.
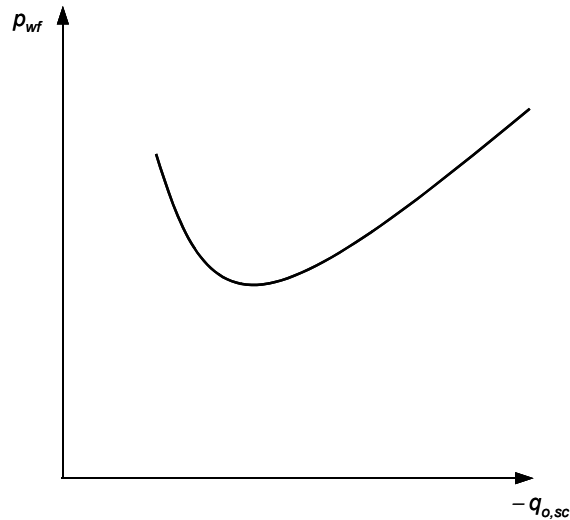
Figure 8.10: Tubing intake pressure curve for varying production rate.

The inflow performance curve (Figure 7.1 of Chapter 7) is shown as Figure 8.9. The intake pressure curve (Figure 6.8 of Chapter 6) is shown as Figure 8.10. Combining these two curves gives us Figure 8.11. This is an example of the combination of an operating point performance curve (the tubing intake pressure curve) and a pressure drop performance curve (the IPR) as was discussed in Section 2.4 where we covered 'nodal analysis'. The curves have two intersection points, and as derived in Section 2.4, the intersection at the right corresponds to a stable operating point and gives us the actual flow rate $q_{o,sc}$ and the actual BHP p_{wf}. The intersection at the left represents an unstable, and therefore physically unrealistic operating point.

Recall that the tubing intake pressure curve has been derived for a fixed THP. If we lower the THP, also the BHP will drop, and the intake pressure curve will shift down. In addition the curve may somewhat change in shape, because the boundaries between the various flow regimes in the tubing may also move. However, the overall effect will be a shift of the stable operating point to the right, corresponding to an increased flow rate. Conversely, if we
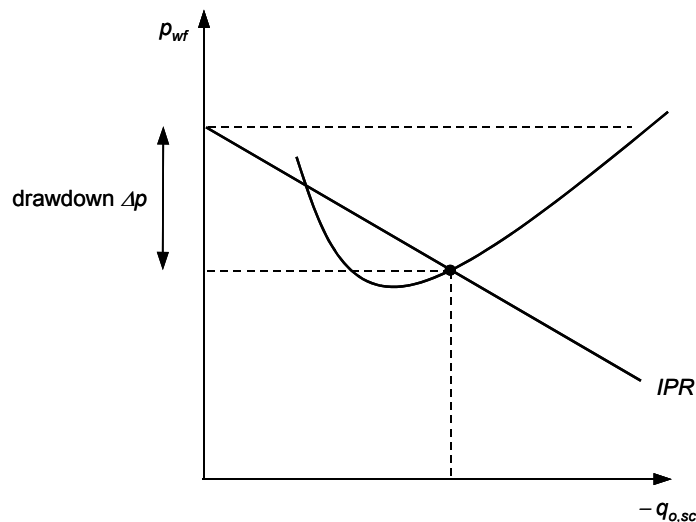
Figure 8.11: Combined plot of inflow performance and intake pressure curves, determining actual production rate.

increase the THP, the production rate will drop. If we increase the THP too much, the well will not flow at all anymore; see Figure 8.12. A similar effect occurs if THP remains constant but the reservoir pressure drops, a situation that frequently happens when an oil field is being depleted. If it is not possible to reduce the THP any further, it may sometimes be possible to bring the well back to production by installing a new tubing with a lower pressure drop. Interestingly, this may be either a larger or a smaller diameter tubing, depending on factors like watercut and GOR. Alternatively, it may be necessary to install a form of artificial lift, such as gas lift, an electric submersible pump (ESP) or a beam pump.

8.5 Production rate of a vertical well operating through a surface choke

In Section 8.4 we assumed that the THP and the reservoir pressure were constant, and calculated the resulting flow rate from the pressure drops over the tubing and the reservoir. However, usually the THP itself will also vary with flow rate. To analyse this effect we need also to consider the flow path downstream of the wellhead, up to a point were we can assume that the pressure remains more or less constant. That point will normally be the first separator which is usually operated with automatic pressure control. The manifold pressure, which is almost the same as the separator pressure, is therefore normally a good system boundary for a complete wellbore pressure drop analysis. Recall that at the other end of the system, i.e. in the reservoir, we have also assumed constant pressure, or at least a pressure that varies only very slowly over time. In conclusion, our problem is to determine the flow rate by considering the pressure drop over the following elements:

- the reservoir (including the near wellbore area and the completion),
- the tubing up to the tubing head,
- the choke, and
- the flowline,

given a constant pressures in the reservoir and the manifold, and constant fluid composition (GOR, watercut).

Here we will restrict ourselves to the analysis of a three-component system consisting of a choke, a tubing and the near wellbore. For this type of analysis it is common practice to choose the analysis node at the top of the tubing and to establish an operating point
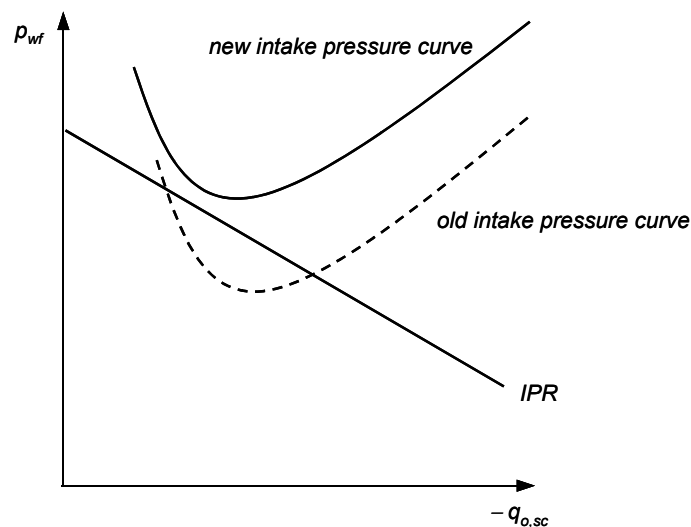
Figure 8.12: Effect of a too large increase in THP: there is no intersection any more between the intake pressure curve and the IPR. As a result the well will no longer flow.

performance curve for the choke and a combined pressure drop performance curve for the tubing and the near wellbore.

For a given flow rate, the inflow performance curve determines the flowing BHP p_{wf}. Using this pressure, and for given tubing diameter, GOR and watercut, the THP p_{tf} can be determined from a wellbore pressure drop analysis, either using a computer or using gradient curves. This gives a relationship between the flow rate $q_{o,sc}$ and the THP p_{tf} which is called the *tubing performance curve*. The procedure for use with gradient curves is illustrated in Figure 8.13. The tubing performance curve gives a total picture of the *deliverability* of the well. Note that the name is slightly misleading. The tubing performance curve is not just dependent on the ability of the tubing to transport the fluids; it also contains the performance of the reservoir and the completion, through the inflow performance relationship. As the reservoir pressure declines, the tubing performance curve will change. So a better name would be the *well performance curve*, but that is not usually used.

The flow through the choke is governed by the linear *choke performance curve* shown in Figure 6.9 of Chapter 7, assuming the flow is above critical. Hence, we can now plot the choke performance curve and the tubing performance curve together to determine the operating point at the tubing head. This has been done for a series of choke performance curves, corresponding to different choke sizes, in Figure 8.14. It has been assumed that the pressure directly downstream of the choke remains constant and equal to the manifold pressure p_m. In theory it is again is possible to obtain two points of intersection, although this is not often the case if we analyse realistic well and choke configurations. It can be proved, following the analysis method from Section 2.4, that the operating point at the lower flow rate will always be unstable.
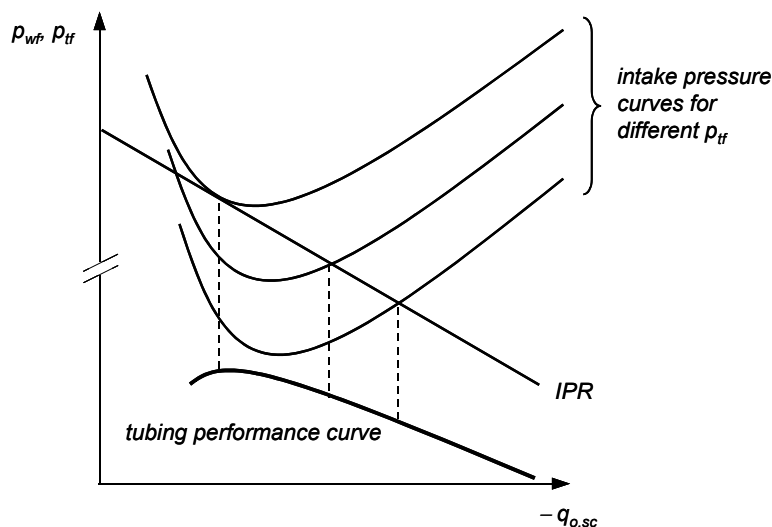
Figure 8.13: Construction of a tubing performance curve: For different THPs p_{tf} we establish the stable operating points at the bottom of the tubing from the intersections of the intake pressure curves and the IPR. Each operating point corresponds to a certain flowing BHP p_{wf} and a flow rate $q_{o,sc}$. Next we compute the pressure drop over the tubing for each of the flow rates, as indicated by the vertical dashed lines. Subtracting the tubing pressure drops from the BHPs gives us the THPs as a function of flow rate, in other words, the tubing performance curve.
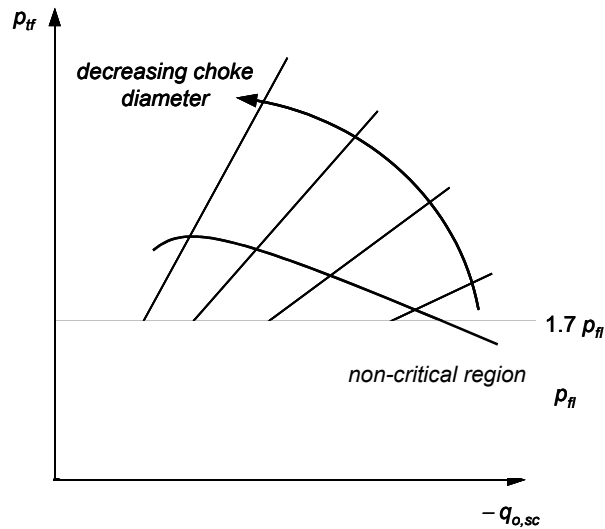
Figure 8.14: Combined plot of tubing and choke performance curves, determining actual production rate.

8.6   Summary of analysis methods

As described above, there are two commonly used methods for analysing the production from oil wells. In each method the behaviour of system to be analysed is reduced to two relationships between pressure and flow rate: a pressure drop performance curve (which determines an unknown pressure *downstream* from a known pressure) and an operating point performance curve (which determines an unknown pressure *upstream* of a known pressure).

In the first method, the analysis is performed downhole. Using the condition at the tubing head and the pressure drop in the tubing, the *tubing intake pressure curve* is calculated at the bottom of the well. The intersection of this curve with the *inflow performance relation (IPR)* determines the production rate. This was illustrated in Figure 8.11. In the second method, the analysis is performed at the tubing head. Using the inflow performance curve and the pressure drop in the tubing, the *tubing performance curve* is calculated at the tubing head. The intersection of this curve with the *choke performance curve* determines the production rate. This was illustrated in Figure 8.14.

As discussed in Chapter 2, the choice of the analysis nodes at either the top or the bottom of the tubing is rather arbitrary and was determined by use of gradient curves for tubing flow before the widespread use of computers. In a cascade system of components the analysis could be performed anywhere at or in between the two system boundaries. Indeed using a computerized analysis method it is would be logical to analyse the pressure drop over the entire system with an algorithm marching from one boundary to the other. The program would than need to change the flow rate in iterative fashion until the pressure drop over the system exactly matches the known difference in pressure between the two boundaries. The advantage of displaying the traditional combinations of a pressure drop performance curve and an operating point performance curve is that they provide quick insight in the flow behaviour of two separate system parts in one graph: one downstream and one upstream of the analysis node. For this reason, most computer programs for wellbore flow analysis still have an option to display the traditional intake pressure and performance curves.

8.7   Field development planning and field management

Well performance analysis plays a crucial role in field development planning for new fields and the management of producing fields.

For a new field, critical questions that must be answered are:

- What form of completion must be installed in the well, and in particular what size tubing?
- For the chosen tubing size, what is the initial production rate of the well, and how will this vary with time?
- How long will the well be able to produce. When is the optimum time to change the tubing size or switch to artificial lift (pumping or gas lifting)?

For a producing field, the following must be considered :

- Is the well producing as expected?
- Is the well impaired, and in need of stimulation to remove the skin?
- Can the well production be improved by changing out the tubing or installing artificial lift? Is the cost justified?
- Can the well performance be improved by increasing the perforated interval?
- Can the well performance be improved by lowering the THP or changing out the choke?
- How long will the well produce? Do plans need to be made for artificial lift?

These issues cannot be decided by a production engineer in isolation; it must make economic sense to increase the production of a single well within the total field plan, taking into account the capacity of the surface facilities. However, the production engineer can greatly improve the economic return from a field by continuous monitoring of all wells and remedial action when the production declines.

The above questions divide into two types: questions about the behaviour of the well in the short term; and questions about the long-term behaviour of the well. We consider these separately.

8.8   Short-term optimisation of well performance

8.8.1   Improved inflow performance

If the well has become impaired then it can be stimulated to improve the inflow performance. Similarly, inflow performance may be improved by additional perforating. To determine the increased production from such operations, we analyse what happens downhole. As shown in Figure 8.15, we draw in the current inflow performance and the improved inflow performance after the operational treatment. The increase in production can be calculated. Generally, for such operations, the increased production more than covers the operational cost.
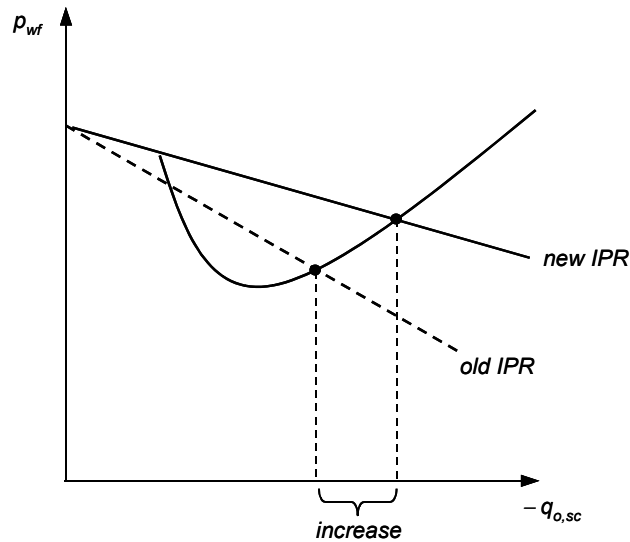
Figure 8.15: Increased production due to improved inflow performance.

8.8.2 Changing the tubing or choke size

Increasing, or decreasing, the tubing diameter can improve production. Changing the choke size can do the same. Analysis of these operations is best done at the tubing head. Changing out a tubing string is expensive, and generally needs to be justified on a long term basis (see below). Changing out a choke is a cheap operation. As shown in Figure 8.16, there is a maximum choke size above which the choke will no longer operate in the critical regime. As explained in Section 6.6, operation in the critical regime is often preferred because it decouples the upstream flow behaviour from the downstream behaviour, and thus shields the well from pressure fluctuations in the production facilities. Associated with the maximum choke size is a maximum flow rate. Sometimes it is required to *bean back* a well, i.e. to reduce the flow rate by installing a smaller choke. A frequently occurring reason for flow reduction is to prevent or delay water or gas coning, or to reduce the amount of gas or water produced once the cone has reached the well. As can be seen in Figure 8.16, there is also a practical minimum choke size, and therefore a minimum flow rate, below which the well will not produce anymore.
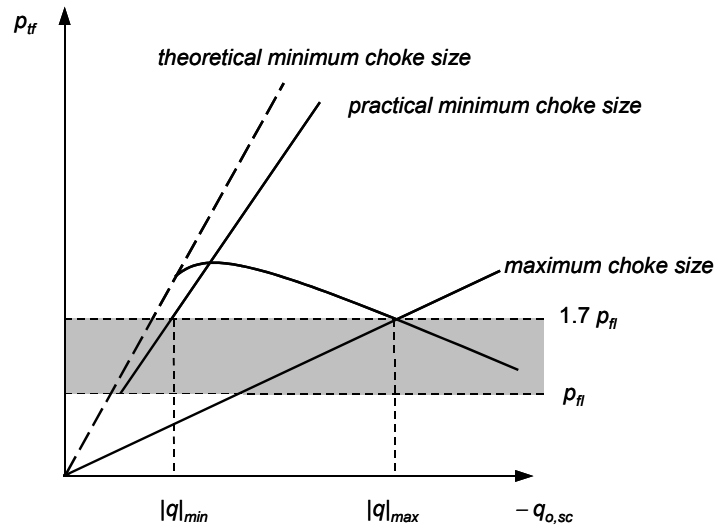
Figure 8.16: Minimum and maximum choke size.

8.9 Long-term optimisation of well performance

8.9.1 Effect of declining reservoir pressure

Analysis of the effect of declining reservoir pressure is best done downhole, using the intake performance curve. Assuming the PI remains constant (no impairment) while the reservoir pressure declines, then as shown in Figure 8.17, the inflow performance curve will move vertically down the pressure axis with time, but keeping the same slope. The corresponding reduction in production can be calculated. If the reservoir pressure drops too far, another (usually smaller) tubing size will need to be installed. By plotting the intake pressure curve for this tubing on the same figure, it will be possible to see for how long this will extend the life of the well, and whether the cost is justified in terms of the extra oil recovered.
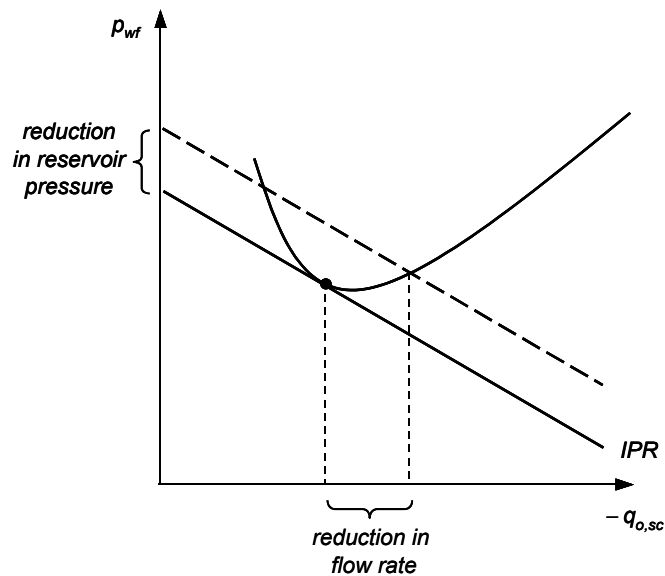
Figure 8.17: Effect of declining reservoir performance on production.

8.9.2 Installation of gas lift

Gas lifting is one of the commonest methods of artificial lift. By injecting extra gas downhole into the tubing, the fluid column becomes lighter, and the total production is increased. We have seen in Chapter 5, that there is an optimum GOR which will minimize the pressure drop over the tubing at a given liquid flow rate; see Figure 6.6. Too much gas increases the pressure drop because of frictional effects. We therefore expect that for a producing well there will be an optimum GOR at which we can inject gas to maximize the oil production rate. This is illustrated in Figure 8.18, which shows the tubing performance curves for varying GOR.

For low GOR, the THP is below the critical choke pressure which may result in erratic well performance. Plotting the production rate as a function of GOR shows that as the GOR is increased, the production increases to a maximum of about 535 bpd, at a GOR of 800. Above this GOR, the oil production starts to decline again. Moreover, we see that adding lift gas to the system is initially very efficient, but the efficiency declines as more gas is added. An increase of 200 scf/stb from 200 to 400 scf/stb gives an increase in production of 325 bpd, but further increases to 600 and 800 give only an additional 140 or 70 bpd. The additional oil must be worth more than the cost of injecting the gas. Thus, the economic optimum GOR may be much lower than 800 scf/stb, the GOR at which the well produces at the maximum rate.

8.10 Productivity of horizontal wells

The analysis of horizontal well productivity requires, in principle, the same techniques as are used for wells with a vertical completion over the reservoir interval. However, the flow in the horizontal section gives additional complications:

- The pressure falls from the 'toe' of the well to the 'heel'. Thus the 'drawdown', the difference between the pressure in the well and the reservoir pressure, varies along the length of the well. The rate of inflow into the well varies along the well.
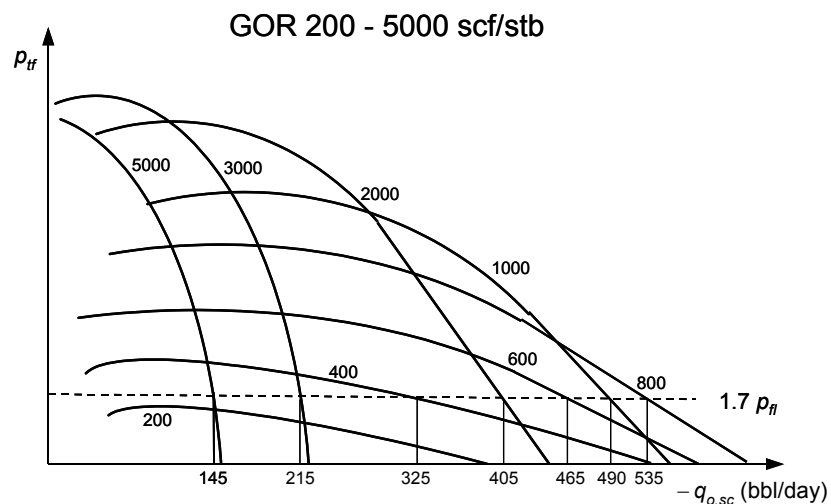
Figure 8.18: Effect of GOR on the production from a well.

- In both vertical and horizontal wells with long completion intervals, the formation properties will vary, resulting in different inflow performance at different points of the well. In uncased holes, and especially uncased horizontal wells, production logging techniques still need to be developed to detect these differences.
- Horizontal wells flowing a mixture of liquid and gas can exhibit difficult multi-phase flow behaviour. Since the well is not perfectly horizontal, liquid can accumulate in lower sections of the well, and cause slugging, or shutting-off of production.

Initial production from horizontal wells is usually high, because the open hole completion reduces impairment and the long production interval helps the inflow. The long-term management of horizontal wells may become a problem, when they start to decline in production or produce water or gas. For more information on horizontal well performance we refer to the textbooks of Joshi (1991), Economides et al. (1994), and Economides et al. (1998). For specific information on the effects of horizontal well pressure drop, see Dikken (1990).

8.11 Related topics that have not been considered in this chapter

- Production from more than one reservoir interval, with different reservoir pressure and inflow performance.
- Gas well performance.

For information on these topics and for further reading on well performance in general, we refer to the textbooks of Nind (1964), Golan and Whitson (1991), Economides et al. (1994), and Economides et al. (1998). The first two books are out of print, but are worth to be looked for in a library.

Appendix A – SI units and field units

A.1 Conversion factors

To obtain SI units, multiply a quantity given in field units with the conversion factor specified in Table A.1.

Table A.1: Conversion factors to convert field units to SI units.				
Physical quantity	*Dimension*	*SI units[1]*	*Field units*	*Conversion factor from field units to SI units[2]*
Area	$[L^2]$	m^2	ft^2	$9.290\ 304 * 10^{-2}$ (exact)
		m^2	$in.^2$	$6.451\ 6 * 10^{-4}$ (exact)
Compressibility	$[L\ m^{-1}\ t^2]$	Pa^{-1}	psi^{-1}	$1.450\ 377 * 10^{-4}$
Density	$[L^{-3}\ m]$	$kg\ m^{-3}$	°API	$141.5*10^3\ /$ $(131.5 + °API)$ (exact)
		$kg\ m^{-3}$	$lbm\ ft^{-3}$	$1.601\ 846 * 10^1$
		$kg\ m^{-3}$	$lbm\ gal^{-1}$	$1.198\ 264 * 10^2$
Energy	$[L\ m^2\ t^{-2}]$	J	cal	4.184 (exact)
Flow rate	$[L^3\ t^{-1}]$	$m^3\ s^{-1}$	bpd	$1.840\ 131 * 10^{-6}$
		$m^3\ d^{-1}$	bpd	$1.589\ 873 * 10^{-1}$
		$m^3\ s^{-1}$	$ft^3\ d^{-1}$	$3.277\ 413 * 10^{-7}$
		$m^3\ d^{-1}$	$ft^3\ d^{-1}$	$2.831\ 685 * 10^{-2}$
Force	$[L\ m\ t^{-2}]$	N	lbf	$4.448\ 222$
Gas-oil ratio (GOR)	[-]	$m^3\ m^{-3}$	$ft^3\ bbl^{-1}$	$1.781\ 076 * 10^{-1}$
Length	$[L]$	m	ft	$3.048 * 10^{-1}$ (exact)
		m	in.	$2.54 * 10^{-2}$ (exact)
Mass	$[m]$	kg	lbm	$4.535\ 924 * 10^{-1}$
Permeability	$[L^2]$	m^2	mD	$9.869\ 233 * 10^{-16}$
Power [3]	$[L\ m^2\ t^{-3}]$	W	hp	$7.456\ 999$
Pressure [4]	$[L^{-1}\ m\ t^{-2}]$	Pa	psi	$6.894\ 757 * 10^3$
Pressure gradient	$[L^{-2}\ m\ t^{-2}]$	$Pa\ m^{-1}$	$psi\ ft^{-1}$	$2.262\ 059 * 10^4$
Productivity Index (PI)	$[L^4\ m^{-1}\ t]$	$m^3\ s^{-1}\ Pa^{-1}$	$bpd\ psi^{-1}$	$2.668\ 884 * 10^{-10}$
		$m^3\ d^{-1}\ Pa^{-1}$	$bpd\ psi^{-1}$	$2.305\ 916 * 10^{-5}$
Specific PI	$[L^3\ m^{-1}\ t]$	$m^2\ s^{-1}\ Pa^{-1}$	$bpd\ psi^{-1}\ ft^{-1}$	$8.756\ 182 * 10^{-10}$
		$m^2\ d^{-1}\ Pa^{-1}$	$bpd\ psi^{-1}\ ft^{-1}$	$7.565\ 341 * 10^{-5}$
Surface tension	$[m\ t^{-2}]$	$N\ m^{-1}$	$dyne\ cm^{-1}$	$1 * 10^{-3}$ (exact)
Temperature [5]	$[T]$	K	°R	$^5/_9$ (exact)
		°C	°F	$(°F – 32) / 1.8$ (exact)
Torque	$[L\ m^2\ t^{-2}]$	N m	lbf ft	$1.355\ 818$
Velocity	$[L\ t^{-1}]$	$m\ s^{-1}$	$ft\ s^{-1}$	$3.048 * 10^{-1}$ (exact)
Viscosity (dynamic)	$[L^{-1}\ m\ t^{-1}]$	Pa s	cp	$1.0 * 10^{-3}$ (exact)

Viscosity (kinematic)	$[L^2 t^{-1}]$	$m^2 s^{-1}$	cSt	$1.0 * 10^{-6}$ (exact)
Volume	$[L^3]$	m^3	ft^3	$2.831\ 685 * 10^{-2}$
		m^3	bbl	$1.589\ 873 * 10^{-1}$

[1] The expression 'SI units' is used loosely to indicate both 'strict' SI units and 'allowable' units. The 'strict' units can be sub-divided in the seven 'base' SI units (m, kg, s, A, K, mol and cd) and 'derived' SI such as °C, N, or J. The 'allowable' SI units are those defined in SPE (1982) and include d (day) and a (year).

[2] Conversion factors have been taken from SPE (1982).

[3] One hp = 550 ft lbf s^{-1}.

[4] Pressure in field units can be expressed in psig (gauge pressure) or psia (absolute pressure) where 0 psig = 14.7 psia. Pressure in SI units is often expressed in bar which is an 'allowable' SI unit, where 1 bar = 100 kPa.

[5] Zero K (Kelvin) is absolute zero in Celsius units. Therefore, the temperature expressed in K equals the temperature expressed in °C + 273.15.

Zero °R (Rankine) is absolute zero in Fahrenheit units. Therefore, the temperature expressed in °R equals the temperature expressed in °F + 459.67.

A.2 SI pre-fixes

Table A.2: SI pre-fixes		
Symbol	*Name*	*Magnitude*
n	nano	10^{-9}
μ	micro	10^{-6}
m	mili	10^{-3}
c	centi	10^{-2}
d	deci	10^{-1}
da	deca	10^{1}
h	hecto	10^{2}
k	kilo	10^{3}
M	mega	10^{6}
G	giga	10^{9}

A.3 Standard conditions

- SI units: 100 kPa and 15 °C. Note: sometimes a standard pressure of 101.325 kPa is used; see SPE (1982). The difference is negligible for normal production engineering purposes.
- Field units: 14.7 psia and 60 °F.
- Density of air at standard conditions: $\rho_{air,sc}$ =1.23 kg m^{-3} (76.3 * 10^{-3} lbm ft^{-3}).
- Density of water at standard conditions: $\rho_{water,sc}$ = 999 kg m^{-3} (62.4 lbm ft^{-3} or 8.34 lbm gal^{-1}).

A.4 Force, mass and acceleration of gravity

The relationship between force and mass is given by *Newton's law* as "force equals mass times acceleration". This can be expressed in SI units as

$$F = m \frac{d^2 x}{dt^2} \ , \tag{A.1}$$

where

  F is force, expressed in N,
  m is mass, expressed in kg,
  x is distance, expressed in m, and
  t is time, expressed in s.

This implies that $N = kg \, m \, s^{-2}$. As a result, a mass of 1 kg experiences an attractive force due to the earth's gravitational field, which has a magnitude $g = 9.80665 \, m \, s^{-2}$, of

$$F_{grav} = 1 \, kg * 9.80665 \, m \, s^{-2} = 9.80665 \, kg \, m \, s^{-2} = 9.80665 \, N \ . \tag{A.2}$$

Field units, however, have been defined purposely such that a mass of 1 lbm experiences an attractive force due to the earth's gravitational field, which has a magnitude $g = 32.174 \, ft \, s^{-2}$, of exactly 1 lbf:

$$F_{grav} = \underbrace{\frac{1}{32.174}}_{g_c} * 1 \, lbm * 32.174 \, ft \, s^{-2} = 1 \, lbf \ . \tag{A.3}$$

This simple result in field units for a mass experiencing the acceleration of gravity, leads however to a more complicated expression for a mass experiencing an arbitrary acceleration. In that case we should write

$$F = \frac{1}{g_c} m \frac{d^2 x}{dt^2} \ , \tag{A.4}$$

where

  F is force, lbf,
  m is mass, lbm,
  x is distance, ft,
  t is time, s, and
  g_c is a dimensionless constant with magnitude 32.174.

This implies that $lbf = g_c^{-1} \, lbm \, ft \, s^{-2}$. Note that the standard acceleration of gravity is specified as $9.80665 \, m \, s^{-2}$ ($32.174 \, ft \, s^{-2}$). In reality, the acceleration of gravity will show slight variations with geographical location and altitude.

A.5 Amount of substance and molar mass

In SI units we express the *amount of substance* in kmol, defined as "the amount of substance of a system which contains as many elementary entities as there are in 12 kg of C_{12}". The *molar mass*, which is the official name in the SI system for what used to be known as the *molecular weight*, is therefore specified in $kg \, kmol^{-1}$. As a result, an amount of n kmol of substance with a molar mass M expressed in $kg \, kmol^{-1}$ has a mass of $n \, M$ kg.

In field units, the amount of substance is expressed in lbm-mole, which is "the amount of substance of a system which contains as many elementary entities as there are in 12 lbm of C_{12}". The molar mass (molecular weight) is expressed accordingly in $lbm \, (lbm\text{-}mole)^{-1}$. As a result, an amount of n lbm-mole of substance with a molar mass M expressed in $lbm \, (lbm\text{-}mole)^{-1}$ has a mass of $n \, M$ lbm.

For gasses, the molar mass M is related to the specific gravity γ_g and the density under standard conditions $\rho_{g,sc}$ according to

SI units:
$$M = \gamma_g M_{air} = \frac{\rho_{g,sc}}{\rho_{air}} M_{air} = \frac{\rho_{g,sc}}{1.23} 28.97 = 23.55 \rho_{g,sc} \ \text{kg kmol}^{-1}, \qquad (A.5)$$

field units: $M = \gamma_g M_{air} = \frac{\rho_{g,sc}}{\rho_{air}} M_{air} = \frac{\rho_{g,sc}}{76.3*10^{-3}} 28.97 = 379.7 \rho_{g,sc} \ \text{lbm} \left(\text{lbm-mole}\right)^{-1}. \quad (A.6)$

Appendix B – Fluid properties and correlations

B.1 Fluid properties

Properties in Table B.1 (in SI units) have been computed from the values in Table B.2 with the aid of the conversion factors presented in Appendix A which, in turn, were taken from SPE (1982). Properties in Table B.2 (in field units) have been taken from GPSA (1998).

Table B.1: Reservoir fluid properties in SI units.				At standard conditions [1]	
Compound	Molar mass M (kg kmol^{-1})	Critical pres. p_c (10^6 Pa)	Critical temp. $T_{c,abs}$ (K)	Gas dens. $\rho_{g,sc}$ (kg m^{-3})	Liquid dens. $\rho_{l,sc}$ (kg m^{-3})
N_2 (nitrogen)	28.01	3.40	126.2	1.18	809 [2]
CO_2 (carbon dioxide)	44.01	7.37	304.1	1.86	817 [3]
H_2S (hydrogen sulphide)	34.08	8.96	373.4	1.44	801 [3]
H_2O (water)	18.02	22.1	647.1	0.77	999
C_1H_4 (methane)	16.04	4.60	190.6	0.68	300 [4]
C_2H_6 (ethane)	30.07	4.88	305.4	1.27	356 [3]
C_3H_8 (propane)	44.10	4.24	369.8	1.86	507 [3]
C_4H_{10} (iso-butane)	58.12	3.64	407.8	2.45	562 [3]
C_4H_{10} (n-butane)	58.12	3.78	425.1	2.45	584 [3]
C_5H_{12} (iso-pentane)	72.15	3.38	460.4	3.05	624
C_5H_{12} (n-pentane)	72.15	3.37	469.7	3.05	631
C_6H_{14} (n-hexane)	86.18	3.03	506.4	3.64	663
C_7H_{16} (n-heptane)	100.20	2.74	539.2	4.23	687
C_8H_{18} (n-octane)	114.23	2.49	568.4	4.82	706
C_9H_{20} (n-nonane)	128.26	2.28	594.7	5.42	721
$C_{10}H_{22}$ (n-decane)	142.29	2.10	617.7	6.00	734

[1] Standard conditions: 100 kPa and 15 °C = 288 K.

[2] Density at the 'normal boiling point', i.e. at boiling temperature (78 K) and 100 kPa. The temperature at standard conditions (288 K) is above the critical temperature (126 K).

[3] Density at saturation pressure (bubble point pressure) and 288 K.

[4] Estimated value. The temperature at standard conditions (288 K) is above the critical temperature (191 K).

Table B.2: Reservoir fluid properties in field units.				At standard conditions [1]	
Compound	Molar mass M (lbm * lbm-mole^{-1})	Critical pres. P_c (psia)	Critical temp. T_c (°F)	Gas specific gravity [2] γ_g (-)	Liquid specific gravity [3] γ_l (-)
N_2 (nitrogen)	28.01	492.8	-232.49	0.9672	0.80940 [4]
CO_2 (carbon dioxide)	44.01	1069.5	87.73	1.5196	0.81801 [5]
H_2S (hydrogen sulphide)	34.08	1300.	212.40	1.1767	0.80143 [5]
H_2O (water)	18.02	3200.1	705.11	0.6220	1.00000
C_1H_4 (methane)	16.04	667.0	-116.66	0.5539	(0.3) [6]
C_2H_6 (ethane)	30.07	707.8	90.07	1.0382	0.35619 [5]
C_3H_8 (propane)	44.10	615.0	205.92	1.5226	0.50698 [5]
C_4H_{10} (iso-butane)	58.12	527.9	274.41	2.0068	0.56286 [5]
C_4H_{10} (n-butane)	58.12	548.8	305.51	2.0068	0.58402 [5]
C_5H_{12} (iso-pentane)	72.15	490.4	368.96	2.4912	0.62441
C_5H_{12} (n-pentane)	72.15	488.1	385.7	2.4912	0.63108
C_6H_{14} (n-hexane)	86.18	439.5	451.8	2.9755	0.66404
C_7H_{16} (n-heptane)	100.20	397.4	510.9	3.4598	0.68805
C_8H_{18} (n-octane)	114.23	361.1	563.5	3.9441	0.70678
C_9H_{20} (n-nonane)	128.26	330.7	610.8	4.4284	0.72193
$C_{10}H_{22}$ (n-decane)	142.29	304.6	652.2	4.9127	0.73417

[1] Standard conditions: 14.7 psia and 60 °F = 520 °R.

[2] With respect to air which has a density at standard conditions of 0.0763 lbm ft^{-3}.

[3] With respect to water which has a density at standard conditions of 8.34 lbm ft^{-3}.

[4] Density at the 'normal boiling point', i.e. at boiling temperature (-320 °F) and 14.7 psia. The temperature at standard conditions (60 °F) is above the critical temperature (-232 °F).

[5] Density at saturation pressure (bubble point pressure) and 60 °F.

[6] Estimated value. The temperature at standard conditions (60 °F) is above the critical temperature (-117 °F).

Table B.3: Typical reservoir fluid gradients.			
Fluid	Density (kg m^{-3})	Gradient (kPa m^{-1})	Gradient (psi ft^{-1})
Gas	100 – 300	1.0 - 2.9	0.04 - 0.13
Oil	800 – 900	7.8 - 8.8	0.35 - 0.39
Water	1000 – 1100	9.8 - 10.8	0.43 - 0.48

B.2 Oil correlations

B.2.1 Black oil correlations

Black oil correlations are based on laboratory tests, most of which were performed on crudes with GOR less then 350 m^3/m^3 (about 2000 scf/stb). In practice, black oil correlations are often used above this limit, but with caution. Note that the numerical values in several of these correlations are not dimensionless. The most widely known black oil correlations are the 'Standing correlations', originally issued in Standing (1947), and Standing (1952). The expressions below have been taken from Appendix II of the 1977 SPE re-issue of Standing (1952). They have been derived based on data from 22 Californian crudes under conditions listed in Table B.4. Note: All correlations in this Appendix have been implemented in MATLAB routines which are available from Blackboard; see the file 'Fluid properties.zip'.

Table B.4: Conditions used to derive Standing correlations		
Property	*SI units*	*Field units*
Bubble point pressure p_b	$0.9 – 48.3 * 10^6$ Pa	130 – 7000 psia
Temperature T	37 – 125 °C	100 – 258 °F
Producing gas-oil ratio R_p	3.5 – 254 m^3/m^3	20 – 1425 scf/bbl
Oil density $\rho_{o,sc}$ or grav. γ_{API}	725 – 956 kg/m^3	16.5 – 63.8 °API
Gas density $\rho_{g,sc}$ or gravity γ_g	0.73 – 1.17 kg/m^3	0.59 – 0.95 (air = 1.00)

B.2.2 Bubble point pressure p_b

Standing's correlation to compute the bubble point pressure p_b from the producing gas-oil ratio R_p of a well is:

$$p_b = 125 * 10^3 \left[\left(\frac{716 R_p}{\rho_{g,sc}} \right)^{0.83} \frac{10^{0.00164 T}}{10^{1768/\rho_{o,sc}}} - 1.4 \right] . \tag{B.1}$$

If the actual GOR R_{go} is used to compute p_b with this correlation, the results are only valid if the gas produced at surface is associated gas. This is the case if the reservoir pressure is above or at the bubble point pressure p_b. It may also be the case if the reservoir pressure is below the bubble point pressure, as long as no gas coning has occurred and the well does not produce gas-cap gas.

B.2.3 Solution gas-oil ratio R_s

We can now estimate R_s, the solution gas-oil ratio at a pressure p other than the bubble point pressure of the mixture. If $p > p_b$, the oil is undersaturated, all gas is in solution and $R_s = R_p$. If $p \le p_b$, the oil is saturated with gas, there is free gas and the pressure p must be the bubble point pressure of the mixture of oil and still-dissolved gas. Hence R_s is given by the inverse of the above Standing correlation, but with pressure p instead of p_b:

$$p \le p_b : R_s = \frac{\rho_{g,sc}}{716} \left[\left(8 * 10^{-6} p + 1.4 \right) 10^{1768/\rho_{o,sc} - 0.00164 T} \right]^{1.2048} . \tag{B.2}$$

B.2.4 Oil formation volume factor B_o

As the pressure changes, the volume it occupies changes due to two effects: compressibility effects and, much more importantly, changes in the amount of dissolved gas. If $p \le p_b$, the oil

is saturated, and the mixture of oil and still-dissolved gas is at its bubble point. We can use Standing's correlation for the oil formation volume factor at the bubble-point pressure:

$$p \leq p_b: \ B_o = 0.9759 + 12*10^{-5} \left[160 R_s \sqrt{(\rho_{g,sc}/\rho_{o,sc})} + 2.25 \, T + 40 \right]^{1.2}. \tag{B.3}$$

If $p > p_b$, the oil is undersaturated and all the gas is dissolved. As pressure changes, all changes are due to changes in density of the mixture; no extra gas is dissolved or comes free. Hence

$$p > p_b: \ B_o = \frac{B_{ob}\rho_{ob}}{\rho_o}, \tag{B.4}$$

where B_{ob} and ρ_{ob} are the oil formation volume factor and the density of the oil at the bubble point pressure p_b, and ρ_o is the density at pressure p. As was shown in Section 4.4.3, this can also be written as:

$$p > p_b: \ B_o = B_{ob} \exp[-c_o(p - p_b)], \tag{B.5}$$

where c_o is the iso-thermal compressibility of the undersaturated oil. A correlation for c_o is given in Section B.2.6 below .

B.2.5 Densities
Using the principle of conservation of mass we can derive that

$$p \leq p_b: \ \rho_o = \frac{\rho_{o,sc} + R_s \rho_{g,sc}}{B_o} . \tag{B.6}$$

The oil density at bubble point conditions, ρ_{ob}, can be obtained from equation (B.6) through substitution of $B_o = B_{ob}$. At other pressures, above p_b, the density is given by

$$p > p_b: \ \rho_o = \rho_{ob} \exp[c_o(p - p_b)] , \tag{B.7}$$

see equation (4.12) in Section 4.4.3. Substitution of relationship (B.7) in equation (B.4) recovers relationship (B.5) for B_o quoted above.

B.2.6 Compressibility
Compressibility is best measured in the laboratory if accurate values are required for the density or B_o. Correlations do exist for the compressibility. One of these is given by Vazquez and Beggs (1980), and has the form

$$p > p_b: \ c_o = \frac{-2541 + 27.8 R_s + 31.0 \, T - 959 \, \rho_{g,100} + 1784*10^3 / \rho_{o,sc}}{10^5 \, p} , \tag{B.8}$$

where $\rho_{g,100}$ is the gas density measured at a pressure of 689 kPa (100 psig = 114.7 psia). This pressure was chosen to reflect a typical separator pressure because usually the gas density is determined from a sample taken from a separator; see Vazquez and Beggs (1980). The relationship between $\rho_{g,100}$ and $\rho_{g,sep}$ measured at any other separator pressure p_{sep} and temperature T_{sep} is given by

$$\rho_{g,100} = \rho_{g,sep} \left[1 + 5.912*10^{-5} \left(\frac{141.5*10^3}{\rho_{o,sc}} - 131.5 \right) (1.8 T_{sep} + 32) \log\left(\frac{p_{sep}}{790.8*10^3} \right) \right] . \tag{B.9}$$

B.2.7 Viscosity

A commonly used empirical correlation for dead oil is that of Beggs and Robinson (1975). It can be expressed as

$$\mu_{od} = 10^{-3}\left(10^a - 1\right) \ , \ a = \frac{10^b}{\left(1.8T + 32\right)^{1.163}}, \ b = 5.693 - \frac{2.863 * 10^3}{\rho_{o,sc}}. \quad \text{(B. 119)}$$

A correlation for saturated oil viscosity is also given by Beggs and Robinson (1975) as

$$\mu_o = \left[4.4065\left(R_s + 17.8\right)^{-0.515}\right]\mu_{od}^c \ , \ c = 3.04\left(R_s + 26.7\right)^{-0.338}. \quad \text{(B.11)}$$

These expressions illustrate that the saturated oil viscosity decreases with increasing temperature and increasing pressure. After reaching the bubble point pressure, however, the viscosity somewhat increases with increasing pressure. Vazquez and Beggs (1980) determined the following empirical correlation for undersaturated oil:

$$\mu_o = \mu_{ob}\left(\frac{p}{p_b}\right)^d \ , \ d = 7.2 * 10^{-5} p^{1.187} \exp\left(-11.513 - 1.30 * 10^{-8} p\right). \quad \text{(B.12)}$$

Table B.5 gives an overview of the conditions under which these correlations were derived; see Beggs and Robinson (1975) and Brill and Mukherjee (1999).

Table B.5: Conditions used to derive viscosity correlations.				
Property	*Equation (B.11), SI units*	*Equation(B.11), field units*	*Equation (B.12), SI units*	*Equation (B.12), field units*
Temperature T	21 – 146 °C	70 – 295 °F		
Pressure p_b	0.1 – 36.3 * MPa	15 – 5265 psia	1.0 – 65.6 MPa	141 – 9515 psia
Solution GOR R_s	3.6 – 369 m³/m³	20 – 2070 scf/stb	16 – 392 m³/m³	90 – 2199 scf/stb
Density $\rho_{o,sc}$, γ_{API}	959 – 747 kg/m³	16 – 58 °API	966 – 739 kg/m³	15 – 60 °API
Density $\rho_{g,sc}$, γ_g			0.63 – 1.66 kg/m³	0.51 – 1.35
Viscosity μ_o			0.12 – 148 mPa s	0.12 – 148 cp

B.2.8 Example 1 – Oil formation volume factor ($p < p_b$)

Consider a well that produces oil and gas at the following rates: $q_{o,sc}$ = 1000 m³ d⁻¹, and $q_{g,sc}$ = 200000 m³ d⁻¹. The production history shows no indication of gas-cap gas production. The density of the oil and gas at standard conditions are given by $\rho_{o,sc}$ = 800 kg m⁻³ and $\rho_{g,sc}$ = 0.98, and the reservoir is at pressure and temperature given by p_R = 20.00 MPa and T_R = 150 °C.

Question
What is the oil formation volume factor B_o at reservoir pressure and temperature?

Answer
The producing GOR is given by the actual GOR as

$$R_p = R_{go} = \frac{q_{g,sc}}{q_{o,sc}} = \frac{200000}{1000} = 200 \ \text{m}^3/\text{m}^3.$$

With the aid of equation (B.1) we find that the bubble point pressure equals

$$p_b = 125 * 10^3 \left[\left(\frac{716 * 200}{0.98} \right)^{0.83} \frac{10^{0.00164 * 150}}{10^{1768/800}} - 1.4 \right] = 26.1 \ \text{MPa},$$

where T has been taken equal to the reservoir temperature. Because the reservoir pressure is below the bubble point pressure, we need to compute the solution gas-oil ratio R_s at reservoir pressure with the aid of equation (B.2):

$$R_s = \frac{0.98}{716} \left[\left(8 * 10^{-6} * 20.0 * 10^6 + 1.4 \right) 10^{1768/800 - 0.00164 * 150} \right]^{1.2048} = 145 \ \text{m}^3/\text{m}^3.$$

The oil formation volume factor now follows from equations (B.3) as:

$$B_o = 0.9759 + 12 * 10^{-5} \left[160 * 145 \sqrt{(0.98/800)} + 2.25 * 150 + 40 \right]^{1.2} = 1.57 \ \text{m}^3/\text{m}^3.$$

Answer with MATLAB

```
» R_p = 200000/1000
R_p = 200
» p_b = pres_bub_Standing(R_p,0.98,800,150)
p_b = 2.6105e+007
» R_s = gas_oil_rat_Standing(20e6,0.98,800,150)
R_s = 145.4194
» B_o = oil_form_vol_fact_Standing(R_s,0.98,800,150)
B_o = 1.5656
```

Alternatively, the black oil properties can be computed directly as:

```
» [B_g,B_o,R_s] = black_oil_Standing(20e6,200,0.98,800,150)
B_g = 0.0068
B_o = 1.5656
R_s = 145.4194
```

B.2.9 Example 2 - Oil formation volume factor ($p > p_b$)

Consider the same situation as in Example 1 in Section B.2.8 above, except for the reservoir pressure which is now given by: $p_R = 40.00$ MPa.

Question

What is the oil formation volume factor B_o at this higher reservoir pressure?

Answer

Because the reservoir pressure is now above the bubble point pressure, the solution gas-oil ratio is equal to the producing gas-oil ratio:

$$R_s = R_p = 200 \ \text{m}^3/\text{m}^3.$$

The corresponding oil formation volume factor B_{ob} is obtained from equation (B.3) as:

$$B_{ob} = 0.9759 + 12*10^{-5}\left[160*15\sqrt{(0.98/800)} + 2.25*150 + 40\right]^{1.2} = 1.75 \text{ m}^3/\text{m}^3.$$

We can now compute the oil formation volume factor from equation (B.5). This requires that we first determine the compressibility c_o from equation (B.8), which, in turn, requires computation of ρ_{g100} from $\rho_{g,sep}$ with the aid of equation (B.9). Because $\rho_{g,sep}$ is in our example equal to $\rho_{g,sc}$, we can enter standard conditions in equation (B.9). This leads to

$$\rho_{g,100} = 0.98\left[1 + 5.912*10^{-5}\left(\frac{141.5*10^3}{800} - 131.5\right)(1.8*15+32)\log\left(\frac{100*10^3}{790.8*10^3}\right)\right] = 0.84,$$

$$c_o = \frac{-2541 + 27.8*200 + 31.0*150 - 959*0.84 + 1784*10^3/800}{10^5*40*10^6} = 2.27*10^{-9} \text{ Pa}^{-1},$$

$$B_o = 1.75\exp\left[-2.27*10^{-9}(40-26)*10^6\right] = 1.70 \text{ m}^3/\text{m}^3.$$

Answer with MATLAB *(continued from previous example)*

```
» B_ob = oil_form_vol_fact_Standing(R_p,0.98,800,150)
B_ob = 1.7515
» rho_g_100 = rho_g_Vazquez_and_Beggs(689e3,0.98,800,15)
rho_g_100 = 0.8407
» c_o = compres_Vazquez_and_Beggs(40e6,R_p,rho_g_100,800,150)
c_o = 2.2732e-009
» B_o = oil_form_vol_fact_undersat(B_ob,c_o,40e6,p_b)
B_o = 1.6970
```

Alternatively, the black oil properties can be computed directly as:

```
» [B_g,B_o,R_s] = black_oil_Standing(40e6,200,0.98,800,150)
B_g = 0
B_o = 1.6970
R_s = 200
```

B.2.10 Example 3 - Oil viscosity

Consider the same situation as in Example 2 in Section B.2.9 above.

Question

What is the oil viscosity μ_o at reservoir pressure and temperature?

Answer

With the aid of equations (B. 119) the dead-oil viscosity follows as:

$$b = 5.693 - \frac{2.863*10^3}{800} = 2.114 \ , \ a = \frac{10^{2.114}}{(1.8*150+32)^{1.163}} = 0.170 \ ,$$

$$\mu_{od} = 10^{-3}\left(10^{0.170} - 1\right) = 0.48*10^{-3} \text{ Pa s } .$$

The oil viscosity at bubble point can then be computed with the aid of equations (B.11) as:

$$c = 3.04(200 + 26.7)^{-0.338} = 0.486 \ ,$$

$$\mu_{ob} = \left[4.4065 \left(200 + 17.8 \right)^{-0.515} \right] \left(0.48 * 10^{-3} \right)^{0.486} = 6.7 * 10^{-3} \text{ Pa s },$$

and the viscosity at reservoir pressure with equation (B.12) as:

$$d = 7.2 * 10^{-5} \left(40 * 10^{6} \right)^{1.187} \exp \left(-11.513 - 1.30 * 10^{-8} * 40 * 10^{6} \right) = 0.45 ,$$

$$\mu_o = 6.7 * 10^{-3} \left(\frac{40 * 10^{6}}{26.1 * 10^{6}} \right)^{0.45} = 8.1 * 10^{-3} \text{ Pa s }.$$

Answer with MATLAB

```
» mu_od = oil_visc_dead_B_and_R(800,150)
mu_od = 4.7851e-004

» mu_ob = oil_visc_sat_B_and_R(mu_od,200)
mu_ob = 0.0067

» mu_o = oil_visc_undersat_V_and_B(mu_ob,40e6,26.1e6)
mu_o = 0.0081
```

Alternatively, the oil viscosity can be computed directly as:

```
» mu_o = oil_viscosity(40e6,200,0.98,800,150)
mu_o = 0.0081
```

B.3 Gas correlations

B.3.1 Pseudo properties

The concepts of critical pressure and temperature are exactly defined for single components. However, for mixtures the concepts are approximations, as indicated by the use of the terms *pseudo-critical* pressure and temperature. We can use the Sutton (1985) correlations to estimate the pseudo-critical properties as function of the gas density:

$$\begin{cases} p_{pc} = 5218 * 10^{3} - 734 * 10^{3} \rho_{g,sc} - 16.4 * 10^{3} \rho_{g,sc}^{2} , \\ T_{pc} = 94.0 + 157.9 \rho_{g,sc} - 27.2 \rho_{g,sc}^{2} . \end{cases} \tag{B.13}$$

Note that the pseudo-critical temperature is expressed in K. If a compositional description of the mixture is available, the pseudo-critical properties can be determined more accurately with the aid of *mixing rules*. For further information, consult the references mentioned in Section 4.2.

The dimensionless pseudo-reduced pressure p_{pr} and pseudo-reduced temperature T_{pr} are defined as:

$$p_{pr} = \frac{p}{p_{pc}}, \ T_{pr} = \frac{T_{abs}}{T_{pc}} . \tag{B.14}$$

B.3.2 Density

For single phase gas flow the gas density follows directly from the non-ideal gas law as

$$\rho_g = \frac{\rho_{g,sc}}{B_g} = \rho_{g,sc} \frac{p T_{sc,abs} Z_{sc}}{p_{sc} T_{abs} Z} . \tag{B.15}$$

In the black oil model, where it is assumed that the gas composition does not change with pressure and temperature, the same expression can be used for the gas density in the two-phase region.

B.3.3 Viscosity

A well known correlation for gas viscosity was presented in graphical form by Carr, Kobayashi and Burrows (1954). A numerical approximation of this correlation was given by Dempsey (1965) and can be represented in two steps as

$$\mu_g = f\left(p_{pr}, T_{pr}\right) * \mu_{g,p_{sc}}\left(M, T\right) , \qquad (B.16)$$

where

$$f = \frac{1}{T_{pr}} \exp\left[\begin{array}{l} a_0 + a_1 p_{pr} + a_2 p_{pr}^2 + a_3 p_{pr}^3 + T_{pr}\left(a_4 + a_5 p_{pr} + a_6 p_{pr}^2 + a_7 p_{pr}^3\right) \\ + T_{pr}^2\left(a_8 + a_9 p_{pr} + a_{10} p_{pr}^2 + a_{11} p_{pr}^3\right) + T_{pr}^3\left(a_{12} + a_{13} p_{pr} + a_{14} p_{pr}^2 + a_{15} p_{pr}^3\right) \end{array}\right] , (B.17)$$

with dimensionless coefficients as given in Table B.6. The variable $\mu_{g,p_{sc}}$ is the viscosity at atmospheric pressure for which the correlation can be expressed as

$$\mu_{g,p_{sc}} = b_0 + b_1 T + b_2 T^2 + b_3 M + b_4 TM + b_5 T^2 M + b_6 M^2 + b_7 TM^2 + b_8 T^2 M^2 , \qquad (B.18)$$

with dimensional coefficients that are also given in Table B.6. The relationship between the molar mass M, the gas density $\rho_{g,sc}$ and the gas specific gravity γ_g was given in equations (A.5) and (A.6). Correlations (B.16) to (B.18) are valid for the following ranges of parameter values:

$$1.0 \le p_{pr} \le 20 , \ 1.2 \le T_{pr} \le 3.0 , \ 16 \le M \le 110 , \ 4°C\left(40°F\right) \le T \le 204°C\left(400°F\right). \ (B.19)$$

The Dempsey (1965) approximations have been programmed in MATLAB routines with which Figures B.1 and B.2 were produced. The graphs are slightly different from the original graphs in Karr, Kobayashi and Burrows (1954), but are accurate enough for most production engineering calculations. In case of the presence of non-hydrocarbon components in the gas, correction factors are needed for the computation of the viscosity at atmospheric pressure. We refer to the original publication of Karr, Kobayashi and Burrows (1954) for further information.

Coefficient	Value	Coefficient	Value
	Table B.6: Coefficients for the Dempsey (1965) approximation of the Carr, Kobayashi and Burrows (1954) gas viscosity correlation.		
a_0	$-2.46211820 * 10^{-00}$	a_{13}	$-1.86408848 * 10^{-01}$
a_1	$2.97054714 * 10^{-00}$	a_{14}	$2.03367881 * 10^{-02}$
a_2	$-2.86264054 * 10^{-01}$	a_{15}	$-6.09579263 * 10^{-04}$
a_3	$8.05420522 * 10^{-03}$		
a_4	$2.80860949 * 10^{-00}$	b_0	$1.11231913 * 10^{-05}$
a_5	$-3.49803305 * 10^{-00}$	b_1	$3.01907887 * 10^{-08}$
a_6	$3.60373020 * 10^{-01}$	b_2	$6.84808007 * 10^{-12}$
a_7	$-1.04432413 * 10^{-02}$	b_3	$-1.09485050 * 10^{-07}$
a_8	$-7.93385684 * 10^{-01}$	b_4	$-1.15256951 * 10^{-10}$
a_9	$1.39643306* 10^{-00}$	b_5	$-2.91397349 * 10^{-13}$
a_{10}	$-1.49144925 * 10^{-01}$	b_6	$4.57735189 * 10^{-10}$
a_{11}	$4.41015512 * 10^{-03}$	b_7	$3.83226102 * 10^{-13}$
a_{12}	$8.39387178 * 10^{-02}$	b_8	$1.28865249 * 10^{-15}$
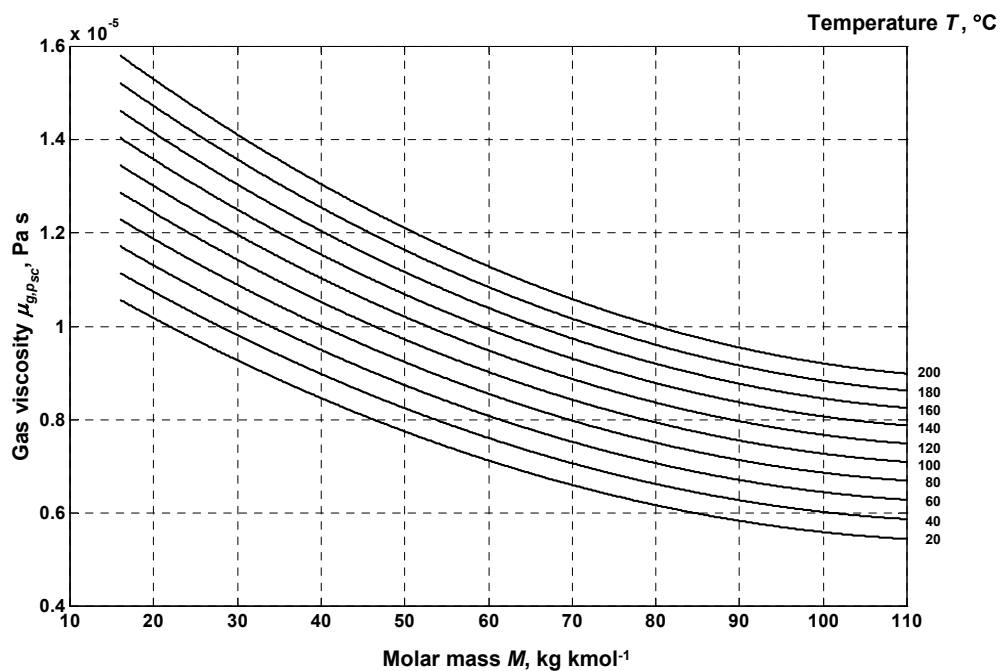
Figure B.1: Gas viscosity at atmospheric pressure. The graph is based on the Dempsey (1965) approximation of the Carr, Kobayashi and Burrows (1954) correlation.
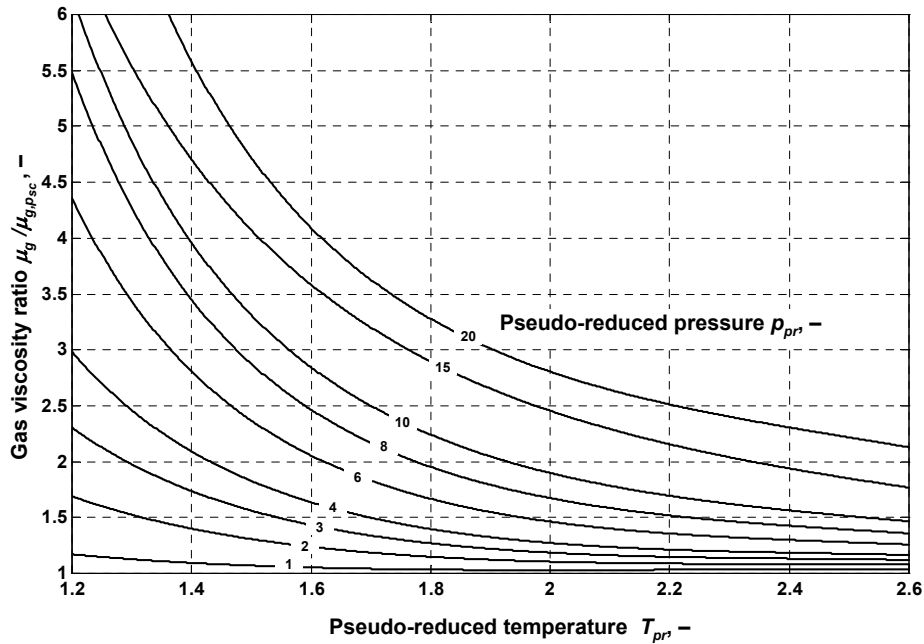
Figure B.2: Gas viscosity ratio. The graph is based on the Dempsey (1965) approximation of the Carr, Kobayashi and Burrows (1954) correlation.

B.3.4 *Z* factor

B.3.5.1 Standing-Katz correlation

The widely accepted correlation for the gas compressibility factor (*Z* factor) for a non-ideal gas or gas mixture was presented by Standing and Katz (1942) in graphical form. Various numerical approximations have been developed over time, and an overview is presented in Takacs (1976). Below we reproduce the approximation by Dranchuk and Abu-Kasem (1975) which is given in the form of an implicit function in terms of *Z*:

$$f(Z) = Z - b_1 Z^{-1} - b_2 Z^{-2} + b_3 Z^{-5} - \left(b_4 Z^{-2} + b_6 Z^{-4}\right)\exp\left(-b_5 Z^{-2}\right) - 1.0 = 0 \ , \quad \text{(B.20)}$$

where

$$b_1 = c\left(a_1 + \frac{a_2}{T_{pr}} + \frac{a_3}{T_{pr}^3} + \frac{a_4}{T_{pr}^4} + \frac{a_5}{T_{pr}^5}\right), \ b_2 = c^2\left(a_6 + \frac{a_7}{T_{pr}} + \frac{a_8}{T_{pr}^2}\right),$$

$$b_3 = c^5 a_9\left(\frac{a_7}{T_{pr}} + \frac{a_8}{T_{pr}^2}\right), \ b_4 = c^2\frac{a_{10}}{T_{pr}^3} \ , \ b_5 = c^2 a_{11} \ , \ b_6 = b_4 b_5 \ .$$

$$\text{(B.21)}$$

Here, a_1 to a_{11} are coefficients as specified in Table B.7, and *c* is a function of the dimensionless pseudo-reduced pressure and temperature:

$$c = 0.27\frac{p_{pr}}{T_{pr}} \ . \tag{B.22}$$

Table B.7: Coefficients for Dranchuk and Abu-Kassem (1975) approximation.	
Coefficient	Value
a_1	0.3265
a_2	-1.0700
a_3	-0.5339
a_4	0.01569
a_5	-0.05165
a_6	0.5475
a_7	-0.7361
a_8	0.1844
a_9	0.1056
a_{10}	0.6134
a_{11}	0.7210

B.3.5.2 Numerical implementation

Because equation (B.20) is implicit in Z it needs to be solved iteratively, e.g. with a Newton Raphson algorithm which we can write as (see Appendix C):

$$(Z)_{k+1} = (Z)_k - \frac{f(Z)_k}{f'(Z)_k} \ . \tag{B.23}$$

Here k is the iteration counter, and $f'(Z)$ is the derivative of $f(Z)$ with respect to Z given by

$$f'(Z) = 1 + b_1 Z^{-2} + 2b_2 Z^{-3} - 5b_3 Z^{-6} + \left(2b_4 Z^{-3} - 2b_4 b_5 Z^{-5} + 4b_6 Z^{-5} - 2b_5 b_6 Z^{-7}\right)\exp\left(-b_5 Z^{-2}\right). \tag{B.24}$$

A convenient starting value for Z is provided by the explicit approximation of Papay quoted in Takacs (1976) as:

$$Z = 1 - \frac{3.52 p_{pr}}{10^{0.9813} T_{pr}} + \frac{0.274 p_{pr}^2}{10^{0.8157} T_{pr}} \ . \tag{B.25}$$

Equation (B.23) can then be used to obtain improved approximations to the desired accuracy.

The Dranchuk and Abu-Kasem approximation to the Standing and Katz correlation has been programmed in a MATLAB file 'Z_factor_DAK.m'. The range of validity for the approximation is

$$0.2 \le p_{pr} \le 30 \ \text{ and } \ 1.05 \le T_{pr} \le 3.0 \ , \tag{B.26}$$

which is sufficient for most applications. Figures B.3.a and B.3.b have been generated with the MATLAB routine, and they closely mimic the original graphical Z-factor chart as presented in Standing and Katz (1942).
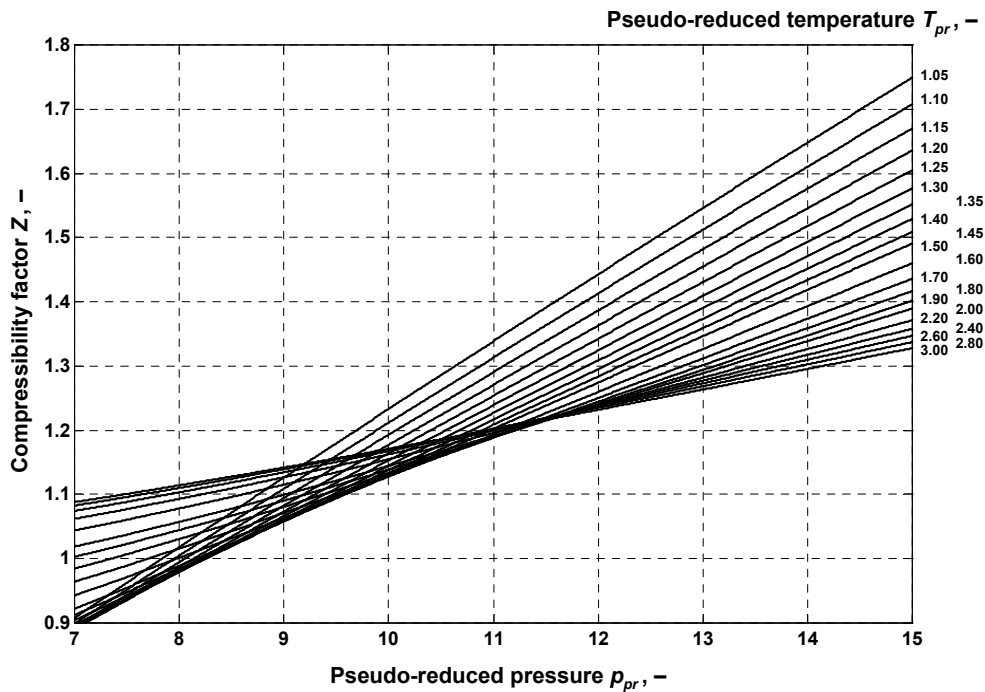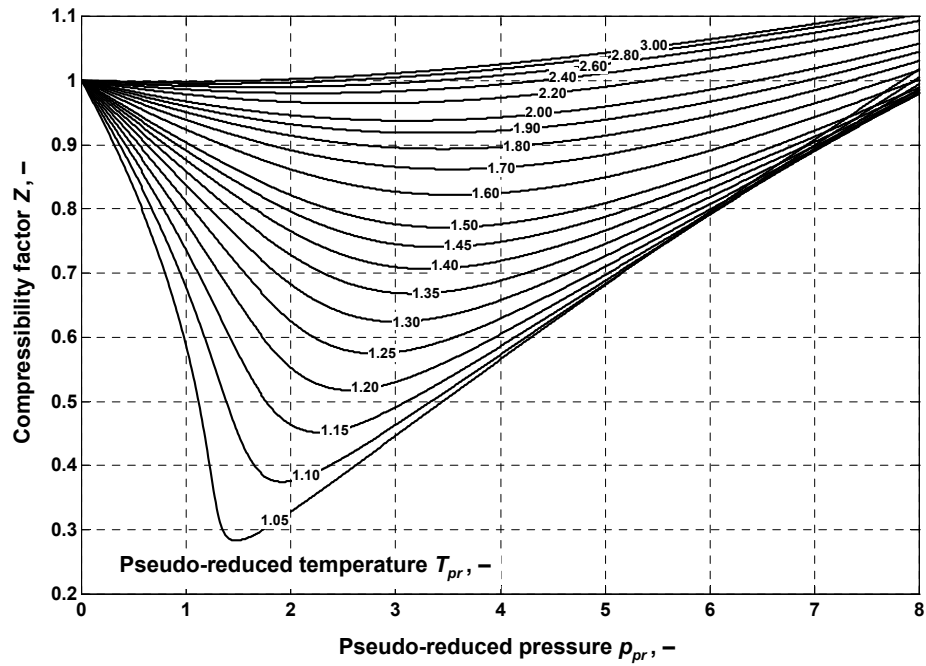
Figure B.3 a) and b). Compressibility factor Z as function of pseudo-reduced pressure p_{pr} and pseudo reduced temperature T_{pr}. The graph is based on the Dranchuk and Abu Kassem (1975) approximation of the Standing and Katz (1942) correlation.

B.3.5 Example 4 - Gas properties

Consider the same situation as in Example 1 in Section B.2.8 above.

Question

What are the gas formation volume factor B_g and the gas viscosity μ_g at reservoir pressure and temperature?

Answer

With the aid of the Sutton correlations (B.13) we find the pseudo-critical properties of the fluid as

$$p_{pc} = 5218*10^3 - 734*10^3 *0.98 - 16.4*10^3 *0.98^2 = 4.48*10^6 \text{ Pa},$$

$$T_{pc,abs} = 94.0 + 157.9*0.98 - 27.2*0.98^2 = 223 \text{ K}.$$

The pseudo-reduced pressure and temperature at the reservoir follow as

$$p_{R,pr} = \frac{p_R}{p_{pc}} = \frac{20*10^6}{4.48*10^6} = 4.46 \text{ and } T_{R,pr} = \frac{T_R}{T_{pc}} = \frac{150+273.15}{223} = 1.90 .$$

With the aid of the Standing-Katz chart in Figure B.3 we find for the compressibility factor, $Z = 0.93$, and with the aid of equation (4.7) for the gas formation volume factor:

$$B_g = \frac{100*10^3 *(150+273.15)*0.93}{20*10^6 *(15+273.15)*1.00} = 6.8*10^{-3} \text{ m}^3/\text{m}^3.$$

The molar mass of the gas follows from equation (A.5) as

$$M = 23.55*0.98 = 23.08 \text{ kg kmol}^{-1}.$$

With the aid of Figures (B.1) and (B.2) we now find for the gas viscosity at atmospheric pressure: $\mu_{g,p_{sc}} = 1.3*10^{-5}$ Pa s, and for the viscosity ratio: $f = 1.4$. The viscosity at reservoir pressure then follows with equation (B.16) as:

$$\mu_g = 1.4*1.3*10^{-5} = 1.8*10^{-5} \text{ Pa s}.$$

Answers with MATLAB

Gas formation volume factor:
```
» p_pc = pres_pseu_crit_Sutton(0.98)
p_pc = 4.4829e+006
» T_pc = temp_pseu_crit_Sutton(0.98)
T_pc = 222.6191
» p_R_pr = 20e6 / p_pc
p_R_pr = 4.4614
» T_R_pr = (150 + 273.15) / T_pc
T_R_pr = 1.9008
» Z = Z_factor_DAK(p_R_pr,T_R_pr)
Z = 0.9284
» B_g = gas_form_vol_fact(20e6,150+273.15,Z)
B_g = 0.0068
```

Gas viscosity:

```
» M = from_kg_per_m3_to_molar_mass(0.98)
M = 23.0790
» mu_g_p_sc = gas_visc_atm_Dempsey(M,150)
mu_g_p_sc = 1.3516e-005
» f = gas_visc_ratio_Dempsey(p_R_pr,T_R_pr)
f = 1.3732
» mu_g = f * mu_g_p_sc
mu_g = 1.8561e-005
```

Alternatively, the gas viscosity can be computed directly as:

```
» mu_g = gas_viscosity(20e6,0.98,150)
mu_g = 1.8561e-005
```

Appendix C – Numerical methods

C.1 Root finding

C.1.1 Newton-Raphson iteration

Consider a function $f(x) = 0$ that has at least one root (zero value) in the interval $D = (-\infty, \infty)$; see Figures C.1a to C.1d. We assume that the function is implicit, i.e. we assume that it is not possible to obtain an explicit expression for the value of x that makes $f(x)$ equal to zero. Therefore we need an iterative procedure to approximate the root. We require that $f(x)$ has a continuous first and second derivative, which implies that the first derivative is smooth and uniquely defined for each value of $x \in D$. We start the iteration with a first guess x_0. To improve the estimate we compute the slope of $f(x)$, i.e. the derivative $f'(x)$, in $x = x_0$, which can also be expressed as:
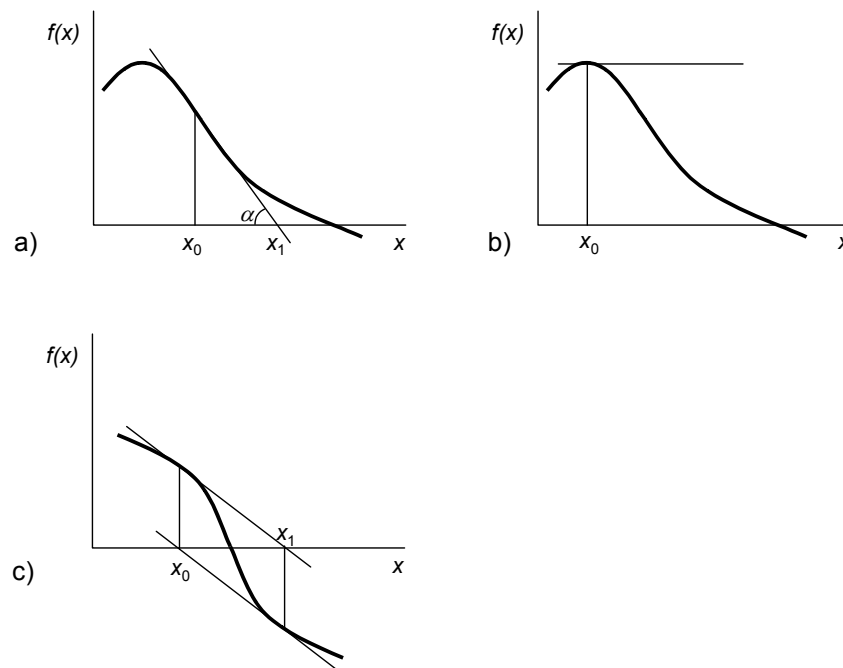
Figure C.1: a) Principle of Newton Raphson iteration; b) Convergence failure caused by a zero value of the derivative in x_0; c) Convergence failure caused by an endless loop.

$$f'(x_0) = \tan \alpha = \frac{f(x_0)}{x_1 - x_0} \quad , \tag{C.1}$$

where α and x_1 have been defined in Figure C-1a. This expression can be rewritten as

$$x_1 = x_0 - \frac{f(x_0)}{f'(x_0)} \quad , \tag{C.2}$$

which gives us a new estimate x_1 for the root. This procedure is called *Newton-Raphson iteration*, and can be generalized by writing

$$x_{k+1} = x_k - \frac{f(x_k)}{f'(x_k)} \;, \tag{C.3}$$

where k is an iteration counter. Expression (C.3) can then be applied until the difference $(x_{k+1} - x_k)$ has been reduced to below a specified value.

C.1.2 Convergence control

Convergence of the Newton-Raphson process is usually very fast if the initial estimate is close enough to the root. However, the process may get in trouble in several situations. It obviously fails for values of $f'(x)$ equal to zero; see Figures C.1b. A more subtle breakdown occurs when the root is located closely to a change in sign of the first derivative, in which case the process may end up in an endless loop; see Figure C.1c. Another type of problem may occur if $f(x)$ has multiple roots in D, in which case the process may convergence to a root that was not intended to be found. Various controls on the iteration process may be introduced to counteract these problems, e.g. a maximum allowed change in x in each iteration step, or restarting the process with a reduced change in x when the iteration fails to converge in a predefined number of steps. Prior inspection of the nature of the function $f(x)$ before using the Newton Raphson process may help to reduce the chance on convergence problems.

C.2 Differential equations

C.2.1 Initial value problems

All steady-state pressure drop equations for pipeline or wellbore flow, such as e.g. equations (5.19) or (5.27), can be expressed as

$$\frac{dp}{ds} = g(s, p) \;, \tag{C.4}$$

where g is a known nonlinear function of s and p. Equation (C.4) is a first-order differential equation that needs one boundary condition specifying a certain value $\hat{p}$ for the pressure at a certain point $\hat{s}$ along the pipeline or the well:

$$s = \hat{s}: \; p(\hat{s}) = \hat{p} \;. \tag{C.5}$$

To obtain the pressure p at any point along the pipeline we can integrate equation (C.4) starting from boundary condition (C.5)

$$p = \hat{p} + \int_{\hat{s}}^{s} g(s, p) \, ds \;. \tag{C.6}$$

This kind of equations is often used to describe problems that depend on time (instead of on distance s as in our case), in which case the boundary condition is usually specified at the start of the time interval. Therefore the boundary condition is often referred to as an initial condition, and the problems as an initial value problem.

C.2.2 Numerical integration

Generally, the integral in equation (C.6) can not be solved analytically, and needs to be evaluated through numerical integration. The most simple approach is to discretise equation (C.4) by replacing the difference dp/ds by a differential $\Delta p/\Delta s$ and to rewrite the result as:

$$\Delta p \approx g(s, p) \Delta s \;. \tag{C.7}$$

This gives us an algorithm to compute an approximate new value p_{k+1} at s_{k+1} from a known value p_k at s_k:

$$p_{k+1} = p_k + \Delta p \approx p_k + g\left(s_k, p_k\right) \Delta s \; . \tag{C.8}$$

where $\Delta s = s_{k+1} - s_k$ and $g(s_k, p_k)$ is a shorthand notation to indicate the evaluation of function $g(s,p)$ at $s = s_k$. More formally, the same result is obtained by using a Taylor expansion for p at s_k:

$$p_{k+1} = p_k + \left[\frac{dp}{ds}\right]_k \Delta s + \frac{1}{2}\left[\frac{d^2 p}{ds^2}\right]_k \left(\Delta s\right)^2 + \dots \; , \tag{C.9}$$

and maintaining only the first-order term. This also illustrates that the truncation error in equation (C.8), which is known as an explicit first-order Euler scheme, is of the order of $(\Delta s)^2$.

Although conceptually very simple, the first-order Euler scheme is not very efficient for use in wellbore flow calculations, and alternative algorithms, with a much smaller error for the same stepsize, should be applied. A popular class of integration algorithms are the Runge-Kutta routines which use multiple evaluations of the function $g(s,p)$ on the interval Δs, instead of only a single evaluation at the beginning of the interval as in the first-order Euler scheme. Especially in combination with an automated strategy to adapt the stepsize in order to achieve a pre-defined accuracy they are very powerfull. Many other schemes have been developed that may have a superior computational performance or accuracy depending on the nature of the function $g(s,p)$. For more information, consult one of the many available textbooks on numerical analysis, e.g. Hoffmann (1992). For our purpose the 4th-order Runge Kutta scheme with variable stepsize that is readily available in MATLAB provides a fit-for-purpose solution.

A simple check on the accuracy of the numerical integration of wellbore or pipeline pressure drop computations can be made by repeating the integration in the opposite direction. For example, after computing the flowing THP through 'bottom-up' integration starting from a known flowing BHP, the flowing BHP is recalculated through 'top-down' integration starting from the flowing THP. The difference between the two BHP values forms a good indication of the accuracy of the numerical integration. Typically a difference of less than a percent of the total pressure drop would be acceptable, although often a much better performance can be achieved. Note, however, that although a small difference is a necessary condition, it is not a sufficient one.

C.2.3 MATLAB implementation

The 4th-order Runge Kutta routine with variable stepsize in MATLAB is named `ode45`. To compute a pressure $p = p_{out}$, at $s = s_{out}$ starting from a known value $p = \hat{p}_{in}$ at $s = \hat{s}_{in}$ the following commands can be used:

```
» interval = [s_in,s_out];
» boundcon = p_in;
» options = [];
» [s,p] = ode45('g_dpds',interval,boundcon,options,p1,p2);
» n = length(p);
» p_out = p(n)
```

The variable `options` is a dummy variable that is required in the argument list of `ode45` but that we do not use. The variable `'g_dpds'` (between quotes) that forms the first element of the

argument list is the name of the user-defined MATLAB function (m-file) that defines the function $g(s,p)$. It is called many times by `ode45` during the Runge-Kutta integration. The function most likely requires various parameters, which can be passed via the argument list after `options`; here we used `p1` and `p2` as examples. The function would typically look something like:

```
function dpds = g_dpds(s,p,flag,p1,p2)
%
% User-defined function to compute the derivative dp/ds.
%
% dpds = pressure gradient, Pa/m
% flag = dummy variable, -
% p = pressure, Pa
% p1 = parameter, -
% p2 = parameter, -
% s  = along-hole coordinate, m
%
dpds = ...;
```

The three dots on the last line should be replaced by the appropriate function definition in terms of `s`, `p`, `p1` and `p2`. The first two elements of the argument list in the function header contain the independent and dependent variables `s` and `p`. The dummy variable `flag` is not used but has to be present as the third element of the argument list. Thereafter follow the parameters. Note that the arguments in the calling sequence of `ode45` are not identical to those in the header of `g_dpds`.

The output of `ode45` consists of a two column vectors with values of the indpendent and the dependent variables (here `s` and `p`) for regularly spaced values of `s`. The last element of vector `p` is the required output pressure `p_out`.

It is possible to integrate a system of first order differential equations, rather than a single equation, in the same fashion. This only requires that the dependent variable and the function definition are defined as vectors instead of scalars. We make use of this feature to compute the individual contributions of gravity, friction and accelleration losses to the total pressure drop in a well bore. For example, the function '`gas_dpds`' has the following header:

```
function dpds = gas_dpds(s,p,flag,...)
```

where the dots indicate parameters. Now, `dpds` is a four-element vector defined as:

```
dpds = [dpds_tot;dpds_grav;dpds_fric;dpds_acc],
```

while the variable `p` in the argument list is also a vector, defined as

```
p = [p_tot;p_grav;p_fric;p_acc].
```

Appendix D - Answers to exercises

D.1 Answers for Chapter 1 - Introduction

1.1 Oil rate: $12000 * 1.840 * 10^{-6} = 0.022$ m^{3}s^{-1}.
Gas rate: $1500 * 12000 * 2.831 * 10^{-2} / (24 * 3600) = 5.9$ m^{3}s^{-1}.
Oil density: $141.5 * 10^3 / (131.5 + 38) = 835$ kg m^{-3}.
Gas density: $0.82 * 1.23 = 1.0$ kg m^{-3}.

```
» from_bpd_to_m3_per_s(12000)
ans = 0.0221
» from_ft3_per_d_to_m3_per_s(1500*12000)
ans = 5.8993
» from_deg_API_to_kg_per_m3(38)
ans = 834.8083
» from_gas_grav_to_kg_per_m3(0.82)
ans = 1.0086
```

1.2 Molar mass of $C_1 = 16.043$ and of $CO_2 = 44.010$.
Total mass: $1* 16.043 + 0.3 * 44.010 = 29.25$ lbm.
Mass: $4.536 * 10^{-1} * 29.25 = 13.27$ kg.
Temperature: $83 * 5/9 = 46.1$ K.
Pressure: $(30 + 14.7) * 6.895 * 10^3 = 308$ kPa.

```
» from_lbm_to_kg(29.25)
ans = 13.2676
» from_deg_R_to_K(83)
ans = 46.1111
» from_psi_to_Pa(30 + 14.7)
ans = 3.0820e+005
```

1.3 Pressure = density * gravity * depth + atmospheric pressure
$= (1.03 * 999) * 9.807 * 2000 + 0.10 = 20.18 * 10^6$ Pa.
Pressure in psi: $20.18 * 10^6 / (6.895 * 10^3) = 2927$ psia.

```
» from_kg_per_m3_to_Pa_per_m(from_liq_grav_to_kg_per_m3(1.03)) *
2000 + 0.1
ans = 2.0181e+007
» from_Pa_to_psi(2.0181e7)
ans = 2.9270e+003
```

1.4 Step 1: Leave the formula in its original form, i.e. expressed in field variables, but enter the variables in SI units divided by their corresponding field-to-SI conversion factors as given in Table A.1.

$$\underbrace{\frac{\Delta p(\text{Pa})}{6.895*10^3}}_{\text{lbf/in}^2} = \underbrace{\frac{\rho(\text{kg}/\text{m}^3)}{1.602*10^1}}_{\text{lbm/ft}^3} \underbrace{\frac{\left(\dfrac{v(\text{m/s})}{3.048*10^{-1}}\right)^2}{\left(\text{ft/s}\right)^2}} \Big/ \left(288*32.174*C^2\right) \quad .$$

Step 2: Solve for Δp and combine all numerical factors:

$$\Delta p = \rho v^2 \big/ \left(2C^2\right) .$$

D.2 Answers for Chapter 2 – Production system modelling

2.1 Refer to equation (2.1) and Table 2.1. The power flow through the motor equals $300 *16 = 4800$ W. Because the motor is only 90% effective, the power flow through the shaft equals $0.9 * 4800 = 4320$ W. The shaft of the motor rotates with 240 rpm $= 240 * 2\pi / 60 = 25.1$ rad/s. The torque is therefore $4320 / 25.1 = 172$ Nm. The reduction gear has an efficiency of 98 %, so the remaining power flow to the pump is $0.98 * 4320 = 4234$ W. The pump creates a pressure differential of $160 * 10^3$ Pa at a flow rate of $22 * 10^{-3}$ m^3/s. The power flow at the liquid end of the pump is therefore $160 * 10^3 * 22 * 10^{-3} = 3520$ W. The efficiency of the pump now follows as $3520 / 4234 * 100 \% = 83$ %.

D.3 Answers for Chapter 3 – Optimisation objectives and constraints

3.1 Using equation (3.4) we find for the discounted value after 5 years:

$$S_{disc} = \frac{S}{\left(1 + R_{disc}/100\right)^n} = \frac{10 * 10^6}{\left(1 + 7/100\right)^5} = 7.13 * 10^6 \$.$$

For $n = 10$ we find $S_{disc} = 5.08 * 10^6$ \$, and for $n = 20$ we find $S_{disc} = 2.58 * 10^6$ \$.

```
» discount(10e6,5,7)
ans = 7.1299e+006
» discount(10e6,10,7)
ans = 5.0835e+006
» discount(10e6,20,7)
ans = 2.5842e+006
```

3.2 See MATLAB output below. Note that with a 15% discount rate the NPV becomes negative.

```
» cash flow = [-5.3,-1.2,1.8,3.9,2.5,1.4]
cash flow = -5.3000 -1.2000 1.8000 3.9000 2.5000 1.4000
» compute_NPV(cashflow,0)
cashflow_disc = -5.3000 -1.2000 1.8000 3.9000 2.5000 1.4000
ans = 3.1000
» compute_NPV(cashflow,15)
cashflow_disc = -4.6087 -0.9074 1.1835 2.2298 1.2429 0.6053
ans = -0.2545
```

3.3 The discounted reduction in CAPEX for the ML wells is depicted in Table D.1 where the discount was calculated according to:

$$\Delta C_{disc} = \Delta C * \left(\frac{1}{1.15}\right)^n,$$

where

ΔC_{disc} is the discounted differential CAPEX
ΔC is the differential CAPEX,
n is time in project years.

For two wells the production is one year delayed which implies

- a small loss of production at the end of the project which can be quantified as $2 * -0.10 = -0.20$ million \$, and, much more importantly,

- an additional one-year discount on the total production of the two wells (minus the contribution from the last year) which can be quantified as
  $2 * (56.58 / 1.15) - 2 * 56.58 = 98.40 - 113.16 = -14.76$ million $.

The total differential cumulative discounted cash flow (differential NPV) is therefore: differential cash-in – differential cash-out = $(- 0.20 - 14.76) - (-8.30) = -6.66$ million $.

The project team therefore has a point that the decreased expenditure for the ML wells is more than offset by the reduced income caused by delayed production. However, a better solution would be to drill the first two wells conventionally, and then replace well 4 to 10 by ML wells. This would give the benefit of reduced expenditure for 8 out of the 10 wells, without suffering a delay in first oil.

Note that this analysis did not take into account that ML wells are technically more complex. The increased risk of overspending and delays should be taken into account in the decision.

Table D.1: Differential expenditure

Year	Expenditure conventional wells (10^6 $)	Expenditure ML wells (10^6 $)	Differential expenditure (10^6 $)	Discounted differential expenditure (10^6 $)
1	10	0	-10	-8.70
2	20	24	4	3.02
3	20	16	-4	-2.63
Total	50	40	-10	-8.30

3.4 The optimal moment to change out the larger tubing is in year 6. The corresponding cashflow calculation is given in Table D.2 below. Although in this case the discounted NPV is somewhat lower than the undiscounted NPV, it is very attractive to start producing through the larger tubing. Only at an oil price as low as 3 $/bbl, the differential NPV becomes negative.

Table D.2: Differential NPV calculation.

Time (year)	Differential production rate (bpd)	Differential annual revenue ($)	Differential annual expenses ($)	Differential annual cash flow ($)	Discounted differential annual cash flow ($)
1	140	766,500	50,000	563,200	502,857
2	140	766,500	0	613,200	488,839
3	140	766,500	0	613,200	436,464
4	105	574,875	0	459,900	292,275
5	0	0	0	0	0
6		0	800,000	-800,000	-405,305
	525	2,874,375	850,000	1,449,500	**1,315,130**

D.4 Answers for Chapter 4 – Properties of reservoir fluids

4.1 The reservoir is below the bubble point pressure and therefore we can use Standing correlation (B.2) to calculate the solution GOR:

$$R_s = \frac{1.11}{716}\left[\left(8*10^{-6}*17*10^6+1.4\right)10^{1768/910-0.00164*76}\right]^{1.2048} = 90.5 \ \text{m}^3/\text{m}^3.$$

```
» R_s = gas_oil_rat_Standing(17e6,1.11,910,76)
R_s = 90.5408
```

4.2 The gas specific gravity at surface, i.e. at standard conditions, is

$$\gamma_g = \frac{\rho_{g,sc}}{\rho_{air}} = \frac{1.11}{1.23} = 0.90 \ \text{kg/m}^3 \ .$$

The gas density just above the gas cap, i.e. at reservoir conditions, can be found with the aid of equation (B.15). For that, we first need to calculate the gas deviation factor Z as follows. With the aid of the Sutton correlations (B.13) we find the pseudo-critical properties of the fluid as

$$p_{pc} = 5218*10^3 - 734*10^3*1.11 - 16.4*10^3*1.11^2 = 4.38*10^6 \ \text{Pa,}$$

$$T_{pc,abs} = 94.0 + 157.9*1.11 - 27.2*1.11^2 = 236 \ \text{K} \ .$$

The pseudo-reduced pressure and temperature at the reservoir follow as

$$p_{R,pr} = \frac{p_R}{p_{pc}} = \frac{17*10^6}{4.38*10^6} = 3.88 \ \text{and} \ T_{R,pr} = \frac{T_R}{T_{pc}} = \frac{76+273.15}{236} = 1.48 \ .$$

With the aid of the Standing-Katz chart in Figure B.3 we find for the compressibility factor, $Z = 0.76$, and with the aid of equation (B.15):

$$\rho_{g,R} = 1.11*\frac{17*10^6*(15+273.15)*1.00}{100*10^3*(76+273.15)*0.76} = 205 \ \text{kg/m}^3 \ .$$

```
» p_pc = pres_pseu_crit_Sutton(1.11)
p_pc = 4.3831e+006
» T_pc = temp_pseu_crit_Sutton(1.11)
T_pc = 235.7559
» p_R_pr = 17e6 / p_pc
p_R_pr = 3.8786
» T_R_pr = (76 + 273.15) / T_pc
T_R_pr = 1.4810
» Z = Z_factor_DAK(p_R_pr,T_R_pr)
Z = 0.7637
» B_g = gas_form_vol_fact(17e6,76+273.15,Z)
B_g = 0.0054
» rho_g_R = 1.11 / B_g
rho_g_R = 203.9255
```

4.3 Consult examples 3 and 4 in Sections B.2.10 and B.3.5 of Appendix B for the principles of the hand calculation. The reservoir pressure is above the bubble point pressure and

therefore the oil is undersaturated. We find for the viscosities $\mu_o = 21*10^{-3}$, and $\mu_g = 25*10^{-6}$ Pa s.

With MATLAB we find for the oil viscosity:

```
» mu_od = oil_visc_dead_B_and_R(910,76)
mu_od = 0.0070
» R_p = gas_oil_rat_Standing(19.5e6,1.11,910,76)
R_p = 106.6472
» mu_ob = oil_visc_sat_B_and_R(mu_od,R_p)
mu_ob = 0.0206
» mu_o = oil_visc_undersat_V_and_B(mu_ob,22e6,19.5e6)
mu_o = 0.0213
```

Alternatively, the oil viscosity can be computed more directly as:

```
» mu_o = oil_viscosity(22e6,R_p,1.11,910,76)
mu_o = 0.0213
```

The MATLAB results for the gas viscosity are:

```
» M = from_kg_per_m3_to_molar_mass(1.11)
M = 26.1405
» mu_g_p_sc = gas_visc_atm_Dempsey(M,76)
mu_g_p_sc = 1.1148e-005
» p_pc = pres_pseu_crit_Sutton(1.11)
p_pc = 4.3831e+006
» T_pc = temp_pseu_crit_Sutton(1.11)
T_pc = 235.7559
» p_R_pr = 22e6 / p_pc
p_R_pr = 5.0193
» T_R_pr = (76 + 273.15) / T_pc
T_R_pr = 1.4810
» f = gas_visc_ratio_Dempsey(p_R_pr,T_R_pr)
f = 2.1619
» mu_g = f * mu_g_p_sc
mu_g = 2.4101e-005
```

Alternatively, also the gas viscosity can be computed directly as:

```
» mu_g = gas_viscosity(22e6,1.11,76)
mu_g = 2.4101e-005
```

4.4 We can use the Vazquez and Beggs correlation (B.8) to calculate c_o. However, we first need expression (B.9) to convert the gas density $\rho_{g,sc}$ to the density at the reference separator pressure $\rho_{g,100}$, which was used to derive correlation (B.8). The values for p_{sep} and T_{sep} are in our case simply the standard conditions p_{sep} = 100 kPa and T_{sep} = 15 °C:

$$\rho_{g,100} = 1.11\left[1+5.912*10^{-5}\left(\frac{141.5*10^3}{910}-131.5\right)(1.8*15+32)\log\left(\frac{100*10^3}{790.8*10^3}\right)\right]=1.03 \ ,$$

$$c_o = \frac{-2541+27.8*90.5+31.0*76-959*1.03+1784*10^3/910}{10^5*22*10^6}=1.71*10^{-9} \ \text{Pa}^{-1}.$$

```
» R_p = gas_oil_rat_Standing(19.5e6,1.11,910,76)
R_p = 106.6472
```

```
» rho_g_100 = rho_g_Vazquez_and_Beggs(100e3,1.11,910,15)
rho_g_100 = 1.0266
» c_o = compres_Vazquez_and_Beggs(22e6,R_p,rho_g_100,910,76)
c_o = 1.7072e-009
```

4.5 Consult examples 1 and 2 in Sections B.2.8 and B.2.9 of Appendix B for the principles of the hand calculation. For p = 15 MPa and T = 85 °C, the oil is saturated and we find B_o = 1.47. For p = 30 MPa and T = 105 °C, the oil is undersaturated, and we find B_o = 2.42. Using MATLAB, the results are:

```
» p_b = pres_bub_Standing(250,1.02,805,85)
p_b = 2.4529e+007
» R_s = gas_oil_rat_Standing(15e6,1.02,805,85)
R_s = 138.9552
» B_o = oil_form_vol_fact_Standing(R_s,1.02,805,85)
B_o = 1.4666
» p_b = pres_bub_Standing(250,1.02,805,105)
p_b = 2.6467e+007
» B_ob = oil_form_vol_fact_Standing(250,1.02,805,105)
B_ob = 1.8790
» rho_g_100 = rho_g_Vazquez_and_Beggs(100e3,1.02,805,15)
rho_g_100 = 0.8785
» c_o = compres_Vazquez_and_Beggs(30e6,250,rho_g_100,805,105)
c_o = 3.0125e-009
» B_o = oil_form_vol_fact_undersat(B_ob,c_o,30e6,p_b)
B_o = 1.8591
```

Also in this case the MATLAB computations can performed more directly as:

```
» [B_g,B_o,R_s] = black_oil_Standing(15e6,250,1.02,805,85)
B_g = 0.0067
B_o = 1.4666
R_s = 138.9552
» [B_g,B_o,R_s] = black_oil_Standing(30e6,250,1.02,805,85)
B_g = 0
B_o = 1.8591
R_s = 250
```

D.5 Answers for Chapter 5 – Single-phase flow in wells and pipelines

5.1 The fluid velocity in the pipeline is given by

$$v = \frac{q}{A} = \frac{q}{\frac{1}{4}\pi d^2} = \frac{-5000/(24*3600)}{\frac{1}{4}\pi 0.232^2} = -1.37 \text{ m/s}^2$$

The oil viscosity can be found from the Dempsey correlation (B. 119) as:

$$b = 5.693 - \frac{2.863*10^3}{850} = 2.325, \; a = \frac{10^{2.325}}{(1.8*45+32)^{1.163}} = 0.866,$$

$$\mu = 10^{-3}\left(10^{0.866} - 1\right) = 6.3*10^{-3} \text{ Pa s }.$$

The Reynolds number and the dimensionless roughness follow from equations (5.10) and (5.11) as

$$N_{Re} = \frac{\rho d |v|}{\mu} = \frac{850*0.232*1.37}{6.3*10^{-3}} = 4.3*10^4 \quad \text{and} \quad \varepsilon = \frac{e}{d} = \frac{3*10^{-6}}{0.232} = 1.3*10^{-5},$$

which allow us to read the friction factor from the Moody diagram in Figure 5.3 as

$$f(\varepsilon, N_{Re}) = f(1.3*10^{-5}, 4.3*10^4) = 0.021 .$$

The pipeline inclination, seen from the origin at the manifold, should be negative to correspond to uphill production flow. Expressed in radians the pipeline inclination therefore becomes

$$\theta = \frac{-1.5*\pi}{180} = -0.0262 \text{ rad} .$$

The pressure at the outlet can now be computed with the aid of equation (5.24) as:

$$p_{out} = \hat{p}_{in} - \left(\rho g \sin\theta + \frac{\rho}{2d} f * v|v| \right)(s - \hat{s})$$

$$= 10*10^5 - \left[850*9.81*\sin(-0.0262) + \frac{850}{2*0.232}*0.021*-1.37^2 \right]*(0 - 3000)$$

$$= 1.29*10^5 \text{ Pa} .$$

5.2 In line with the sign convention for production flow that was choosen in the lecture notes, the MATLAB m-file `flowline_p_mf` has been defined such that the origin of the coordinate along the flowline is at the manifold. Therefore, flow towards the manifold, as occurs in production wells, has a negative sign. Furthermore, a negative value of the flowline inclination indicates a decreasing flow line elevation, seen from the manifold. The m-file can be used for single-phase liquid flow, single-phase gas flow or multi-phase flow, depending on the value of the parameter `fluid`. In case of single-phase oil flow, the input values for gas and water flowrates and densities may be assigned an arbitrary value. See scriptfile `exercise_5_2.m` for the MATLAB implementation. The output is:
`p_mf = 1.2149e+005`

5.3 The average absolute temperature along the well is $T_{av,abs}$ = 273.15 + (120+30)/2 = 348.15 K. The coefficients k_1 and k_2 are given by equations (5.32) and (5.33) as

$$k_1 = -\frac{Mg \sin\theta_{av}}{Z_{av} R T_{av,abs}} = -\frac{23.55*0.95*9.81*\sin(-\pi/2)}{0.96*8314*348.15} = 7.90*10^{-5} \text{ m}^{-1}, \text{ and}$$

$$k_2 = -\frac{8 Z_{av} R T_{av,abs} f_{av} \rho_{g,sc}^2 q_{g,sc} |q_{g,sc}|}{\pi^2 d^5 M}$$

$$= -\frac{8*0.96*8314*348.15*0.0166*0.95^2*(-8.62)*8.62}{\pi^2*(62.3*10^{-3})^5*23.55*0.95} = 1.19*10^{11} \text{ Pa}^2/\text{m}.$$

With the aid of equation (5.37) we now find that

$$p_{wf} = \sqrt{\left(\hat{p}_{tf}^2 + \frac{k_2}{k_1}\right)\exp\left[2k_1\left(s-\hat{s}\right)\right] - \frac{k_2}{k_1}}$$

$$= \sqrt{\left[\left(1.5*10^6\right)^2 + \frac{1.19*10^{11}}{7.90*10^{-5}}\right]\exp\left[2*7.90*10^{-5}*\left(3000-0\right)\right] - \frac{1.19*10^{11}}{7.90*10^{-5}}}$$

$$= 30.3*10^6 \text{ Pa},$$

which is reasonably close to the numerical result of $29.0*10^6$ Pa. See scriptfile `exercise_5_3.m` for the MATLAB implementation.

5.4 See scriptfile `exercise_5_4.m` for the MATLAB implementation. The pressure drop over the wellbore is $27.5*10^6$ Pa. The absolute error is -375 Pa, which gives a relative error of only $-1.36*10^{-5}$

D.6 Answers for Chapter 6 – Multi-phase flow in wells, pipelines and chokes

6.1 See Figure 6.3.
$$A_l = \frac{q_l}{v_l} = \frac{0.3*q_g}{v_g/1.2} = 0.36*A_g \;\;;$$

$$\lambda_l = \frac{q_l}{q_g + q_l} = \frac{0.3*q_g}{\left(1+0.3\right)q_g} = 0.23 \;\;; \;\; H_l = \frac{A_l}{A_g + A_l} = \frac{0.36*A_g}{\left(1+0.36\right)A_g} = 0.26 \;\;.$$

6.2 The local phase rates can be obtained from equations (4.21) as

$$\begin{bmatrix} q_g \\ q_o \\ q_w \end{bmatrix} = \begin{bmatrix} 0.05 & -0.05*10.1 & 0 \\ 0 & 1.15 & 0 \\ 0 & 0 & 1 \end{bmatrix}\begin{bmatrix} 238 \\ 1 \\ \dfrac{0.23}{1-0.23} \end{bmatrix}*18.4*10^{-3} = \begin{bmatrix} 2.6 \\ 21.2 \\ 5.5 \end{bmatrix}*10^{-3}\text{m}^3.$$

The pipe's surface area is given by $A = \frac{1}{4}\,\pi d^2 = 0.0117$ m^2. Thus we find:

$$\lambda_l = \frac{q_l}{q_g + q_l} = \frac{\left(21.2+5.5\right)*10^{-3}}{\left(2.6+21.2+5.5\right)*10^{-3}} = 0.91 \;\;; \;\; H_l = 1.05*\lambda_l = 1.05*0.91 = 0.96 \;\;;$$

$$v_{sg} = \frac{q_g}{A} = \frac{2.6*10^{-3}}{0.0117} = 0.22 \text{ m/s} \;\;; \;\; v_{sl} = \frac{q_o + q_w}{A} = \frac{\left(21.2+5.5\right)*10^{-3}}{0.0117} = 2.28 \text{ m/s} \;\;;$$

$$v_g = \frac{v_{sg}}{\left(1-H_l\right)} = \frac{0.22}{\left(1-0.96\right)} = 5.50 \text{ m/s} \;\;; \;\; v_g = \frac{v_{sl}}{H_l} = \frac{2.28}{0.96} = 2.38 \text{ m/s} \;\;.$$

Appendix E – MATLAB m-files

E.1 Conversion factors

```
from_bbl_to_m3.m                    from_lbm_per_ft3_to_Pa_per_m.m
from_bpd_psi_ft_to_m2_per_d_Pa.m    from_lbm_per_ft3_to_psi_per_ft.m
from_bpd_psi_ft_to_m2_per_s_Pa.m    from_lbm_to_kg.m
from_bpd_psi_to_m3_per_d_Pa.m       from_liq_grav_to_deg_API.m
from_bpd_psi_to_m3_per_s_Pa.m       from_liq_grav_to_kg_per_m3.m
from_bpd_to_m3_per_d.m              from_m2_per_d_Pa_to_bpd_psi_ft.m
from_bpd_to_m3_per_s.m              from_m2_per_s_Pa_to_bpd_psi_ft.m
from_cal_to_J.m                     from_m2_per_s_to_cSt.m
from_cp_to_Pa_s.m                   from_m2_to_ft2.m
from_cSt_to_m2_per_s.m              from_m2_to_in2.m
from_deg_API_to_kg_per_m3.m         from_m2_to_mD.m
from_deg_API_to_liq_grav.m          from_m3_per_d_Pa_to_bpd_psi.m
from_deg_C_to_deg_F.m               from_m3_per_d_to_bpd.m
from_deg_F_to_deg_C.m               from_m3_per_d_to_ft3_per_d.m
from_deg_R_to_K.m                   from_m3_per_m3_to_ft3_per_bbl.m
from_deg_to_rad.m                   from_m3_per_s_Pa_to_bpd_psi.m
from_dyne_per_cm_to_N_per_m.m       from_m3_per_s_to_bpd.m
from_ft2_to_m2.m                    from_m3_per_s_to_ft3_per_d.m
from_ft3_per_bbl_to_m3_per_m3.m     from_m3_per_s_to_ft3_per_s.m
from_ft3_per_d_to_m3_per_d.m        from_m3_to_bbl.m
from_ft3_per_d_to_m3_per_s.m        from_m3_to_ft3.m
from_ft3_per_s_to_m3_per_s.m        from_m_per_s_to_ft_per_s.m
from_ft3_per_s_to_m3_per_s.m        from_m_to_ft.m
from_ft3_to_m3.m                    from_m_to_in.m
from_ft_per_s_to_m_per_s.m          from_mD_to_m2.m
from_ft_to_m.m                      from_molar_mass_to_gas_grav.m
from_gas_grav_to_kg_per_m3.m        from_molar_mass_to_kg_per_m3.m
from_gas_grav_to_molar_mass.m       from_N_m_to_lbf_ft.m
from_hp_to_W.m                      from_N_per_m_to_dyne_per_cm.m
from_in2_to_m2.m                    from_N_to_lbf.m
from_in_to_m.m                      from_Pa_per_m_to_kg_per_m3.m
from_J_to_cal.m                     from_Pa_per_m_to_lbm_per_ft3.m
from_K_to_deg_R.m                   from_Pa_per_m_to_psi_per_ft.m
from_kg_per_m3_to_deg_API.m         from_Pa_s_to_cp.m
from_kg_per_m3_to_gas_grav.m        from_Pa_to_psi.m
from_kg_per_m3_to_lbm_per_ft3.m     from_per_Pa_to_per_psi.m
from_kg_per_m3_to_liq_grav.m        from_per_psi_to_per_Pa.m
from_kg_per_m3_to_molar_mass.m      from_ppg_to_kg_per_m3.m
from_kg_per_m3_to_Pa_per_m.m        from_psi_per_ft_to_kg_per_m3.m
from_kg_per_m3_to_ppg.m             from_psi_per_ft_to_lbm_per_ft3.m
from_kg_per_m3_to_psi_per_ft.m      from_psi_per_ft_to_Pa_per_m.m
from_kg_to_lbm.m                    from_psi_to_Pa.m
from_lbf_ft_to_N_m.m                from_rad_to_deg.m
from_lbf_to_N.m                     from_W_to_hp.m
from_lbm_per_ft3_to_kg_per_m3.m
```

E.2 Economics

```
compute_NPV.m                       discount.m
```

E.3 Exercises

```
exercise_5.2.m                      exercise_5.4.m
exercise_5.3.m
```

E.4 Fluid flow

```
Beggs_Brill_dpds.m                  example_flowline.m
choke_critical_p_tf.m               example_intake_curve.m
```

```
example_traverse.m              liquid_near_well_p_wf.m
example_wellbore.m              Moody_friction_factor.m
flowline_p_fl.m                 Muk_Brill_dpds.m
flowline_p_mf.m                 Reynolds_number.m
gas_dpds.m                      well_p_tf.m
gas_near_well_p_wf.m            well_p_wf.m
liquid_dpds.m                   Zig_and_Syl_fric_fact.m
```

E.4 Fluid properties

```
black_oil_Standing.m            oil_visc_dead_B_and_R.m
compres_Vazquez_and_Beggs.m     oil_visc_sat_B_and_R.m
gas_form_vol_fact.m             oil_visc_undersat_V_and_B.m
gas_oil_rat_Standing.m          oil_viscosity.m
gas_visc_atm_Dempsey.m          pres_bub_Standing.m
gas_visc_ratio_Dempsey.m        pres_pseu_crit_Sutton.m
gas_viscosity.m                 rho_g_Vazquez_and_Beggs.m
interfacial_tensions.m          temp_pseu_crit_Sutton.m
local_q_and_rho.m               water_viscosity.m
oil_form_vol_fact_Standing.m    Z_factor_DAK
oil_form_vol_fact_undersat.m
```

References

Ahmed, T., 1989: *Hydrocarbon phase behaviour*, Gulf, Houston.

Arnold, K. and Stewart, M., 1998: *Surface production operations, 2nd ed.*, Vols. 1 and 2, Gulf, Houston.

Bear, J., 1972: *Dynamics of Fluids in Porous Media*, Elsevier. Reprinted by Dover, 1988.

Beggs, H.D. and Robinson, J.R., 1975: Estimating the viscosity of crude oil systems, *J. Petr. Techn.*, 1140-1141.

Beggs, H.D., 1991: *Production optimisation using NODAL analysis*, Oil and Gas Consultants International Publications, Tulsa.

Bird, R.B., Stewart, W.E. and Lightfoot, E.N., 2002: *Transport phenomena, 2nd ed.*, Wiley, New York.

Bobok, E., 1993: *Fluid mechanics for petroleum engineers*, Elsevier, Amsterdam.

Boyce, W.E. and DiPrima, R.C., 2000: *Ordinary differential equations and boundary value problems, 7th ed.*, Wiley, New York.

Brill, J.P. and Mukherjee, H., 1999: Multi-phase flow in wells, *SPE Monograph Series,* **17**, SPE, Richardson.

Brown, K.E., 1984: *The technology of artificial lift methods, Vol. 4 - Production optimisation of oil and gas wells by nodal systems analysis*, PennWell, Tulsa.

Carr, N.L., Kobayashi, R. and Burrows, D.B., 1954: Viscosity of hydrocarbon gases under pressure, *Trans. AIME,* **201**, 264-272.

Chilingarian, G.V., Robertson, J.O. and Kumar, S., 1987: *Surface operations in petroleum production*, Vols. 1 and 2, Elsevier, Amsterdam.

Civan, F., 2000: *Reservoir Formation Damage*, Gulf, Houston.

Colebrook, C.F., 1939: Turbulent flow in pipes with particular reference to the transition region between the smooth and rough pipe laws, *J. Inst. Civil Eng.*, **11**, 133-156.

Currie, P.K., 1999: Drilling, completion and facilities, *Lecture notes ta3430, Delft University of Technology*.

Dake, L.P., 1978: *Fundamentals of reservoir engineering*, Elsevier.

Danesh, A., 1998: *PVT and phase behaviour of petroleum reservoir fluids*, Elsevier.

Dempsey, J.R., 1965: Computer routine treats gas viscosity as a variable, *Oil and Gas J.*, Aug. 16, 141-142.

Dietz, D.N. (1965): Determination of average reservoir pressure from build-up surveys*, J. Petr. Techn.*, Aug., 955-959.

Dikken, B.J., 1990: Pressure drop in horizontal wells and its effect on production performance, *J. Petr. Techn.*, Nov., 1426-1433.

Dranchuk, P.M. and Abu-Kasem, J.H., 1975: Calculation of Z-factors for natural gasses using equations-of-state, *J. Can. Petr. Techn.*, July-September, **14**, 34-36.

Duns, H. and Ros, N.C.J., 1963: Vertical flow of gas and liquid mixtures in wells, *Proc. 6th World Petroleum Congress*, section II, 451-465, paper 22-PD6.

Economides, M.J., Hill, A.D. and Ehlig-Economides, C., 1994: *Petroleum production systems*, Prentice Hall.

Economides, M.J., Watters, L.T. and Dunn-Norman, S., 1998: *Petroleum well construction*, Wiley.

Fetkovich, M.J., 1973: The isochronal testing of oil wells, *Proc. 48th Ann. Fall Meeting SPE, Las Vegas*, paper SPE 4529.

Firoozabadi, A., 1999: *Thermodynamics of hydrocarbon reservoirs*, McGraw-Hill, New York.

Gilbert, W.E., 1954: Flowing and gas-lift well performance. *Drill. & Prod. Prac. (API) 143*.

Golan, M. and Whitson, C.H., 1991: *Well performance, 2nd ed.*, Prentice Hall, Englewood Cliffs.

GPSA, 1998, *Engineering data book 11th ed. - FPS*, Gas Processors Suppliers Association, Tulsa.

Hassan, A.R. and Kabir, C.S., 2002: *Fluid flow and heat transfer in wellbores*, SPE, Richardson.

Hoffman, J.D., 1992: *Numerical methods for engineers and scientists*, McGraw-Hill, New York.

Joshi, S.D., 1991: *Horizontal well technology*, PennWell, Tulsa.

Karnopp, D.C., Margolis, D.L. and Rosenberg, R.C., 2000: *System dynamics, 3rd ed.*, Wiley, New York.

McCain, W.D., 1990: *The properties of petroleum fluids, 2nd ed.*, PennWell, Tulsa.

Moody, L.F., 1944: Friction factors for pipe flow, *Trans. Am. Soc. Mech. Eng.*, **66**, 671-684.

Moran, M.J. and Shapiro, H.N., 1998: *Fundamentals of engineering thermodynamics, 3rd ed.*, Wiley.

Nind, T.E.W., 1964: *Principles of oil well production*, McGraw-Hill, New York.

Oliemans, R.V.A., 1998: Applied multi-phase flows, *Lecture notes tn3782, Delft University of Technology*.

Pedersen, K.S., Fredenslund, Aa. and Thomassen, P., 1989: *Properties of oils and natural gases*, Gulf, Houston.

Rachford, H.H. and Rice, J.D., 1952: Procedure for use of electronic digital computers in calculating flash vaporization hydrocarbon equilibrium, *J. Petr. Techn.*, October, Section 1, 19, Section 2, 3.

Reis, J.C., 1996: *Environmental control in petroleum engineering*, Gulf, Houston.

Ros, N.C.J., 1960: An analysis of critical simultaneous gas-liquid flow through a restriction and its application to flow metering, *Appl. Sci. Res*. **9,** section A 374.

Rossi, D.J., Gurpinar, O., Nelson, R. and Jacobsen, S., 2000: Discussion on integrating monitoring data into the reservoir management process, *Proc. SPE European Petroleum Conference, Paris*, paper SPE 65150.

Seba, R.D., 1998: *Economics of worldwide petroleum production*, Oil & Gas Consultants International, Tulsa.

SPE, 1982: *The SI metric system of units and SPE metric standard*, SPE, Richardson.

SPE, 1993: *SPE letter and computer symbols standard*, SPE, Richardson.

Standing, M.B., 1947: A pressure-volume-temperature correlation for mixtures of California oils and gases, *API Drilling and Production Practice*, 275-287.

Standing, M.B., 1952: *Volumetric and phase behaviour of oil field hydrocarbon systems*, Reinhold, New York, Reprinted by SPE, Dallas, 1977.

Standing, M.B. and Katz, D.L., 1942: Density of natural gases, *Trans. AIME,* **146**, 140-149.

Strang, G., 1986: *Introduction to applied mathematics*, Wellesley-Cambridge.

Sutton, R.P., 1985: Compressibility factors for high-molecular weight reservoir gases, *Proc. SPE Ann. Techn. Conf. and Exhib., Las Vegas*, September, paper SPE 14265.

Takacs, G., 1976: Comparisons made for computer Z-factor calculations, Oil and Gas J., December 20, 64-66.

Vazquez, M. and Beggs, H.D., 1980: Correlations for fluid physical property predictions, *J. Petr. Techn.*, June, 968-970.

Vogel, J.V., 1968: Inflow performance relationships for solution-gas drive wells*, J. Petr. Techn.*, January, 83-92.

Wallis, G.B., 1969: *One-dimensional two-phase flow*, McGraw-Hill, New York.

Whitson, C.H. and Brulé, M.R., 2000: Phase behaviour, *SPE Monograph Series,* **20**, SPE, Richardson.

Zitha, P.L.J. and Currie, P.K., 2000: Properties of hydrocarbons and oilfield fluids, *Lecture notes ta3410, Delft University of Technology*.

Glossary

AHD	Along-Hole Depth
AIME	American Institute of Mining and Metallurgical Engineers
AOFP	Absolute Open Flowing Potential
API	American Petroleum Institute
bbl	barrel
BHP	Bottomhole Pressure
BHT	Bottomhole Temperature
bpd	barrel per day
BSW	Base Sediment and Water
CAPEX	Capital Expenditure
CGR	Condensate-Gas Ratio
EMV	Expected Monetary Value
EOS	Equation Of State
ESP	Electric Submersible Pump
E&P	Exploration and Production
FDP	Field Development Plan(ning)
FBHP	Flowing BottomHole Pressure
FBHT	Flowing BottomHole Temperature
FTHP	Flowing Tubing Head Pressure
FTHT	Flowing Tubing Head Temperature
FVF	Formation Volume Factor
GLR	Gas-Liquid Ratio
GOC	Gas-Oil Contact
GOR	Gas-Oil Ratio
GWC	Gas-Water Contact
II	Injectivity Index
IPR	Inflow Performance Relationship
MD	Measured Depth
ML	Multi-Lateral
NPV	Net Present Value
OCR	Oil-Condensate Ratio
OGR	Oil-Gas Ratio
OPEX	Operating Expenditure
OWC	Oil-Water Contact
PDG	Permanent Downhole Gauge
PI	Productivity Index
ppg	pounds per gallon
PVT	Pressure, Volume, Temperature
rpm	revolutions per minute
scf	standard cubic foot
SCSSV	Surface-Controlled Subsurface Safety Valve
SPE	Society of Petroleum Engineers
stb	standard barrel
THP	Tubing Head Pressure
THT	Tubing Head Temperature
TVD	True Vertical Depth
UTC	Unit Technical Costs
VLE	Vapour-Liquid Equilibrium

WOR   Water-Oil Ratio

Index